

Lunar Lander Propellant Production for a Multiple Site Exploration Mission

by

Joshua Neubert

B.S. Earth, Atmospheric and Planetary Science
Massachusetts Institute of Technology, 2003

SUBMITTED TO THE DEPARTMENT OF EARTH, ATMOSPHERIC AND PLANETARY SCIENCE IN PARTIAL FULFILLMENT OF THE REQUIREMENTS FOR THE DEGREE OF

MASTERS OF SCIENCE IN EARTH, ATMOSPHERIC AND PLANETARY SCIENCE
AT THE
MASSACHUSETTS INSTITUTE OF TECHNOLOGY

MAY 2004
[June 2004]

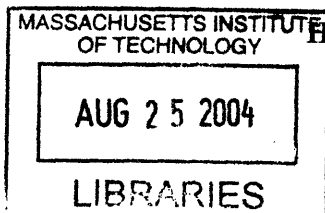
Copyright © 2004 Joshua R. Neubert. All rights reserved.

The author hereby grants to MIT permission to reproduce and to distribute publicly paper and electronic copies of this thesis document in whole or in part.

Signature of Author: _____
Department of Earth, Atmospheric and Planetary Science
May 7, 2004

Certified by: _____
Dr. Jeffrey Hoffman
Professor of the practice of Aerospace Engineering
Thesis Supervisor

Accepted by: _____
Dr. Maria Zuber
E. A. Griswold Professor of Geophysics
Head of the Department of Earth, Atmospheric and Planetary Science



ARCHIVES

Lunar Lander Propellant Production for a Multiple Site Exploration Mission

By

Joshua R. Neubert

Submitted to the Department of Earth, Atmospheric and Planetary Science on May 7, 2004
in Partial Fulfillment of the Requirements for the Degree of Master of Science in Earth,
Atmospheric and Planetary Science

ABSTRACT

A model has been developed to analyze the benefit of utilizing a processing plant architecture so that a lunar oxygen production demonstration mission can also provide a significant exploration and scientific return. This architecture will send one lander to the lunar surface with the capability of producing its own propellant to launch itself to multiple sites of scientific interest. It is compared with two other possible planetary exploration architectures: the multiple mission architecture which sends one mission to each landing site of interest, and the fully fueled architecture which sends one mission with enough propellant to launch itself to all selected landing sites. A value of the total mass savings of the processing plant architecture over these two architectures is used as a means of quantifying the benefit for future lunar exploration. The mass of the power system is found to be the dominant component of the overall system mass for all cases using a Cassini type RTG. Results from model runs have shown that at Cassini RTG efficiencies this architecture will not be beneficial in highland regions; however, a significant benefit is shown when using mare and glassy type feedstocks. Further data and analysis is needed to confirm the extent of this benefit. At Cassini RTG efficiencies, a processing plant architecture exhibits significant benefit in mare regions when launching once every ~2 months or longer. Launching every 2 months creates a benefit for a minimum of 12 launches with a launch range of up to ~10km. Using pyroclastic glasses as the feedstock produces a benefit when launching once every ~2 months or longer as well. Launching every 2 months creates a benefit for a minimum of 12 launches with a launch range up to ~13km. Utilizing a longer time between launches significantly increases the launch capabilities. In the near future, RTGs are expected to quadruple in efficiency. With the expected RTG efficiencies the processing plant architecture has an even higher range of benefit for mare and glassy feedstocks. Highland region exploration is only expected to be beneficial with this architecture if further advances in RTG efficiency are made and if system degradation is not severe over a mission timeframe of several years. Advanced RTG technology is identified as the primary technology of need for increasing the benefit of possible processing plant missions. Future versions of this model will be created to better understand and quantify the exact benefit and system dynamics of this architecture.

Thesis supervisor: Dr. Jeffrey Hoffman

Title: Professor of the Practice of Aerospace Engineering

TABLE OF CONTENTS

page number

List of Tables and Figures	5
1. Introduction	6
1.1 Past lunar exploration	6
1.2 Lunar ice discovery	8
1.3 Current/future lunar exploration plans	10
2. Lunar Resources	11
2.1 Lunar compositional regions	12
2.1.1 Mare	12
2.1.2 Highlands	13
2.1.3 The lunar regolith	14
2.2 Resources available	15
2.2.1 Oxygen	15
2.2.2 Water ice	16
2.2.3 Lunar concrete	16
2.2.4 Structural metals	17
2.2.5 Solar panels	17
3. Oxygen Production Methods	18
3.1 Ice extraction	19
3.2 Hydrothermal regolith reduction	20
3.3 Carbothermal regolith reduction	22
4. Lunar Exploration Architectures	23
4.1 Multiple mission architecture	24
4.2 Fully fueled architecture	24
4.3 Processing plant architecture	25
5. Model Development and Analysis Methods	27
5.1 Model parameters	29
5.2 Model design and assumptions	32
5.2.1 Multiple mission architecture design	33
5.2.2 Fully fueled architecture design	35
5.2.3 Processing plant architecture desing	38
5.2.3.1 Propellant and tank calculations	40
5.2.3.2 Oxygen yield	41
5.2.3.3 Regolith and batch conversions	44
5.2.3.4 Furnace calculations	44
5.2.3.5 Power system calculations	45
5.3 Analysis method	49
6. Analysis Results	50
6.1 Equatorial highland feedstocks	51
6.1.1 Preheating time	52
6.1.2 Maximum range of feasibility	56
6.1.3 Batch processing time	58
6.1.4 Launch number	60
6.1.5 Mass benefit and system feasibility	63
6.1.5.1 Benefit vs. multiple mission architecture	63

6.1.5.2	Benefit vs. fully fueled architecture	66
6.2	Equatorial mare feedstocks	77
6.2.1	Preheating time	78
6.2.2	Maximum range of feasibility	84
6.2.3	Batch processing time	86
6.2.4	Launch number	87
6.2.5	Mass benefit and system feasibility	90
6.2.5.1	Benefit vs. multiple mission architecture	91
6.2.5.2	Benefit vs. fully fueled architecture	95
6.2.5.3	Overall system feasibility	98
6.3	Equatorial Glassy feedstocks	102
6.3.1	Preheating time	103
6.3.2	Maximum range of feasibility	107
6.3.3	Batch processing time	109
6.3.4	Launch number	110
6.3.5	Mass benefit and system feasibility	113
6.3.5.1	Benefit vs. multiple mission architecture	114
6.3.5.2	Benefit vs. fully fueled architecture	117
6.3.5.3	Overall system feasibility	121
7.	Polar Ice Deposits	129
8.	Technological Improvements of Importance	131
8.1	Hydrothermal processing system	131
8.2	Power production systems	132
9.	Error Analysis	137
10.	Discussion and conclusions	139
References	142

LIST OF TABLES AND FIGURES

page number

Table 1 – Architecture pros and cons	26
Table 2 – List of model parameters	30
Table 3 – List of oxygen yields	43
Table 4 – Heat energies	46
Table 5 – Highland feedstock optimal heating times	55
Table 6 – Highland feedstock range of feasibility	57
Table 7 – Mare feedstock optimal heating times	81
Table 8 – Mare feedstock range of feasibility	85
Table 9 – Mare total system masses and distances	100-101
Table 10 – Glassy feedstock optimal heating times	106
Table 11 – Glassy feedstock range of feasibility	108
Table 12A:C – Glassy total system masses and distances	123-126
Figure 1 – Multiple mission architecture flowchart	35
Figure 2 – Fully fueled architecture flowchart	38
Figure 3 – Processing plant architecture flowchart	39
Figure 4A:D – Highland system mass vs. heating times	53-54
Figure 5 – Highland batch processing time comparisons	59
Figure 6A:D – Highland launch number comparisons	61-62
Figure 7A:D – Highland mass benefit vs. multiple mission architecture	64-65
Figure 8A:D – Highland mass benefit vs. fully fueled architecture	67-69
Figure 9 – Highland Delta benefit vs. fully fueled architecture	72
Figure 10 – 2000hr highland mass benefit vs. multiple mission architecture	74
Figure 11 – 2000hr highland mass benefit vs. fully fueled architecture	75
Figure 12A:D – Mare system mass vs. heating time	79-80
Figure 13 – Optimal heating time affects on system mass	82
Figure 14 – Affect of heating time on batch size	83
Figure 15 – Mare batch processing time comparisons	86
Figure 16A:D – Mare launch number comparisons	88-89
Figure 17 – Mare total processing time comparisons	90
Figure 18A:D – Mare mass benefit vs. multiple mission architecture	91-93
Figure 19 – Mare maximum beneficial range	94
Figure 20A:D – Mare mass benefit vs. fully fueled architecture	95-97
Figure 21A:D – Glassy system mass vs. heating times	104-105
Figure 22 – Glassy batch processing time comparisons	109
Figure 23A:D – Glassy launch number comparisons	110-112
Figure 24 – Glassy total processing time comparison	113
Figure 25A:E – Glassy mass benefit vs. multiple mission architecture	114-116
Figure 26 – Glassy maximum beneficial range	117
Figure 27A:E – Glassy mass benefit vs. fully fueled architecture	118-120
Figure 28A:B – Glassy system masses vs. total mission range	127
Figure 29A:B – System mass breakdown	135
Figure 30 – Thermal RTG total mission time comparisons	136

1. Introduction

Hundreds of years before mankind could even dream about sending a man into space, astronomers and other scientists focused their attention on the moon. Early observers mapped the path of the Moon in the sky to keep track of important dates for farming and other needs. Over time our instruments of observation improved and so did our scientific discoveries.

1.1 Past lunar exploration

Long after humanity first began studying the moon, nations began setting much more lofty goals. From the very inception of our ability to enter space, lunar exploration has been a key target. Throughout the 1960s and into the 1970s both the American and Russian space programs focused heavily on the Moon. In 1959 the Russians launched the first ever lunar flyby, Luna1. Shortly afterwards, America responded to the Russian's lunar activity with the Apollo program, which had the single primary goal of landing a man on the moon. This push to the Moon was largely a result of the cold war between the two superpowers and produced the only successful missions to ever put a human on another planetary body to date. The Apollo program successfully landed humans on the lunar surface six times.

The Apollo missions and their precursor robotic explorers provided detailed data on many aspects of lunar exploration. Apollo 11, 12, 14, 15, 16, and 17 all achieved the goal of landing on the lunar surface. Each landing site was chosen with both science and

engineering constraints in mind. The multiple missions were able to land in very different regions of the lunar surface; however, they were all limited to mostly mare regions due to the engineering constraints of the landing process. Apollo 1 through 6 were all test missions for analyzing the mission designs. Apollo 7 and 9 were designed as Earth orbiting missions to test the Command and Lunar Modules. Apollo 8 and 10 were lunar orbiting missions that did not land on the surface. These orbiting missions were key to future Apollo missions by supplying important high resolution photography of possible landing sites. Apollo 13 was planned to land on the moon but was unable to do so. At the end of the program six Apollo missions had landed on the Moon returning a wealth of data and almost 400 kilograms of lunar samples for study. The ability to analyze lunar samples in laboratories on Earth provided a great amount of information on lunar composition and mineralogy that could not have been obtained without the sample return. These analyses also provided knowledge about the formation of the moon and the compositional variability between the mare and highland regions. The mare regions were found to be volcanic in origin with high iron content, similar to volcanic basalts found here on the Earth. In general, the highland soils were noted to be much older than the volcanic mare and to have a more anorthositic mineralogy [Heiken].

The Apollo program provided much knowledge about human aspects of space exploration as well as lunar science. Before the program it was not known how the human body would react to long stays in space, or how the Moon's lower gravity and lunar environment could affect humans. The lunar missions provided scientists with valuable data on the human body's reaction to the space environment. Unfortunately, as the cold war wound down, so

did our nation's desire and inspiration to continue the expensive program of lunar exploration. The only missions since the Apollo program to study the moon were both unmanned orbiters sent in the 1990s – Clementine and Lunar Prospector, both of which were able to provide tantalizing new data about various aspects of the moon.

1.2 Lunar ice discovery

Both Lunar Prospector and Clementine made a number of great discoveries in lunar science, the most notable of which has been data showing evidence for possible water ice at the lunar poles. Clementine was launched on January 25, 1994 and began returning data shortly thereafter. Clementine's radar experiment showed a reflectance signature which has been interpreted as a sign of water ice [Nozette]. The results of the experiment showed a significant backscatter increase from one orbit over the south-pole; however, little signal indicative of water ice was detected over the north-pole. This data did not show signs of large standing bodies of water ice, but rather of water ice crystals intermixed with the rocky silicate soils. Further data is still needed to determine definitively the existence and concentrations of any ice deposits.

In the lunar environment it is impossible for liquid water to exist. Ice deposits can only exist in areas that are permanently shaded. Solid ices will automatically sublime and be lost into space if solar energy reaches the ice deposit. The polar regions are the only places that can have permanently shaded areas where ice can exist for long periods of time, due to the low solar incidence angle. Time sequenced images from the Clementine mission were pieced together from which researchers were able to determine that there were specific

regions of several craters near the lunar south-pole that the sun never reached. It was shown that the signatures of water ice found with other experiments closely matched the areas of permanent shadow. However, the resolution of these images was not high enough to definitely discern the location of possible ice deposits.

Several years after Clementine, Lunar Prospector explored the poles with its suite of instruments, including several spectrometers. The neutron spectrometer detected signs of hydrogen, which were then interpreted as indicating water ice deposits. Hydrogen absorbs a higher concentration of epithermal neutrons. Therefore, in the presence of an increased hydrogen source such as water, the epithermal neutron count will be diminished. The neutron spectrometer showed a significant reduction in epithermal neutrons over both the north and south-pole regions [Feldman 2000, 2001].

This experiment provides compelling evidence for water ice at the lunar poles; however, it is not conclusive. Solar wind hydrogen has also been proposed as a possible source of the epithermal neutron data count [Hodges, E2 2002; Crider 2000]. Scientists still argue over the neutron data today. A general consensus has been reached that there is some amount of water ice trapped at the poles. Feldman estimated 1.5 ± 0.8 wt% ice held within the lunar cold traps in the south-pole [Feldman, 2000]; however, these numbers are contested by other scientists. Hodges notes that other thermal neutron signatures should be seen as a result of water ice; however, he claims that they are not present in the data [Hodges E2 2002]. Instead, he proposes a simple mineralogical anomaly such as a deficit in CaO to explain the epithermal neutron count found by Lunar Prospector [Hodges E12 2002]. As a

last effort to glean further evidence for water ice, the Lunar Prospector spacecraft was crashed into the southern pole in hopes of releasing a cloud of volatiles that would be detectable by Earth observers. Unfortunately, no such cloud was detected and further experiments are still needed to definitively determine the existence and concentration of ice at the pole.

1.3 Current/future lunar exploration plans

Recently, President Bush has introduced a new space exploration proposal including a return to the moon as a primary goal. There are also several missions currently being planned, or already in route to the Moon. ESA's Smart-1, Japan's SELENE, and a privately funded mission by Transorbital Inc. will all shortly be studying the lunar environment. Towards the end of the decade NASA plans to launch both a lunar orbiter and lander.

The discovery of possible water ice at the lunar poles has helped spark new enthusiasm for returning to the moon that is now apparent in the space community, as can be seen in the numerous new missions being planned to the moon. China has also expressed interest in taking its new and developing space program to the moon. A white paper published on the official Chinese National Space Agency's website states that a future development target for their agency is to study "outer space exploration centering on the exploration of the moon" [<http://www.cnsa.gov.cn>].

In the 1990s the NRC-NAS decadal survey determined a south-pole Aitken Basin sample return mission to be a high priority in coming years for NASA. The President's plan for

space exploration proposed in January of 2004 has listed a lunar return as a primary goal. With this renewed interest in returning to the moon it is important to determine what resources can be used and how to use them. This study is a step towards understanding the benefits of oxygen as a lunar resource and how it will be useful in future years. The in-situ production of oxygen alone could drastically alter the future of not only lunar exploration, but exploration of the rest of the solar system as well.

2. Lunar Resources

The lunar surface is host to a wide variety of minerals that can be processed into usable materials for future lunar exploration and development. Different resources will be needed for different types of missions. For example, manned missions need more resources for life support and other human operations. Robotic missions primarily need energy and propellant. However, many robotic missions are used to prepare resources for future human missions as well. The ease with which any given mineral can be processed into a usable resource depends on what resource you are trying to gain and the energy needed to separate out the required elements. For any given resource there are specific lunar minerals which most easily yield the desired elements. Therefore, producing a needed resource at one landing site may not be as easy as at the next due to compositional variability. This makes it very important to understand lunar composition and mineralogy as well as any resource production processes.

2.1 Lunar compositional regions.

On the most basic level, the lunar surface can be divided into two major regions of compositional variability: the highlands and the mare. A third division must be made between the regolith layer and the underlying rocks within these regions when considering the resource capabilities of each region. There are a few immediately noticeable differences between the mare and the highland regions. First, the mare are visibly much darker than the highlands. Secondly, the highland regions are older and more densely cratered than the mare terrain. Going into further detail, one can determine the mineralogical differences between these regions. There has been much research on the mineralogy and variability of both the mare and highland regions; however, for this study it is only important here to understand the relative mineralogies and compositions as they relate to resource processing. Heiken has compiled vast amounts of data in great detail on lunar composition and mineralogy in “The Lunar Sourcebook” [Heiken].

2.1.1 Mare

Mare regions are comprised of various ancient basaltic lava flows. These regions cover nearly 20% of the near-side of the Moon, but less than 1% of the far-side. Specific regions of the mare can be related to individual impact basins. The Imbrium basin is one example of an ancient impact which resulted in a large lava flow and is now a basaltic mare deposit. Lunar volcanism has long since ceased being an active force on the moon. This means that all basaltic mare were laid down long ago and have been undergoing space weathering effects for over a billion years. The moon has suffered a large number of impacts since the

last active volcanism. All sizes of impacts have thrown ejecta material across the lunar surface. Large tracts of very early basaltic lava flows have been covered by these ejecta blankets and are now primarily considered to be highland regions. These ancient, covered mare are termed crypto-mare. Compositionally the mare are primarily basaltic; however, there is a fairly wide range in the exact mineralogy from one mare deposit to another. A major distinction in compositional variability within the mare regions is in the titanium and iron contents. These two elements are usually linked through the mineral ilmenite [FeTiO₃]. This mineral has been identified as a primary source for several oxygen processing systems. Mare regions can be divided into two sub-categories, one of high-Titanium basalts, and low titanium basalts. Regions of high-titanium basalts are preferable for a number of oxygen production methods because of their increased abundance of Ilmenite. The mare also have a relatively high abundance of the pyroxene minerals [(Ca,Mg,Fe)SiO₃]. The variability among the pyroxene minerals from one mare region to another is noticeably larger than pyroxene variabilities among Earth's basalts [Heiken]. The compositional variability and uncertainties in lunar mineralogy add complications to determining the resource capabilities of any region. However, a major note of importance for all mare regions is that they are significantly enriched in oxide minerals relative to the highland regions.

2.1.2 Highlands

Highland regions are all older than the most recent mare deposits. Chemically, they are enriched in calcium and aluminum and dominantly composed of feldspar rich rocks. Highland rock types have been split into three major categories: ferroan anorthosites, magnesium rich rocks, and KREEP rocks. Ferroan anorthosites are rich in calcium and

aluminum, and composed primarily of the mineral plagioclase. Magnesium rich rocks can be similar in their plagioclase content, but they also contain significant amounts of high-magnesium content minerals such as olivine $[(Mg,Fe)_2SiO_4]$ and pyroxenes. The KREEP rocks are crystalline highland rocks containing a chemical component rich in potassium, rare Earth elements, and/or phosphorus. Physically the highland regions are impact-shocked terrain punctuated with large boulders and rocks strewn over the relatively rough landscape. This is a heavy contrast to the smoother mare plains. The mineralogy of the highland regions has been important in discoveries of lunar formation; however, it is important to note that for many processing methods the mineralogy of highland material makes resource extraction (specifically oxygen) an expensive undertaking.

2.1.3 The lunar regolith

Beyond the initial distinction between mare and highland regions one must also recognize the difference between the lunar regolith and the region's rocks. The regolith is defined as the layer of fragmented fine grained soil covering the surface. It includes rock debris and fragments that have been pulverized from millennia of impact cratering. The entire moon, with the exception of high topography regions and rock outcroppings, is covered with a layer of fine grained regolith to varying depths. The regolith thickness on the mare is typically only a few meters with an average range of about 4-5 meters. The highland regions are estimated to be covered on average by 10-15 meters of regolith material [Heiken]. Because of the complex evolution of the regolith over billions of years the variability in the composition of regolith material can be extreme over only a few meters distance. The cratering process itself can transport material hundreds of kilometers across

the lunar surface, and over time this creates a well mixed fine-grained material. Highland region regolith material is primarily feldspathic, and mare regolith is basaltic. The regolith layers covering both highland and mare regions have been found to be compositionally similar to the bedrock composition of the region. The mean grain size of regolith soils ranges from approximately 40 microns to 800 microns. Because most resource processing systems require a fine-grained source material to maximize the efficiency of the process, the regolith layer has become a prime target for most lunar resource development ideas. The regolith also includes glassy agglutinates which turn can be extremely useful on their own for several resource processing systems.

2.2 Resources available

Lunar minerals can provide a large number of elements essential to future exploration architectures. Many studies have been conducted on utilizing lunar materials for resource extraction, and a large number of resources have been named as potential in-situ production candidates. Resources that have been studied for in-situ production include oxygen, water, lunar concrete, structural metals, and solar panels.

2.2.1 Oxygen

Oxygen is the most abundant element on the moon. It is primarily trapped in oxide minerals in high concentrations in the mare. As a resource for future exploration missions, oxygen has many uses. One major use of in-situ oxygen is for propulsion systems. Liquid oxygen is heavily used in the majority of today's rocket engines. It can also be useful for fuel cells on rovers. When considering human exploration, it can be used for breathable air

and for possible combination with hydrogen for use as water for human life support. However, it has been shown that other constraints will limit these life support issues. For example, if an atmosphere needs to be replenished for a lunar base or habitat, nitrogen would be the critical gas which is much less abundant on the moon than oxygen [Sherwood]. Fuel cells are also a very regenerative system and the oxygen losses are expected to be small. Propulsion is likely to be the most beneficial use for in-situ oxygen production.

2.2.2 Water

Water is the most important resource for any human space mission. It can be used for life support, propellant production (both H_2 and O_2), and to produce breathable air. The existence of water ice at the lunar poles has not been definitively confirmed, but even in small amounts this may be a very important resource. Although hydrogen does exist on the lunar surface due to implantation from the solar wind [Crider, 2000], it is relatively scarce on the moon and would probably have to be brought from the Earth for use in rocket engines or for the creation of water for life-support if ice deposits do not exist. Water is a very important resource for exploration because of its ease of processing and multiple uses. If sizeable quantities are discovered at the lunar poles it will greatly enhance the capabilities of future missions.

2.2.3 Concrete

When establishing a manned lunar base, creating strong structures will be a necessity. A number of different ways of creating habitats on the lunar surface have been proposed.

Many methods ranging from digging caves, to enclosing craters with a sealed dome, to bringing inflatable habitats from Earth have been analyzed, specific designs and uses of concrete are shown in the Lunar Base Handbook [Ekhart]. Lunar concrete has been studied in Earth laboratories and has been shown to be relatively inexpensive to create. This could be a valuable resource for future lunar base applications. For the production of lunar concrete, water will be required either from polar ice deposits or supplied directly from the Earth.

2.2.4 Structural Metals

Many metals are also contained in lunar minerals. Oxides have been proposed as a good source of metals for structural materials. Fairly simple reduction processes could process oxides and separate out the constituent metal phases. These metals could then be processed into usable structural materials. This same process is also a leading candidate for oxygen extraction from the lunar regolith and is discussed in further detail in following sections. Stefanescu has shown that Titanium alloys are the most well suited for use on the Moon [Stefanescu].

2.2.5 Solar panels

Solar panels are a key resource for any space mission. The amount of power required has always been a limiting factor for planetary missions. Lunar solar panel arrays have even been proposed as a means of supplying power to the Earth [Criswell]. Several studies have been conducted on the ability to produce solar arrays in-situ on the lunar surface. It is possible to create low efficiency solar cells from lunar highland materials with a somewhat

complex processing system. The majority of the studies that have analyzed solar panel production have done so assuming that humans would be available on the surface to monitor this production system. However, Michael Duke has proposed a robotic lunar crawler system that could create large solar arrays automatically in preparation for a human presence [Duke]. This ability to produce power capability in-situ could be another key architecture for future lunar exploration.

3. Oxygen Production Methods

Oxygen is going to be a key resource for any lunar mission. Robotic missions could use oxygen to re-supply depleted propellant reserves, while human missions will require oxygen for life support as well. Given the large amount of oxygen on the moon and its high potential benefit for future missions, much research has been conducted on in-situ oxygen production. There are over twenty methods that have been proposed. Many involve advanced concepts and will require a large number of technological advances before they become feasible for lunar production systems. The proposed processes can be grouped into several categories: Solid/gas interactions, silicate/oxide melts, pyrolysis, and aqueous dissolution [Taylor]. Solid gas interactions involve fluxing a gas through a solid feedstock sample, usually at high temperatures, to reduce the sample and release oxygen. Silicate/oxide melt reactions involve heating the lunar silicates and oxides to a molten state and using electrolysis or pyrochemical techniques to recover oxygen. Pyrolysis is the application of heat to induce a chemical change in the process feedstock. This change will

usually take the form of a partial decomposition of oxides and the vaporization of the associated oxygen, which can then be collected. Aqueous dissolution processes involve taking the feedstock and dissolving it in an aqueous acid. This produces several bi-products through complicated processing steps. One of these products is water, which is then electrolyzed to obtain oxygen. A majority of the proposed oxygen extraction processes are very complicated and will not be ready for actual lunar missions in the near future. However, there are several processes which have been studied in greater detail and which do not have major technological leaps to overcome before they are ready for a lunar mission. The more developed methods are discussed below.

3.1 Ice extraction

Data provided by Clementine and Lunar Prospector has excited many scientists about the prospect of water on the lunar surface. Water itself is a very useful resource, as mentioned above; however, it is also a readily accessible source of oxygen. Water is relatively easily electrolyzed into its constituent hydrogen and oxygen gases. Both gases have their uses on the moon. Obtaining oxygen from lunar ice deposits is very beneficial, because it will require a fairly low amount of power for the extraction process. The quantity of ice estimated to be in the south pole cold traps by Feldman et al is 1.35×10^8 metric tons. This amount is spread out over approximately 2250 square kilometers in the south-pole with a concentration of 1.5 +/- 0.8wt%. In order to gain a sizeable amount of water or oxygen from this source a large amount of regolith must be processed. There are several other limitations to using polar ice deposits as an oxygen source. First, any mission using this resource will be limited to the polar regions. If a lunar base is reliant upon this source for

oxygen it will need to be placed close to the lunar poles or have a system for transporting polar material to equatorial regions. The fact that this material is in permanent shadow places thermal and power constraints on any extraction system and the mission as a whole.

3.2 Hydrothermal regolith reduction

This simplest chemical method of extracting oxygen from the lunar regolith is to use hydrogen as a reducing agent. Hydrogen reduction of lunar materials has only two processing steps. First, oxides in the regolith are reduced by the hydrogen to produce a metal bi-product slag and water. Iron oxide is the most easily reduced mineral oxide in the lunar regolith. The activation energy for this reaction to occur requires processing temperatures above approximately 800 degrees centigrade. However, experiments have shown that if the temperature of the reaction chamber reaches above 1050 degrees centigrade the lunar regolith begins to sinter. This effectively blocks the hydrogen flow from reaching a portion of the available oxygen and thereby lowers the total oxygen yield of the system [Chambers]. The primary chemical reaction for this process is:



Other in reality other oxides are also substituted for iron oxide in this equation, but in a lesser amount. The water produced from the reduction of the oxides is then electrolyzed into hydrogen and oxygen gases. The hydrogen gas can be recycled back into the system, and the oxygen can then be utilized for propulsion or life-support systems as it is required. Iron oxide is not found as a mineral phase itself in lunar materials. It is primarily found in

the mineral Ilmenite (FeTiO_3). Other mineral phases are reduced to a lesser extent by hydrogen, yet they can add significantly to the overall oxygen yield of the system. These phases include primarily olivines [$(\text{Mg,Fe})_2\text{SiO}_4$] and pyroxenes [$(\text{Ca,Mg,Fe})\text{SiO}_3$]. Suboxide reduction of titanium phases in ilmenite has also been shown to add to the total oxygen yield [Allen]. The mare contain the highest concentrations of ilmenite and pyroxene. Ilmenite concentrations vary widely between high-Titanium mare basalts and low-titanium basalts. At the high end the ilmenite content can reach above 20 wt%. A stoichiometric yield from ilmenite releases 10.5 wt% oxygen from the sample; using a bulk regolith could produce an oxygen yield of 2.1 wt%, assuming only the iron oxide in ilmenite is reduced. Experiments conducted by Allen have shown that total oxygen yield is highly correlated with the initial FeO content of the feedstock. Experiments were conducted on regolith basalts, regolith soils, and pyroclastic glasses. Soil samples were found to release 1.2 to 3.6 wt% oxygen, with higher oxygen yields being derived from high FeO content feedstocks. Pyroclastic glass samples released even higher yields of oxygen, 4.3-4.7 wt%. Therefore, Allen concluded that oxides other than FeO must contribute significantly to the total oxygen yield, but that the yield is still highly correlated to initial iron content [Allen]. At these concentrations, both bulk lunar regolith and pyroclastic glasses can be considered prime targets for an oxygen production facility using a hydrogen reduction system. The ability to use bulk regolith eliminates the potentially massive and costly beneficiation system. For this reason and the simplicity of the process, this study analyzes the possible benefit of the hydrogen reduction system for future lunar exploration architectures. Ogiwara studied the hydrothermal reduction process on lunar simulants

showing similar results to those found by Allen [Ogiwara]. In these experiments, Ogiwara noted that the grain size is a key factor controlling the rate of the reaction.

3.3 Carbothermal regolith reduction

Another method of releasing oxygen from lunar materials is by Carbothermal reduction.

The basis behind this process is similar to the hydrothermal system, but instead of using hydrogen as the reducing agent, a carbon compound is employed. Several different carbon compounds have been studied for this system, with carbon monoxide and methane as the leading candidates. Zhao and Shadman have conducted laboratory experiments on ilmenite reduction with both hydrogen and carbon monoxide. They concluded that the reduction rate using hydrogen was faster than using carbon monoxide for pure ilmenite feedstocks [Zhao]. Dr. Eric Rice and the Orbitec corporation have done extensive research on the reduction of lunar materials with methane [Rice]. Rosenberg has designed several large scale production plants using the carbothermal reduction method for future lunar base uses [Rosenberg].

This system has three major processing steps: reduction of oxides and silicates with methane, the hydrogenation of carbon monoxide, and the electrolysis of water. As with the hydrothermal system, oxide phases in the lunar regolith will be most easily reduced.

However, carbothermal reduction will also readily reduce some silicate phases. The highest yield lunar mineral estimated for this process is olivine, but other silicate phases such as pyroxenes should work equally well. This means that bulk regolith can also be used to achieve a high oxygen yield. The maximum yield expected from the carbothermal reduction of bulk regolith is closer to 20 wt%, which is significantly higher than the yield for hydrothermal reduction. Unfortunately, this benefit in oxygen yield comes at the

expense of system complexity and power requirements. The operating temperatures for the carbothermal process are between 1600-1800 degrees centigrade – much higher than the temperatures required for the hydrothermal process. The added processing steps, power requirements, and complexity make carbothermal reduction less desirable for an early stage of lunar exploration. As more lunar missions are conducted and larger architectures set in place, carbothermal reduction may well be the oxygen production process of choice; however, in this early stage of exploration the simplest process is deemed the most beneficial and is therefore the reason that the carbothermal system is not being analyzed for this study.

4. Lunar Exploration Architectures

Over the next several decades, understanding how to optimize lunar exploration architectures will become increasingly important. Before any human missions are even planned, many robotic explorers will be required to gain further scientific data, allowing space agencies to better prepare future human missions. There are two major planetary mission types: orbiters and landers. Orbiting missions can conduct many experiments and gather large amounts of data; however, they are limited in their resolution and in the types of experiments that they can conduct. In order to gain detailed scientific knowledge about the surface, and to understand the lunar environment to the degree needed to properly support human missions, robotic landers will be required. The more sites that can be explored robotically, the better the data set will be to characterize the lunar surface and to

choose future human landing sites. There are three methods of exploration in which multiple landing sites can be explored: sending multiple missions from the Earth, sending one fully fueled mission capable of launching itself to multiple sites, and sending one mission with a processing plant to produce the required propellant to launch itself to the desired sites.

4.1 Multiple mission architecture

In the first mission architecture, each site would be visited by a completely separate spacecraft. These missions would all have their own payload of instruments and equipment necessary to land on the lunar surface. This is how all missions to date have been conducted. The Viking missions to Mars, the Surveyor missions to the moon, and the recent Mars Exploration Rovers are all examples of the multiple mission exploration architecture. In each case, an entire spacecraft is launched from the Earth for each landing site to be visited. Usually the spacecrafts have the same or similar designs for easy data comparisons between sites. For the remainder of this study this method will be termed the “multiple mission architecture”. If the mission contains a rover, a larger area can be explored, limited by rover mobility and mission life.

4.2 Fully fueled architecture

One mission can be launched from the Earth and sent to the first landing site with all the propellant necessary to launch itself to a number of landing sites. In this system, there is only one payload of scientific instruments being launched. This may, in some sense, limit the amount of scientific return from the mission because new or different instruments

cannot be used for each landing site, and the missions cannot utilize improvements from the knowledge gained by each mission. However, if these missions are being sent as precursors to human missions, significant technological advances in scientific instrumentation is unlikely to occur over the time frame between missions. The fact that the same instruments are often employed on each mission of a multiple mission architecture can be used to conclude that there is not a significant scientific loss by utilizing a fully fueled architecture. The benefit of the fully fueled architecture is that the landing stage and payload mass (including everything but the propulsion system) only has to be launched from the Earth once to visit multiple sites. This method of exploration is called the “fully fueled architecture.”

4.3 Processing plant architecture

The third method of surface exploration is to land one spacecraft at the first desired site with a processing plant capable of producing the oxygen required to launch itself to the next site. At each site the mission will remain long enough to both explore the surface and refuel by processing in-situ resources. Then the craft will launch itself to the next site. Scientific constraints similar to those seen with the fully fueled architecture apply here. The difference between this and the fully fueled system is in the mass of the total propellant needed for the fueled system versus the mass of the production plant.

Hydrogen deposited by the solar wind is accessible in very small quantities over the entire lunar surface. It is estimated that the equatorial regions contain solar wind implanted hydrogen on the order of 50 ppm [Feldman, Crider]. In another study, Bustin estimated

lunar hydrogen content to be between 0.01 and 0.06 grams per kilogram of regolith depending upon the maturity of the soil. The more mature the soil, the longer it has been exposed to the solar wind and therefore the more hydrogen has been implanted [Mendell].

Architecture Type	Pros	Cons
Multiple Mission	<ol style="list-style-type: none"> 1. Use of different or improved instruments for each mission. 2. System robustness- if one fails still have others that can reach different sites. 3. Global access- can reach landing sites anywhere on the lunar surface. 	<ol style="list-style-type: none"> 1. Large launch cost from the Earth. 2. Must launch total craft mass multiple times.
Fully Fueled	<ol style="list-style-type: none"> 1. Potential mass savings by launching only one craft from the Earth. 	<ol style="list-style-type: none"> 1. Limited to one instrument set for all landing sites. 2. Range and number of sites is limited by amount of propellant it can carry. 3. Not a robust architecture- If the mission fails, all sites are lost. 4. Long lifetime requirement to visit multiple sites.
Processing Plant	<ol style="list-style-type: none"> 1. Potential mass savings by launching only one craft from the Earth. 2. Can demonstrate a new exploration technology while at the same time enhancing the exploration potential of the mission. 	<ol style="list-style-type: none"> 1. Limited to one instrument set for all landing sites. 2. Limited by amount of hydrogen it can carry. 3. Limited by amount of oxygen it can produce. 3. Not a robust architecture- If the mission fails, all sites are lost. 4. Long lifetime requirement to visit multiple sites.

Table 1: Architecture pros and cons

At these low levels of hydrogen abundance, a production plant would need to process between 10 and 180 cubic meters of regolith to yield enough hydrogen to launch a MER sized craft of only 200kg over a distance of just 1 kilometer. At the lunar poles, ice deposits

may make in-situ hydrogen production more feasible; however, because of the low equatorial hydrogen content, the production of hydrogen in-situ is not being considered as an option for this architecture. All the hydrogen for the lunar launches will be carried with the spacecraft from the Earth and only oxygen will be produced in-situ. Therefore, the mission will be limited by the mass of hydrogen that it can carry. This third method of exploration is called the “production plant architecture” for the remainder of this study. Table 1 lists a summary of each architecture’s overall pros and cons.

The fully fueled and processing plant architectures have several associated cons that the multiple mission architecture does not. A quantitative analysis of the lifetime of such systems cannot be conducted because there is no data concerning the development of these architectures. The focus of this study is on the pros and cons created by the total mass differences between the architectures – a con for the multiple mission architecture and a pro for the fully fueled and processing plant architectures.

5. Model Development and Analysis Methods

A model is developed to analyze the three exploration architectures. The goal is to better understand which architecture is most beneficial (lowest cost) for various sets of mission parameters, and to determine the conditions under which the processing plant architecture is a feasible method of lunar exploration. This architecture takes a technology which has yet to be demonstrated in space and calculates how it can be used to enhance lunar

exploration capabilities. A simple demonstration mission could be conducted initially to prove the technology; however, this model is designed to develop and analyze a mission so that it not only demonstrates the technology, but also creates a significant exploration mission with large scientific gains.

The systems unique to the processing plant architecture are modeled to the highest level of detail, while general systems such as structure and communications are not modeled at all. Through this model the effect of each system parameter on the overall benefit of each architecture is characterized. There are both scientific and engineering concerns that need to be considered when attempting to determine the best designs for future missions.

Scientific concerns, such as instrument design choices and data transfer are not accounted for in this model. Only the scientific data affecting the processing yield is of concern. The number of sites visited, and therefore the total scientific data gathered, is modeled by simply assuming that at each site the spacecraft will provide the same scientific data as at all previous sites. The more sites visited, the better the scientific return.

The mass of all the systems besides processing and propulsion are combined into one general payload value which is used as an input to the model. The total system mass required to land that payload on the lunar surface is then calculated for each architecture. A generic lunar transit stage is considered applicable for all missions. Therefore, an estimate of the benefit of one architecture over another is determined based upon the total system mass in lunar orbit. The architecture with the minimal lunar orbit mass is considered to be the most beneficial.

5.1 Model parameters

There are a large number of parameters, each affecting several others in the model.

Because the total benefit of any architecture over another is determined by its total mass, the model focuses on how the mass of each component flows through the system. Several initial parameters control values that affect the mass of one or more components. For each run the model iterates all values until the total system mass in orbit converges to a change of less than 0.001 kg per iteration. Table 2 lists the parameters of importance to the model.

A total of nine input parameters can be varied to study the feasibility of the processing architecture and to compare it against the other mission types. These variables are: initial payload mass, lunar launch range, number of launches, feedstock water content, feedstock type, batch processing time, processing temperature, pre-heating time, and total processing time. Only the number of launches and the initial payload mass affect the multiple mission architecture. The more launches the processing plant can achieve, the more landing sites the multiple mission architecture must send spacecraft to for an equivalent exploration return. There are a total of three input variables that affect the fully fueled system: launch range, number of launches, and payload mass. All nine input parameters are essential for evaluating the processing plant system. For simplicity of comparison, the initial payload mass is limited to two values: 200kg and 1000kg. A 200 kilogram payload is suggestive of a MER sized lander, while a 1000kg is closer to a Viking style mission. Lunar launch range is analyzed for values up to 2000km. This value is chosen as an upper limit based upon the fact that this range will nearly complete a launch from the lunar pole to equator.

Parameter Name	Model Value	Description
Payload Mass	200 or 1000kg	The mass of the general mission systems: includes everything not in the propellant, tank, or processing systems
Lunar launch range	1-2000km	Distance between lunar landing sites
Number of launches	1-20	Number of launches that the fully fueled and processing plant are designed to achieve. Equal to the number of sites visited minus one for the multiple mission
Water content	0.7-2.3wt%	How much water is contained in the polar regolith, equal to zero for equatorial regolith
Feedstock type	Highland, Mare, Glassy	One of three major feedstock distinctions for an input to the processing system
=Batch time	1 or 3 hrs	Time to process one batch of regolith, multiple batches are used to produce the total oxygen to launch to the next site
Processing temperature	900C or 1050C	Temperature at which the processing furnace is held during reduction
Heating time	(0-10hrs)	Length of time to preheat the regolith feedstock before reduction begins
Total processing time	500 or 1000hrs	Total time allowed for all batches to produce oxygen required to launch to next site
Lunar Delta V	2200 m/s	Delta V to go from lunar orbit to a softlanding on the lunar surface
Propellant Isp	450 sec	Isp of the hydrogen/oxygen propellant system
Heat energy	HL: 3267 kJ/kg; Mare: 3262 kJ/kg; Glassy: 3365 kJ/kg	The amount of energy it takes to heat the feedstock up to the processing temperature
Power loss function	10%	How much thermal energy is lost due to radiation through the furnace walls
RTG power density	250W per 1.44kg	Amount of power produced per kilogram of RTG
Propellant mass fraction	Dependant variable	Fractional mass required to launch a total mass to a certain distance
Oxygen yield	dependant variable	The weight percentage of oxygen that can be taken out of the regolith feedstock
Spacecraft orbital mass	output value	Total mass of the spacecraft in lunar orbit
Spacecraft landed mass	output value	Total mass of the spacecraft once initial landing has occurred
Landing H2	output value	Hydrogen mass needed to land total spacecraft mass
Landing O2	output value	Oxygen mass needed to land total spacecraft mass
Launch H2	output value	Hydrogen mass needed to launch total craft to next site
Launch O2	output value	Oxygen mass needed to launch total craft to next site
O2 tank mass	output value	Mass of oxygen storage tank
H2 tank mass	output value	Mass of hydrogen storage tank
Total regolith volume	output value	Volume of regolith that needs to be processed to produce the oxygen required for launch
Total regolith mass	output value	Mass of regolith needed to be processed to produce oxygen required for launch
number of batches	output value	Total number of batches run per launch cycle.
batch regolith volume	output value	The volume of the regolith that must be processed each batch
batch regolith mass	output value	The mass of the regolith that must be processed each batch
Furnace volume	output value	Size of the furnace to hold the given amount of regolith
Furnace mass	output value	Mass of the furnace to hold the given amount of regolith
Reduction power	output value	Maximum power required to conduct the regolith reduction process
Electrolysis power	output value	Maximum power required to electrolyze the water produced from the reduction process
RTG mass	output value	Total mass of the RTG power system to provide power to reduction and electrolysis systems

Table 2: List of model parameters, with values and descriptions. Input parameters and constants are given with their possible values listed. Output parameters of the model are listed as outputs.

The number of launches that the processing plant mission can conduct is varied between 1 and 20 launches. It is to be expected that any actual mission employing a multiple launch system will undergo some range of degradation over time. The extent of this degradation has not been modeled but it can be expected that large launch number values will be physically unreasonable based upon sheer time limitations. The exact number of launches any mission is capable of cannot yet be quantified. The regolith water content is held to the high and low values of 0.7 to 2.3wt% suggested by Feldman [Feldman]. The processing plant mission architecture could be extremely different between equatorial regions with no water content and polar regions with ice contained in the soils. The term “equatorial” is used for any 0% water content soil outside the polar cold traps. The choice of feedstock is limited to either highland, mare, or glassy type regoliths. Several generalities are created when using three broad categories to estimate all possible feedstock types. However, because of the lack of detailed compositional knowledge of the entire lunar surface and the large differences between these three feedstocks, this general separation serves as a good estimate for yield values expected from the processing system. Batch time values are limited to either 1 or 3 hours. Laboratory experiments have shown that after the first hour of processing the majority of the available oxygen is already reduced. After three hours the reduction process is considered to be complete [Allen]. The exact time of a complete sample reduction will vary based upon grain size, and other physical properties of the feedstock. These variations are assumed to be small. It is estimated that any mission will be able to select feedstocks so that the variation in regolith properties is a minimum. With this assumption the oxygen yield will not vary significantly within any of the three categories of feedstocks. Above 1050C the regolith begins to sinter, causing a reduction in oxygen

yield. Below 900C the reaction proceeds at a significantly slower rate [Mckay]. For this reason, values of 900C and 1050C were chosen as high and low end process temperatures. The pre-heating time is separate from the batch processing time because the regolith is heated before the hydrogen is released to begin the reaction. The total processing time is the amount of time for all the batches to be completed so that the proper amount of oxygen for the next launch is provided within this time.

5.2 Model design and assumptions

To create this model it is necessary to make some assumptions due to insufficient knowledge about the processing apparatus. These assumptions lessen the complexity of the modeled system to a level that can be analyzed with the current state of knowledge of each system. Initial assumptions are made concerning the launch capability from the Earth and transit stage to the moon. The model for all three architectures begins with an initial payload mass in lunar orbit and iterates the mass of each system from there based upon the parameter values supplied. This payload mass includes many system masses that would vary based upon the size of the processing system or the amount of propellant, such as the mass of the support structures to hold the spacecraft together throughout its lifetime. However, this model does not incorporate these systems designs for analysis. Assumptions about the detailed kinetic properties of the reaction are also included in this model. It is assumed that each regolith reduction reaction will proceed with the same kinetics as were found in Allen's laboratory experiments [Allen]. One process required to produce the oxygen in a form usable as a propellant is the oxygen liquification system. This system is not modeled in this study. The mass of the liquification system is assumed to be built into

the initial payload mass. In Orbitec’s study on carbothermal oxygen production the liquification system was approximately ½ the size of the oxygen storage tank [Rice]. However, this system is not easily scalable and is therefore left as an assumed constant mass included in the payload.

5.2.1 Multiple mission architecture design

The design of the multiple mission architecture is very simple. The initial payload mass is taken as an input value. In this system, the payload mass includes everything except for the propellant and tank masses. The propellant mass – both hydrogen and oxygen – required to land the initial payload mass on the lunar surface is calculated from the propellant Isp and lunar delta V requirement. Tank masses to hold the required liquefied hydrogen and oxygen are then calculated from Orbitec’s work on a carbothermal oxygen production system. A spherical tank is utilized to optimize the volume to tank wall mass ratio. The mass per unit area of the tank wall is calculated from Orbitec’s study to be 8g/cm². The density of oxygen within the tank is approximately 9 metric tons per cubic meter [Rice]. These values are then used to calculate the mass of the tanks required for different hydrogen and oxygen masses. Equation 2 shows the calculation for the tank masses. One assumption in this system is that the hydrogen and oxygen tank densities are the same.

$$M_{\text{tank}} = 4\pi * [3/(4\pi) * M_{\text{prop}} / \rho_{\text{prop}}]^{2/3} * \rho_{\text{A(tank)}} \quad (2)$$

In this equation M_{prop} is the mass of the propellant (either hydrogen or oxygen), ρ_{prop} is the density of the propellant (9mt/m³), and $\rho_{\text{A(tank)}}$ is the surface area density of the tank (8g/cm²). Finally the tank masses and propellant masses are added on to the initial payload

mass. The orbiting spacecraft mass is then given the new payload mass which is the old payload mass plus the propellant and tank masses. The propellant and tank masses must then be recalculated using this new payload mass in an iteration process, which is repeated until the masses converge to less than a 0.001 kg change. The equation below describes the iteration process:

$$\mathbf{M}_{\text{mission}(i+1)} = \mathbf{M}_{\text{mission}(i)} + \delta\mathbf{M}_{\text{PL}} \quad (3)$$

where $\mathbf{M}_{\text{mission}(0)}$ is equal to the initial payload mass and,

$$\delta\mathbf{M}_{\text{PL}} = \mathbf{M}_{\text{OxTank}} + \mathbf{M}_{\text{Htank}} + \mathbf{M}_{\text{H,landing}} + \mathbf{M}_{\text{Ox,landing}}$$

The mass of the oxygen tank, $\mathbf{M}_{\text{OxTank}}$, and the mass of the hydrogen tank, $\mathbf{M}_{\text{Htank}}$, are both functions of the mass of oxygen and hydrogen respectively.

To obtain the total mass of this architecture, the mass of an individual mission is multiplied by the number of sites that are to be explored. In order to compare this with the other architectures, the number of sites explored is the same as the number of launches plus one for the other architectures. A flowchart of the multiple mission architecture is shown in figure 1.

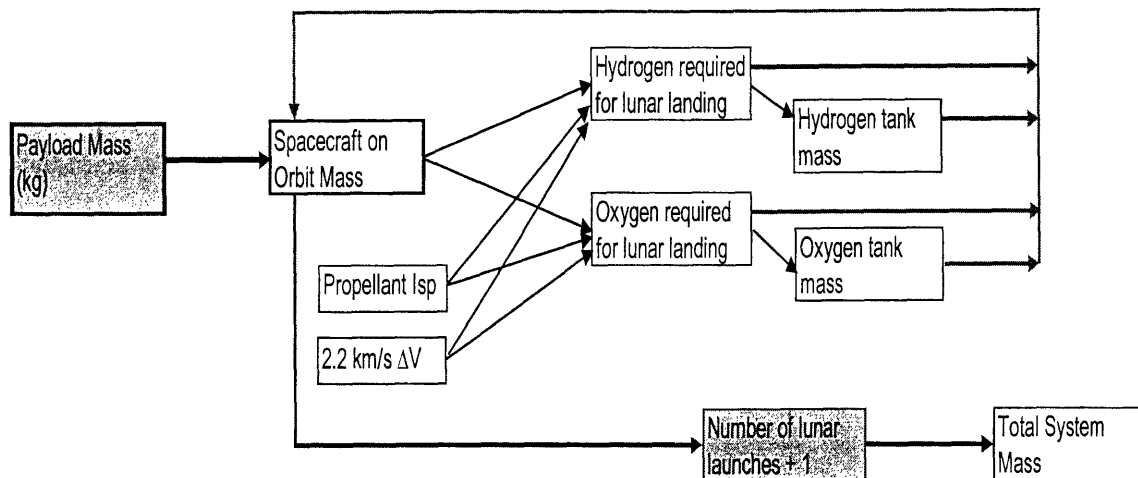


Figure 1: Multiple mission architecture flowchart.

The input parameters of importance for this architecture are shown in the grey boxes. It should be noted that only two of the nine input parameters modeled affect the outcome of this system.

5.2.2 Fully fueled architecture design

The fully fueled architecture starts again with an initial payload mass including everything but the propellant and tank masses. However, unlike the multiple mission system the total propellant now includes the hydrogen and oxygen needed for each lunar launch as well as for the initial landing. A distinction must be made between the orbital craft mass and the landed craft mass. The orbital mass includes everything, while the landed craft mass does not include the propellant required for the initial landing, because it has already been used. To calculate the amount of propellant required for each subsequent launch, the landed craft

mass is used; however, it is the orbital mass that is important for the benefit analysis. The amounts of hydrogen and oxygen required for the initial landing are calculated in the same manner as in the multiple mission architecture. To begin the model both the orbital mass and the landed mass are given the value of the payload mass. The propellant for the initial lunar landing and for all launches is then calculated. This propellant mass and the tank masses are added to the initial payload mass and then recalculated. This iteration process is again described by equation 3. However, for the fully fueled architecture,

$$\delta M_{PL} = M_{H,land} + M_{Ox,land} + \sum M_{H,launch} + \sum M_{Ox,launch} + M_{Htank} + M_{OxTank}$$

where the oxygen tank mass and hydrogen tank mass are now functions of both the respective propellant component required for the initial lunar landing, and the propellant for all the lunar launches.

$$M_{OxTank} = M_{OxTank} (M_{Ox,land} + \sum M_{Ox,launch})$$

$$M_{Htank} = M_{Htank} (M_{H,land} + \sum M_{H,launch})$$

Calculating the propellant for each launch is more complicated than calculating the propellant for the initial landing because after each launch the total craft has a little less mass due to the propellant that was used up on the previous launch. Launch propellants are calculated using the propellant mass fraction which is derived from the equation:

$$m_f = 1 - \text{EXP}(-(\text{SQRT}(\text{Range} * 1000 * G_{\text{moon}}) / (\text{Isp} * G_{\text{earth}}))) \quad (4)$$

This accounts for the ΔV needed both to launch the spacecraft into a parabolic trajectory and then to make a soft landing at the next exploration site. The mass of the propellant is calculated by taking the launch mass and multiplying it by the propellant mass fraction. The propellant needed to launch to the last site can be significantly less than the propellant required to launch to the first site. This is taken into account in the model by calculating the propellant masses for each launch individually. At each subsequent iteration, new propellant masses for all launches are calculated. The equation for the propellant of each launch is:

$$P_i = (M_c + \sum P_{i+N}) * m_f \quad (5)$$

where P_i is the propellant of that launch, M_c is the spacecraft mass, and m_f is the propellant mass fraction. The sum in this equation is over N , ranging 1 to the number of launches minus 1. So the highest P_i will be calculated with the mass of the spacecraft plus the mass of all the launches. Therefore, if there are a total of three launches, P_3 is the mass of propellant for the first launch, and P_1 is the mass of propellant for the last launch. In this manner the propellant of each successive launch is calculated taking into account the mass lost due to previous launches. To calculate the total propellant required for all launches the P_i 's must be summed. At each iteration equation 5 is used to recalculate the propellants required for all the launches. The total propellant for all the launches and for the initial landing are combined to calculate the hydrogen and oxygen storage tank masses. The tank masses are calculated the same way as in the multiple mission architecture.

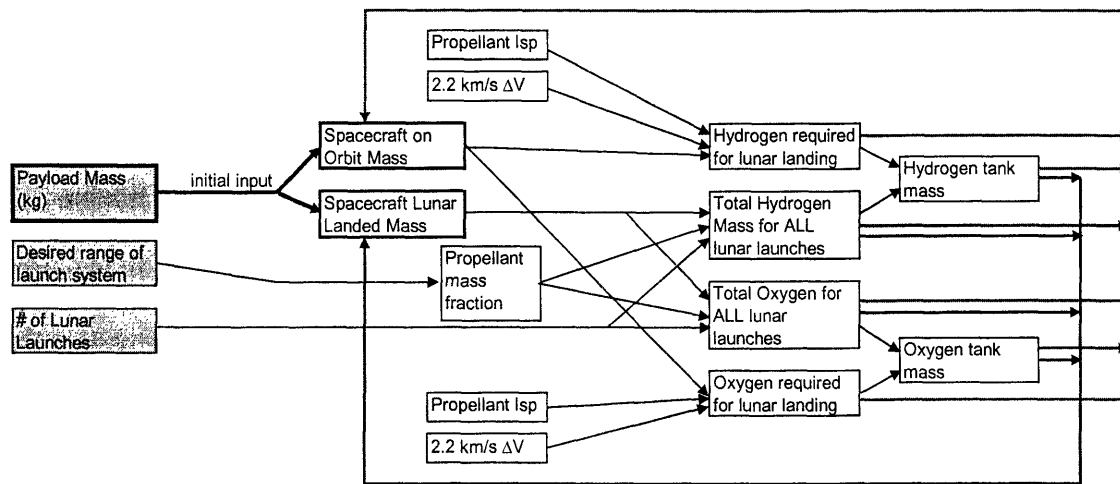


Figure 2: Fully fueled architecture flowchart. Input parameters are shown in the grey boxes on the left.

These four masses – hydrogen, oxygen, hydrogen tank, and oxygen tank – are added to the landed and orbital mass values appropriately, and the system is then iterated until convergence is achieved. A diagram of the fully fueled architecture is presented in figure 2. Again the input parameters of importance are shown in grey boxes. All other boxes show variables that result from a combination of these input parameters and the calculations mentioned above.

5.2.3 Processing plant architecture design

The processing plant architecture model is more complicated than the previous two architectures because of the added processing system details. An initial payload mass is again the starting point in which all scientific, structural, and other masses not associated with the processing and propellant systems are included. Because of the larger number of

variables affecting the overall output of the processing plant model there are many more interactions to be considered. A flowchart of these interactions is shown in figure 3. The nine input parameters are displayed in grey on the left of the figure. It can immediately be seen that most of the input parameters have multiple affects on the overall system. For this reason it is hard to intuitively analyze the behavior of the system. The model is initiated by setting the input parameters to the desired values, and taking the payload mass as the starting point for the orbital and landed spacecraft masses.

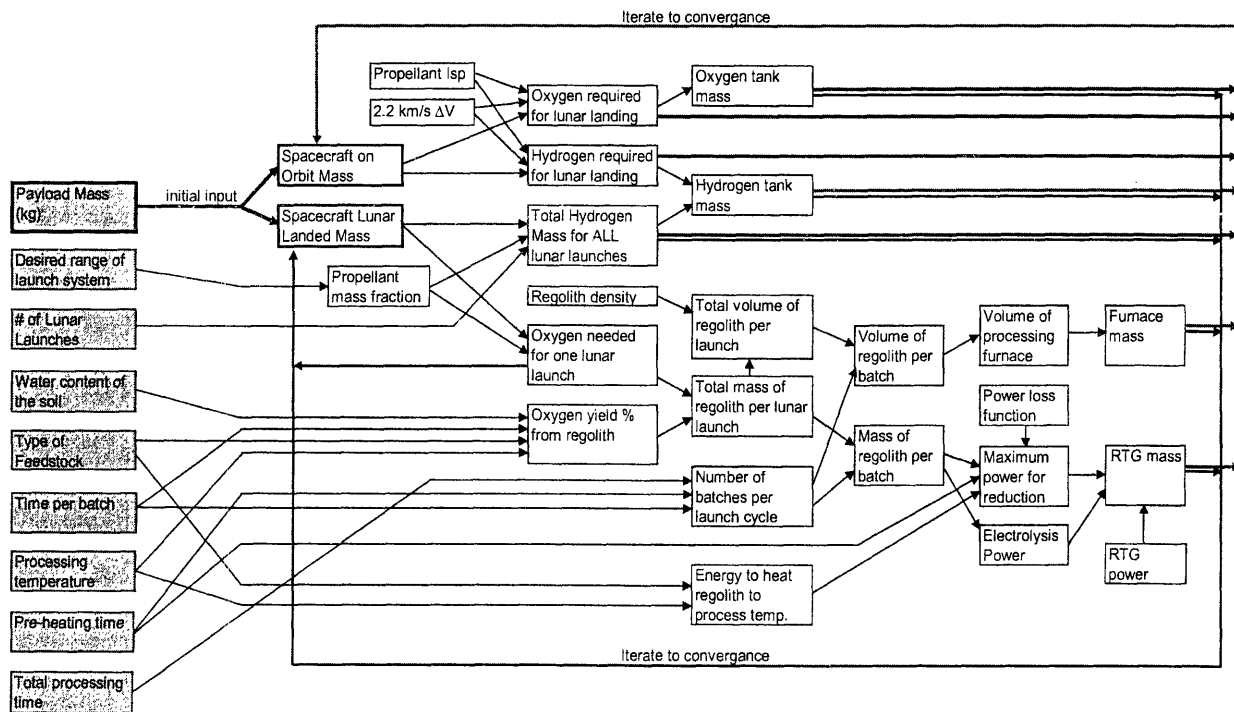


Figure 3: Processing plant architecture flowchart. This flowchart shows the nine input parameters in grey on the left and their affect on the various aspects of the processing plant system.

The total on orbit mass is then iterated by adding each component's mass, calculated as described in equation 3 above. For the processing plant mission, the change in the initial

payload mass after each iteration, δM_{PL} , is slightly more complicated than in the other architectures. This is shown the equation 6,

$$\delta M_{PL} = M_{H,land} + M_{Ox,land} + \sum M_{H,launch} + M_{Htank} + M_{OxTank} + M_f + M_{RTG} \quad (6)$$

where the hydrogen tank, M_{Htank} , is a function of both the hydrogen required for the initial lunar landing and the sum of the hydrogen masses required for each lunar launch; however, the oxygen tank, M_{OxTank} , is just a function of the oxygen required for the initial lunar landing. The furnace mass, M_f , is a function of the size of the batch, which is a function of the total amount of regolith required and the number of batches. The total amount of regolith required comes from the oxygen required for the first lunar launch and the oxygen yield percent of the feedstock in use. Ultimately the furnace mass can be said to be a function of the launch range because the amount of oxygen required for the first lunar launch depends only upon the launch range. The RTG mass, M_{RTG} , is also a function of the oxygen required for the first lunar launch and therefore the launch range as well as the input processing system parameter values. Which parameters affect each of these masses is shown in figure 3 above.

5.2.3.1 Propellant and tank calculations

The propellant required for the initial landing is calculated from the spacecraft orbital mass as mentioned for the previous two architectures. Because this architecture produces all the oxygen needed for the lunar launches in-situ, the oxygen tank mass is not a function of the oxygen mass for the lunar launches, and therefore will be sized only from the oxygen

required for the initial landing. It can be assumed that the amount of oxygen required to land the spacecraft from orbit will be significantly more than that needed for subsequent launches and landings. Therefore, the launch oxygen mass will not require another tank. The oxygen needed for a each lunar launch is dependant on the mass of the craft and the launch range. However, instead of being a factor for the tank mass, it is now taken as an input into the processing section of the model.

Hydrogen on the other hand is not being produced in-situ from the regolith, so the spacecraft must carry enough hydrogen in its tank for the initial landing and all launches. The landing hydrogen is simply calculated from the propellant Isp and the ΔV for landing as mentioned in equation 4. The hydrogen required for each launch is again dependant upon the mass of the vehicle and the range of the launch as in the fully fueled architecture described above. Each successive launch will require slightly less hydrogen than the previous one because of the mass lost in the spent fuel. This difference in hydrogen required for successive launches is incorporated into the model through equation 5. The hydrogen tank mass can then be calculated from the total hydrogen of all the launches and the initial landing.

5.2.3.2 Oxygen yield

The oxygen yield of the processing system is a key value that depends upon four of the initial input parameters: water content, type of feedstock, batch processing time, and processing temperature. The water content of the soil can add significantly to the total oxygen yield. Oxygen from the water content does not take the full processing energy to be

released. Simply heating the regolith above the ambient temperature of the permanently shadowed craters will release the water from the soil. However, if oxygen from the reduction of the regolith is still required to produce the desired amount of oxygen for the launch then the regolith will still need to be heated for the reduction process. The type of feedstock has a large impact on the amount of oxygen yield achievable. Highland soils have a relatively low iron content as was previously mentioned. This means a lower oxygen yield than either the mare soils or glassy type soil. The batch processing time affects the oxygen yield in that longer batches increase the amount of oxygen released from the soil. However, Allen found that after approximately three hours the majority of the oxygen had been released. The processing temperature does not have a strong affect on the oxygen yield of the mare or highland soils; however, it is noted by McKay that glassy soils have a highly temperature dependant oxygen yield [McKay].

Table 3 shows the oxygen yield values used in this model for each combination of these four input variables. In the polar regions there may be some small deposits of glassy or mare material from impacts; however, both the north and south poles are primarily composed of highland material. For this reason one should not expect to utilize mare or glassy soils with any water content. Because of the increased amount of water ice, it can be expected that another system architecture designed to supply all the required oxygen from the ice deposits could be more beneficial in the polar regions than the processing plant architecture. Such an architecture is discussed, but not modeled in detail in this study.

Type of Feedstock	Water content weight%	Batch processing time(hr)	Temperature (deg C)	Oxygen Yield %
Highland	0%	1	1050	0.8
			900	0.8
		3	1050	1.2
			900	1.2
	0.70%	1	1050	1.5
			900	1.5
		3	1050	1.9
			900	1.9
	2.30%	1	1050	3.1
			900	3.1
		3	1050	3.5
			900	3.5
Mare	0%	1	1050	3.0
			900	3.0
		3	1050	3.6
			900	3.6
	0.70%	1	1050	3.7
			900	3.7
		3	1050	4.3
			900	4.3
	2.30%	1	1050	5.3
			900	5.3
		3	1050	5.9
			900	5.9
Glassy	0%	1	1050	3.6
			900	1.8
		3	1050	4.3
			900	2.0
	0.70%	1	1050	4.3
			900	2.5
		3	1050	5.0
			900	2.7
	2.30%	1	1050	5.9
			900	4.1
		3	1050	6.6
			900	4.3

Table 3: Oxygen yields. This table lists the expected oxygen yield for all combinations of important parameters as found by Allen.

5.2.3.3 *Regolith and Batch conversions*

The oxygen required for a lunar launch is divided by the oxygen yield achieved under the given parameter values to calculate the total mass of regolith that must be processed in order to obtain the oxygen. The regolith mass is converted into a volume amount by using 1.75 g/cm^3 as the regolith density. Taking the total mass and volume of regolith, the model calculates the mass and volume of each batch by dividing the totals by the number of batches. The number of batches per launch cycle is dependant upon three input parameters: the total processing time, the pre-heating time, and the time per batch. Increasing the total processing time increases the number of batches. Conversely, increasing either the pre-heating time or the batch processing time decreases the total number of batches for a launch. The equation for calculating the number of batches per launch cycle is:

$$N_{\text{batch}} = T_{\text{total}} / (T_{\text{preheating}} + T_{\text{batch}}) \quad (7)$$

This then yields the equation for the batch volume and mass to be:

$$[V_{\text{batch}}, M_{\text{batch}}] = [V_{\text{tot}}, M_{\text{tot}}] / N_{\text{batch}} \quad (8)$$

5.2.3.4 *Furnace calculations*

The batch volume is used to calculate the size of the processing furnace. Orbitec Corp utilized a graphite and fire brick furnace for a carbothermal reduction system [Rice]. Many hydrogen reduction furnaces in laboratories on Earth are created from an Inconel alloy which was also employed in laboratory tests on lunar simulant soils by Ogiwara [Ogiwara]. For this model the furnace design from the Orbitec carbothermal study is utilized. A

spherical furnace design is used to maximize the volume to surface area ratio. This furnace is designed to withstand the thermal stresses of the carbothermal reduction process, which are significantly higher than those for the hydrothermal process. Therefore, it can be assumed that the furnace masses being calculated are high end estimates. The mass of the furnace wall is calculated to be 8.5 g/cm^2 . In calculating the furnace mass, a 15% contingency is added to the volume of the batch to account for the volume of the gaseous flow in the furnace. This total volume is then used to calculate the surface area required to reduce a batch of the given size, which can in turn be used to calculate the mass of the furnace from the above surface density. Other plant masses are not included in the processing system mass calculations. The mass of heat exchangers and other miscellaneous items in the reduction plant from the Orbitec design only amount to approximately 10% of the furnace mass. Inconel furnaces utilized in earth laboratories are not properly designed for space missions. In the future, more detailed studies of furnace designs and configurations will be needed. Because of the lack of detailed furnace designs for the hydrothermal production system, the Orbitec carbothermal furnace is taken as the best high-end estimate for the furnace mass. At the level of detail achieved by this model, the furnace mass estimates stated above are sufficient.

5.2.3.5 Power system calculations

There are two major options for producing power for a lunar mission: solar cells or nuclear. The amount of power required for the reduction process is on the order of kilowatts. Under the best conditions, using solar cells with an efficiency of 30% this power requirement leads to a solar panel area of at least 10 m^2 . For a mission that must launch itself from one

landing site to another, this would be a severe engineering challenge. For this reason a nuclear power source is optimal and used in the power system mass calculations. Radio-isotope thermoelectric generators (RTGs) are utilized as the power source for the processing unit. The design specifics of the RTGs in this model are taken from the Cassini mission to Saturn. These RTGs have an overall power density of 4 watts of electrical power per kilogram. There are two power requirements that are modeled in this system: the maximum power for reduction and the power for electrolysis of the water released from the furnace. Power requirements related to systems other than the processing plant are not modeled in this study. It is estimated that the power required for systems such as communications and science instruments is much less than that for the processing plant. These requirements could most likely be met by the RTGs at times when the peak processing power is not needed.

Feedstock Type	Temperature	
	900 C	1050 C
Highland	235 kJ/mol	284 kJ/mol
Mare	221 kJ/mol	268 kJ/mol
Glassy	215 kJ/mol	260 kJ/mol

Table 4: Heat energy values required to heat the various lunar regolith types to their operating temperatures are displayed.

The maximum power required for the processing plant occurs during the preheating stage before the actual reaction has begun. The energy required for the reaction is approximately 12kJ/mol while the energy required to heat the regolith to the processing temperature is over an order of magnitude above that. Table 4 shows the amount of energy required to heat the three regolith types to the operating temperatures for the reduction reaction [Robie].

These energy requirements are calculated by taking average regolith compositions for each type of feedstock from the Apollo 15 and 17 sites [Heikin]. Because the composition of the regolith is substantially variable within these major divisions, the energy values could vary by approximately +/- 10 kJ/mol. However, this variation does not significantly change the power requirement. Until better analyses of a furnace design for this process are available, compositional average values are sufficiently accurate to produce significant power supply requirements. The major piece of information in these energy calculations is that the heating energy is approximately 20 times larger than that needed to sustain the reaction. Therefore the power requirement will be a maximum during the preheating time, and some smaller amount of power will be required during the batch processing time to sustain the temperature and the reaction.

The furnace is not going to be a perfect insulator; some portion of the energy input will be lost due to radiation through the furnace walls and conduction to other parts of the spacecraft. Because the furnace being used is taken from the Orbitec furnace design, the power loss function is also modeled from that design. This power loss function is a simple 10% loss of energy per hour due to radiation. In reality this function should be more complicated, but for our purposes a simple power loss function will do. A power profile throughout the entire cycle is not analyzed in this model. The only value needed by the model is the maximum power requirement, which is used to size the RTG mass. Equation 9 describes the reduction reaction power requirements,

$$P = [(E * M_{\text{mol}} + 0.1 * E * M_{\text{mol}} * T_{\text{heat}}) * M_{\text{batch}}] / T_{\text{heat}} \quad (9)$$

P is the power requirement in watts, E is the energy required in kJ/mol, M_{mol} is the molar mass of the feedstock in mol/kg, T_{heat} is the preheating time of the system, and M_{batch} is the mass of the batch.

The maximum power required also includes the power to conduct electrolysis on the water produced from the regolith reduction. To minimize the time it takes to produce the required amount of oxygen for a launch, the electrolysis cell will be operating throughout the batch processing and preheating times for the reduction process. The energy needed to electrolyze water is 285kJ/mol. The electrolysis power requirement is modeled by the equation:

$$P = \{[(M_{\text{ox}} * 18/16) / N_{\text{batch}}] * E * M_{\text{mol}}\} / (T_{\text{heat}} + T_{\text{batch}}) \quad (10)$$

Where P is the power, M_{ox} is the mass of oxygen required for the launch, N_{batch} is the number of batches, E is the energy required to electrolyze water (285 kJ/mol), M_{mol} is the molar mass of water, and T_{heat} and T_{batch} are the heating and batch times respectively.

Once the two power requirements are calculated, the total RTG mass required for the system is computed. This is simply done by summing the two power requirements and dividing by the power density of the RTG (4W/kg). The RTG mass is the last mass of the processing plant architecture that is calculated in the model. Once this mass is calculated all the masses are added back to the spacecraft landed and on-orbit masses. The landed mass

does not include the mass of the oxygen or hydrogen needed for the initial landing, but the on-orbit mass includes everything. These calculations are then repeated and iterated until convergence on the order of 0.001 kilograms is achieved in the total on-orbit mass.

5.3 Analysis method

In order to calculate the total mass of the system the model iterates the mass of all the components and adds them to the initial payload mass after each iteration. This new mass is then used for the next iteration and this process is repeated. Once each of the three architectures has been iterated to convergence the system masses can be analyzed and compared. The overall system mass on orbit is used as a base of comparison. Whichever architecture has the lowest orbital mass is deemed a more beneficial architecture for that set of parameters. Each input parameter can be varied at will. For each trial run the model outputs the system mass of the fully fueled and processing plant architectures for a number of launch ranges. The system mass of the multiple mission architecture is constant for all launch ranges. The system masses are then used to graph the mass benefit for the processing plant architecture over the other two architectures at each launch range. The model is run many times varying each parameter in turn. Many parameters can be optimized and limited to that value by holding all other parameters constant. As each parameter's optimal values are found, that parameter is then limited to that value for the remaining parameter and system mass analyses. Ultimately the parameter values that produce a mass benefit over both architectures are found. These parameter values are then used to graph the total system mass of the processing plant mission at all beneficial launch ranges.

6. Analysis Results

Due to the numerous variables in this analysis there are many trade studies to be considered, and many different ways to display the results. A number of trade studies have been conducted taking each of the nine input variables into consideration at a time.

Combinations of these variables affect the amount of regolith required, the total mass of the spacecraft, the size of each batch, and therefore the total mass savings of utilizing this exploration architecture. For all trade studies, values of the input variables are limited as mentioned in section 5. The ultimate measure of the processing plant architecture's benefit to lunar exploration is in mass savings compared to the other two possible exploration architectures.

Once the parameter values have been input to the model the payload mass is held constant before it is set to iterate by adding the additional system masses calculated through the model. If the additional masses that are to be added to the system in the first iteration are greater than the initial payload mass the total system mass will diverge as the model iterates. This provides a baseline limitation on the launch range that the processing plant mission can feasibly conduct. In parameter value terms, if the equation

$$PL_{initial} < \sum M_{H,launch} + M_{H\ tank} + M_{Ox,land} + M_{Ox\ tank} + M_{furnace} + M_{RTG} \quad (11)$$

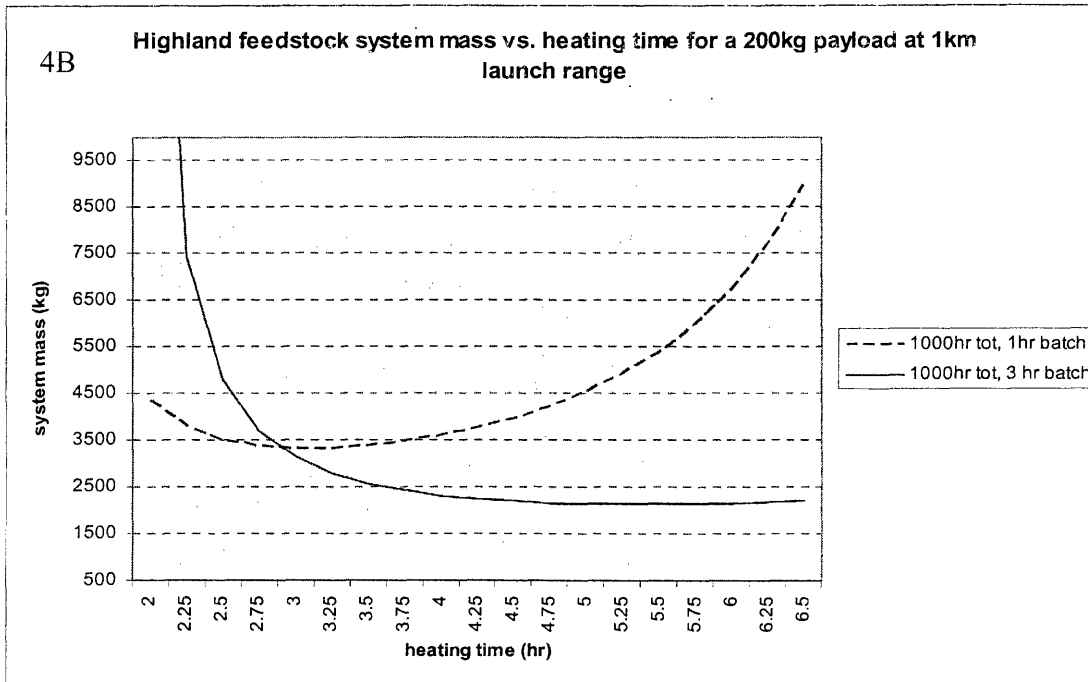
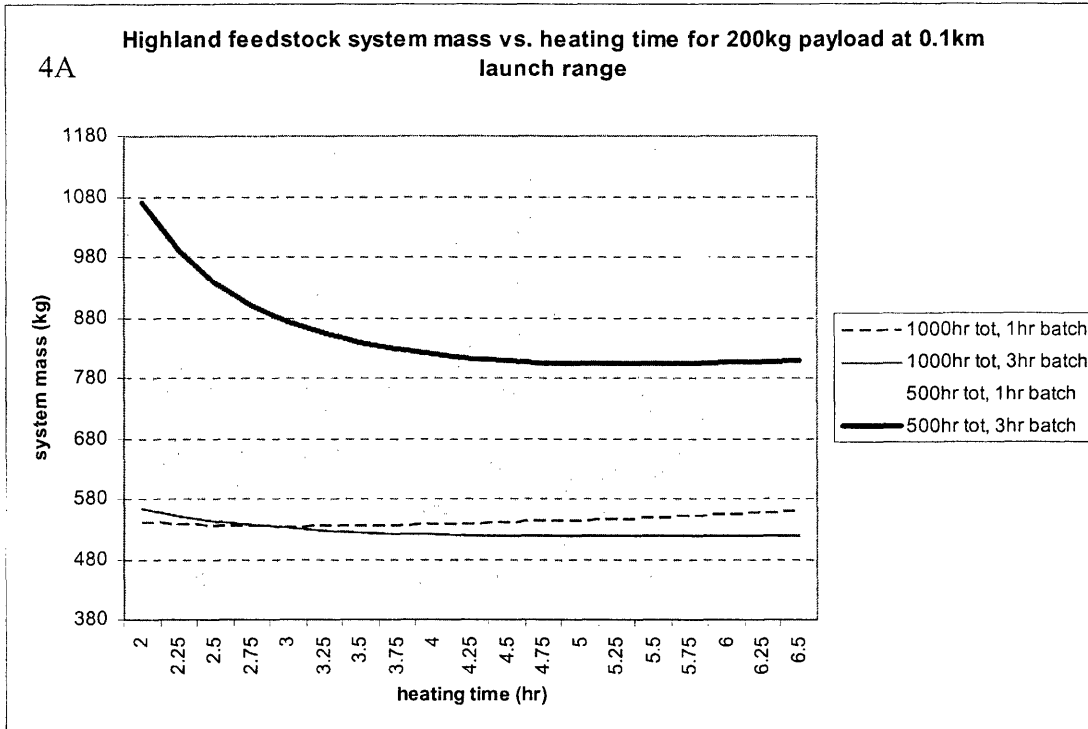
is true, the total system mass required blows up as the system is iterated and a feasible system is never achieved. In this equation PL_{initial} is the payload mass being input to the model, $\sum M_{H,\text{launch}}$ is the hydrogen mass for all lunar launches, $M_{H \text{ tank}}$ is the mass of the tank required to hold the hydrogen, M_{ox} is the mass of the oxygen required for one lunar launch of mass PL_{initial} , $M_{\text{Ox tank}}$ is the mass of the oxygen tank required to hold the oxygen, M_{furnace} is the mass of the processing furnace, and M_{RTG} is the mass of the RTG needed to power the processing system. The launch range at which this equation becomes true is termed the “Range of feasibility” for the system. Any launch range greater than this will be physically impossible to achieve. Using this as a baseline requirement we can set a limitation on the launch range for each combination of other parameter values being analyzed.

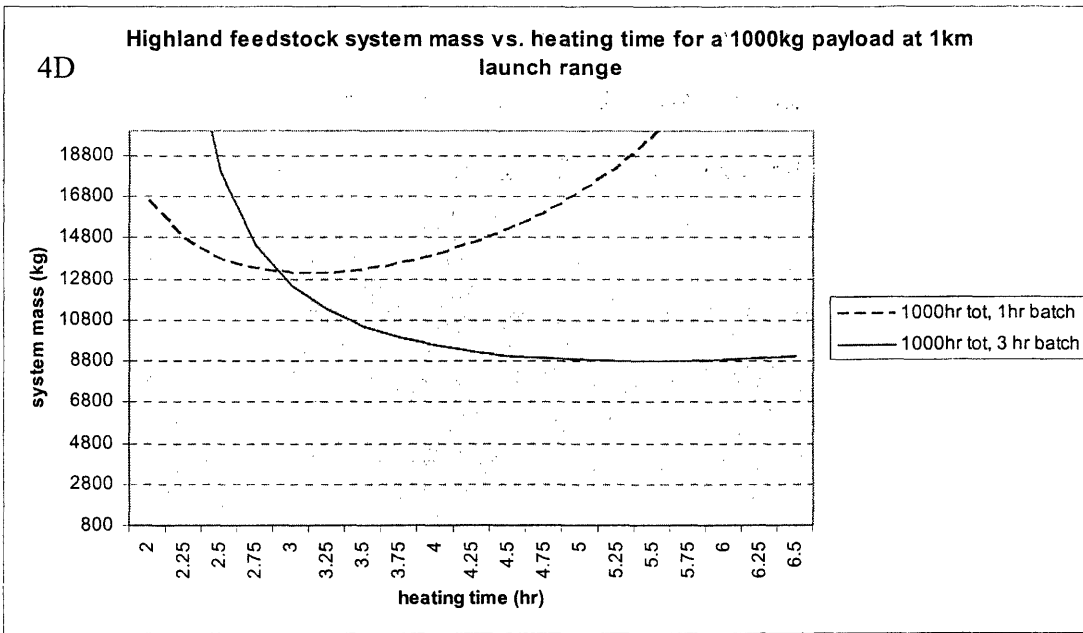
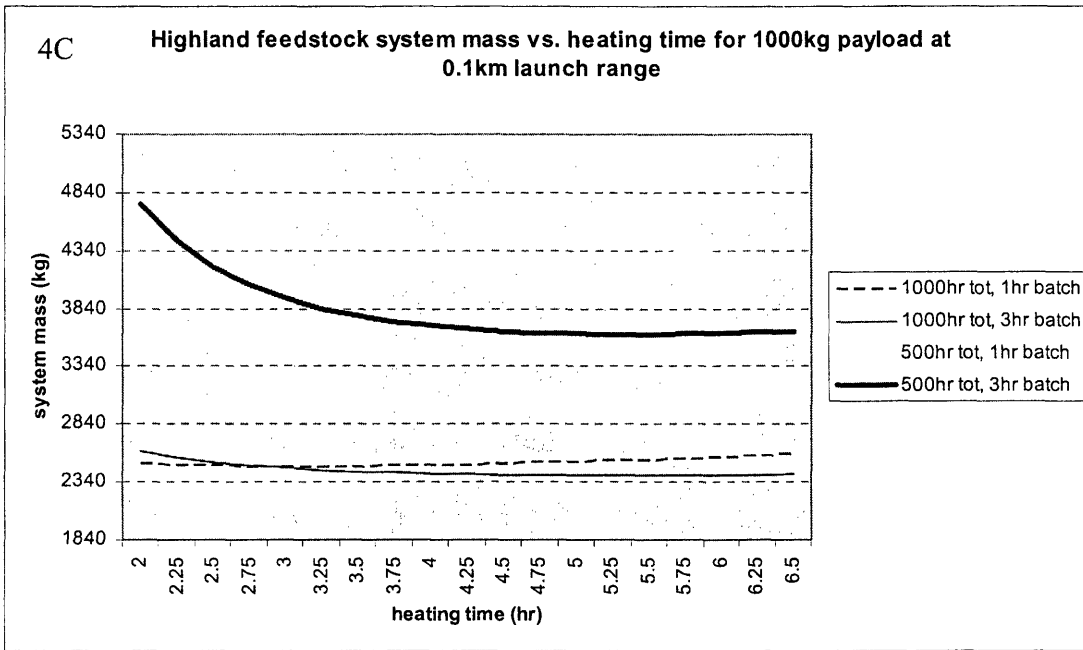
6.1 Equatorial highland feedstocks

Highland soils have a much lower iron content than mare and glassy soils, as has been seen from the Apollo samples. This translates into a lower yield of between 0.8 and 1.2 wt% oxygen. McKay and Allen have shown that the yield obtained from the reduction of highland soils does not vary significantly over the temperature range of 900-1050C [McKay]. Higher temperatures will increase the power requirement of the system without providing a substantial rise in the oxygen yield. For this reason all highland studies use only a 900C processing temperature. Using an equatorial water content of 0% leaves six variables to be analyzed for a highland feedstock processing system: batch processing time, preheating time, payload mass, total processing time, number of launches, and launch range.

6.1.1 Preheating time

The feedstock heating time affects the total system mass in two ways. First, it has an inverse relationship on the power system mass. The maximum power is a simple relationship of the energy delivered per time. So as heating time decreases the required power increases. Heating time also has an inverse affect on the total number of batches. Longer heating times leave less time for batch processing assuming the total time is held constant. If the batch processing time is held constant as well, the number of batches must decrease. In order to process the same amount of feedstock each batch must therefore be larger, which requires a larger amount of energy. In the end these two effects oppose each other, although unequally. Optimal heating times for various processing scenarios can be determined by finding the value that minimizes the scenario's system mass. These optimal values vary based upon other system parameters – total processing time, batch processing time, payload mass, launch range, and number of launches. The change in system mass produced from different parameter values creates a slightly different optimal heating time. The total processing time, batch time, payload mass, and launch range have significant affects on the overall system mass and will noticeably change the optimal heating time by greater than 0.01 hours. However, the number of lunar launches only adds a small amount of hydrogen and tank mass to the system mass which is not a significant change.





Figures 4A-4D- Highland feedstock system mass vs. heating times for a 200kg payload at 0.1km (A) and 1km (B) launch range, and for a 1000kg payload also at 0.1km (C) and 1km (D) launch ranges

This therefore creates a relatively small change – less than 0.01 hours per additional launch – in the optimal heating times. This change in preheating times will not produce a noticeable change in the overall benefit of the system. The affects of heating time on the system mass for missions with a 200kg payload are shown in figures 4A and 4B, and for missions with a 1000kg payload in figures 4C and 4D.

Highland type feedstock Optimal Heating times						
Total Time (hr)	Payload Mass (kg)	Batch Time (hr)	# of launches	Launch Range of Optimization (km)		
				0.1	0.5	1
				Optimal heating times (hrs)		
1000	200	1	1	3.02	3.07	3.11
			3	3.02	3.07	3.11
			5	3.02	3.07	3.11
1000	200	3	1	5.25	5.33	5.38
			3	5.25	5.33	5.38
			5	5.25	5.33	5.38
1000	1000	1	1	3.07	3.11	3.12
			3	3.07	3.11	3.12
			5	3.08	3.11	3.12
1000	1000	3	1	5.34	5.39	5.41
			3	5.34	5.39	5.41
			5	5.34	5.39	5.41
500	200	1	1	3.06	N/A	N/A
			3	3.06	N/A	N/A
			5	3.06	N/A	N/A
500	200	3	1	5.32	N/A	N/A
			3	5.32	N/A	N/A
			5	5.32	N/A	N/A
500	1000	1	1	3.10	N/A	N/A
			3	3.10	N/A	N/A
			5	3.10	N/A	N/A
500	1000	3	1	5.38	N/A	N/A
			3	5.38	N/A	N/A
			5	5.38	N/A	N/A

Table 5: Highland feedstock scenario’s optimal heating times. Each optimal heating time is listed for all parameter scenario combinations being analyzed with a highland type feedstock.

The preheating time value which produces the minimum mass in each data series is the optimal heating time for that set of parameters. In graphs B and D only the 1000hr total processing time scenarios are shown because the system mass for a 500hr total processing time system has blown up at the 1 kilometer launch range. Optimal heating time values for eight parameter scenarios using equatorial highland feedstocks are listed in table 5. This table shows the change in optimal heating times caused by varying each parameter independently. The largest change is caused by the batch time. This is the only parameter which causes variability on the order of an hour. Each of the other parameters causes a change of several hundredths of an hour. For the heating time optimization analysis the launch range has been limited to 0.5 kilometers for a highland type feedstock with a total processing time of 500hrs. Any range above this value causes the system mass to diverge thereby making such a mission unrealistic. For high values where the masses diverge the model loses accuracy as well. Scenarios with longer total processing times produce feasible system mass at larger launch ranges. Therefore with increased total time it is important to consider optimal heating times at higher launch range values. The range applicable for a 1000hr total processing time is approximately 1 kilometer. The heating times found to be optimal for each combination of parameters are used in all further analyses. This maximizes the total system benefit over the other exploration architectures.

6.1.2 Maximum range of feasibility

From the optimal heating times the optimal range of feasibility can be found. This is the maximum distance that any system will be able to physically achieve. A launch range greater than this causes the change in system mass required to launch to this range to be

greater than the initial payload mass, as stated in equation 11. This causes the system mass to blow up when iterated through the model.

Highland type feedstock range of feasibility				
Total Time (hr)	Payload Mass (kg)	Batch Time (hr)	# of launches	Range of Feasibility (km)
1000	200	1	1	1.17
			5	1.14
			10	1.10
			15	1.07
			20	1.04
1000	200	3	1	1.37
			5	1.33
			10	1.29
			15	1.25
			20	1.21
1000	1000	1	1	1.30
			5	1.27
			10	1.24
			15	1.21
			20	1.18
1000	1000	3	1	1.54
			5	1.50
			10	1.46
			15	1.42
			20	1.38
500	200	1	1	0.29
			5	0.29
			10	0.28
			15	0.28
			20	0.27
500	200	3	1	0.34
			5	0.34
			10	0.33
			15	0.33
			20	0.32
500	1000	1	1	0.33
			5	0.32
			10	0.32
			15	0.31
			20	0.31
500	1000	3	1	0.38
			5	0.38
			10	0.37
			15	0.37
			20	0.36

Table 6: Highland feedstock range of feasibility. Listed are the maximum range of feasibility for each parameter scenario at 1 to 20 launches.

The maximum range of feasibility for each of the eight scenarios mentioned above is listed in table 6. Further analysis of system parameters is limited to launch ranges below the maximum range of feasibility for each scenario. A 1000hr total processing time system is capable of launching to a much greater range than a 500hr total processing time system with the same mass. It is noted that doubling the total processing time quadruples the range of feasibility for all eight parameter scenarios with only 1 launch. Increasing the payload mass by a factor of 5 translates to only a short increase in launch range, approximately 0.05km, which is similar to the level of increase caused by changing between a 1 and 3 hour batch processing time.

Increasing the number of launches decreases the range of feasibility by approximately 0.01 km per five launches. This is caused by the added hydrogen and hydrogen tank mass for each additional launch. The range of feasibility as defined above decreases with each launch that is added to the system because more hydrogen and hydrogen tank mass is added into equation 11. Using parameter values previously mentioned, the launch range at which the system mass diverges is less than 1 kilometer for equatorial highland feedstock scenarios using a 500hr total processing time, and less than 2 kilometers using a 1000hr total time. Therefore when conducting further highland analysis, launch ranges will be held to below these values.

6.1.3 Batch processing time

Varying the batch time between 1 and 3 hours can create fairly different system dynamics when designing the production plant architecture. Increasing the batch time has two major

affects on the system. First it increases the oxygen yield from the feedstock. For a highland type feedstock a 1 hour batch yields 0.8wt% oxygen while a 3 hour batch yields 1.2wt% oxygen. Longer batch processing times also lower the total number of batches that can be accomplished in any set amount of total processing time. Therefore, by holding the total time constant the differences between a 1 hour and 3 hour batch cycle can be analyzed.

It can be seen in figures 4A through 4D above that when analyzing a system for feasible highland system launch ranges, a 3 hour batch time yields a lower overall system mass if optimal heating times are used.

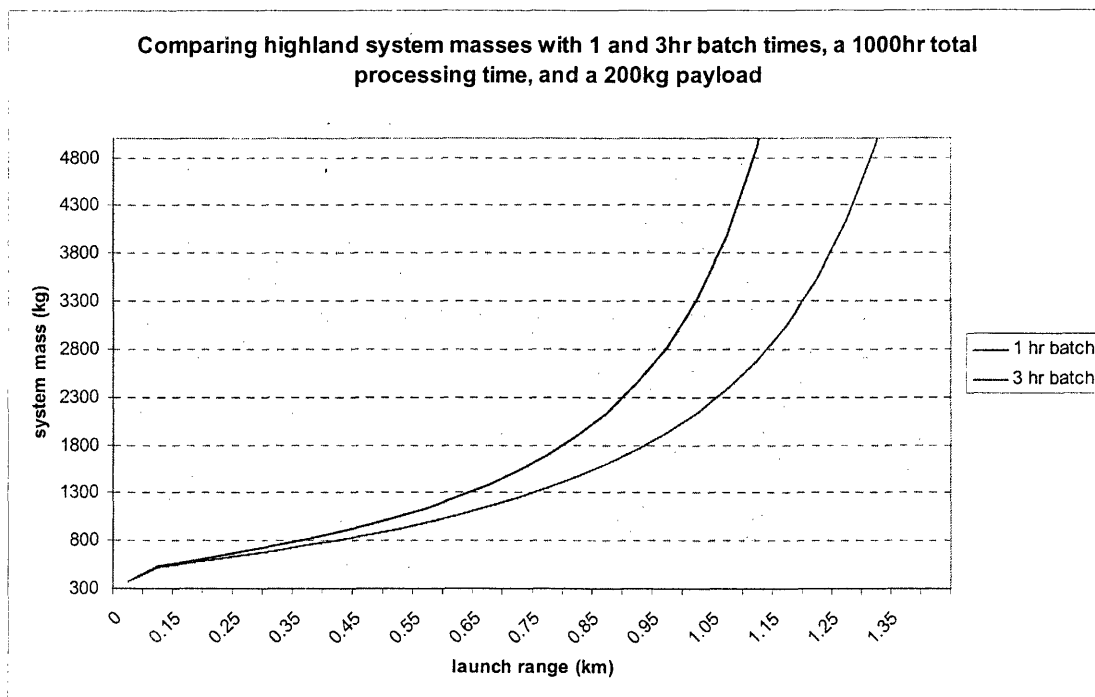


Figure 5: Highland feedstock batch time comparisons. Batch times of both 1 and 3 hours are compared over all feasible launch ranges for a 1000hr total processing time with a 200kg payload to demonstrate the affect that different batch times has on the system mass.

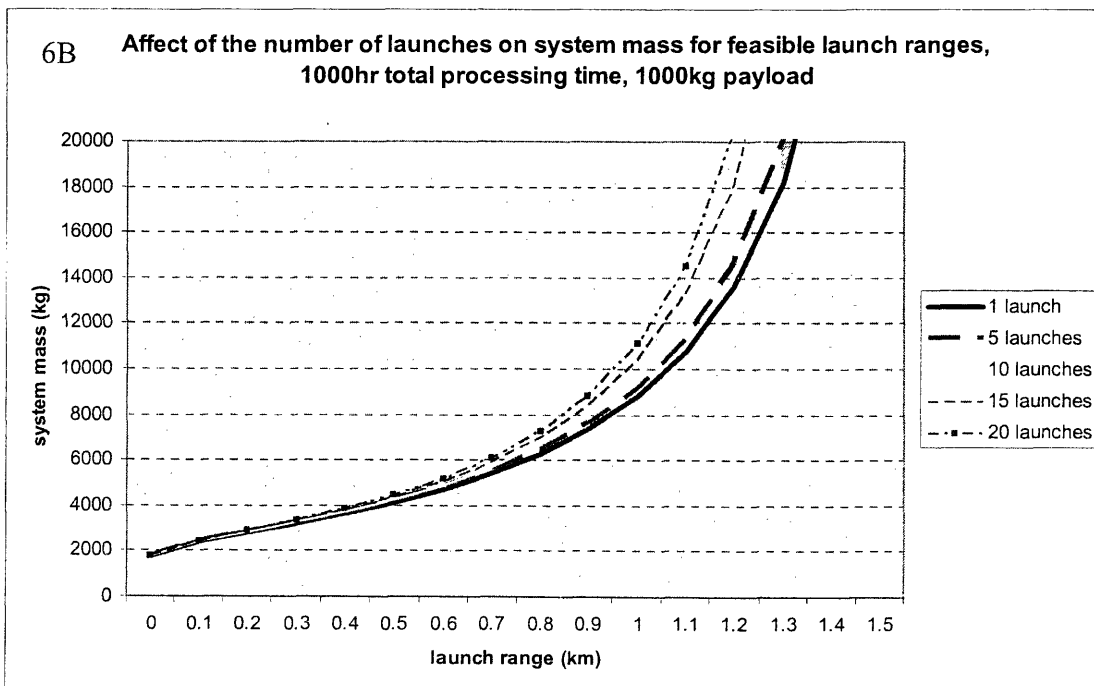
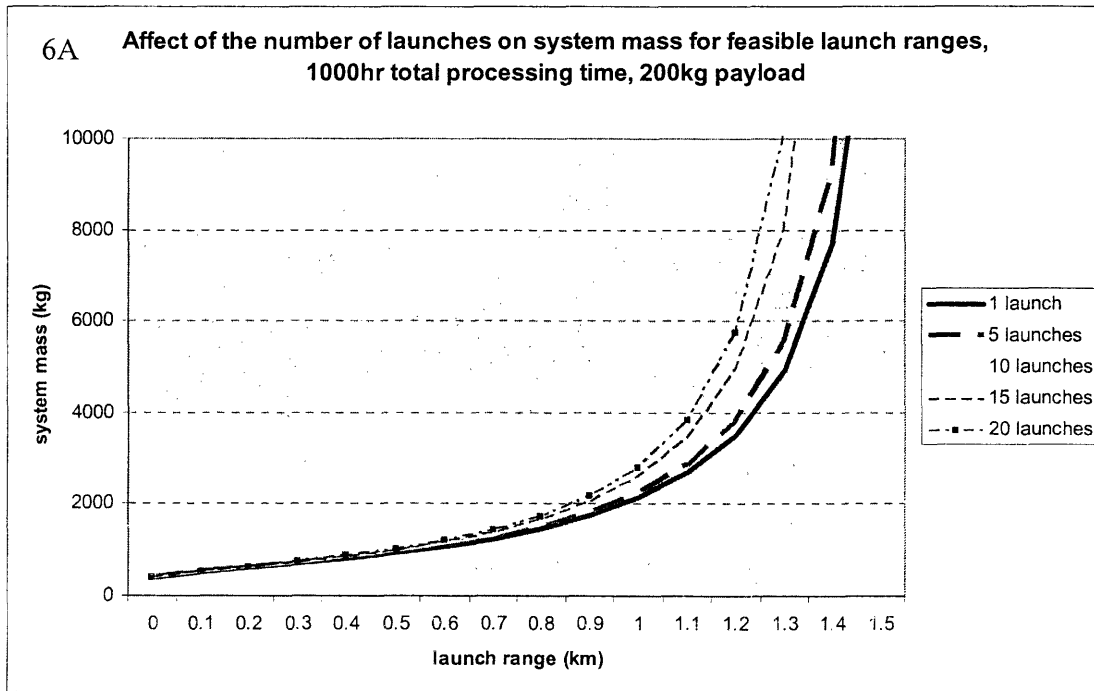
The mass benefit of using a 3 hr batch over a 1 hr batch at these launch ranges varies greatly upon the other system parameters. However, in all systems it is noted to be a significant value. As the desired launch range of the system is increased, the difference in system mass between a 1 and 3 hour batch also increases. Figure 5 shows the system masses for both a 1 and 3 hour batch processing time for a scenario using a 1000hr total processing time, 200kg payload, and 1 launch. At higher launch ranges the mass benefit of a 3 hour batch over a 1 hr batch is on the order of 1000kg. When designing a system using highland regolith as the feedstock a 3 hr batch is recommended for all parameter scenarios.

6.1.4 Launch number

The number of lunar launches that the system is designed to complete has a large affect on the overall system composition. Additional lunar launches will require a larger hydrogen and tank mass. Both the heating time and batch processing time can now be limited to their optimal values (3 hr batch and heating times mentioned in table 5) which leaves four scenarios over which to analyze how the number of launches affects the system. These scenarios are:

1. 1000hr total processing time, 200kg payload
2. 1000hr total processing time, 1000kg payload
3. 500hr total processing time, 200kg payload
4. 500hr total processing time, 1000kg payload

Each scenario is analyzed over the entire set of feasible launch ranges, and the number of launches set between 1 and 20.



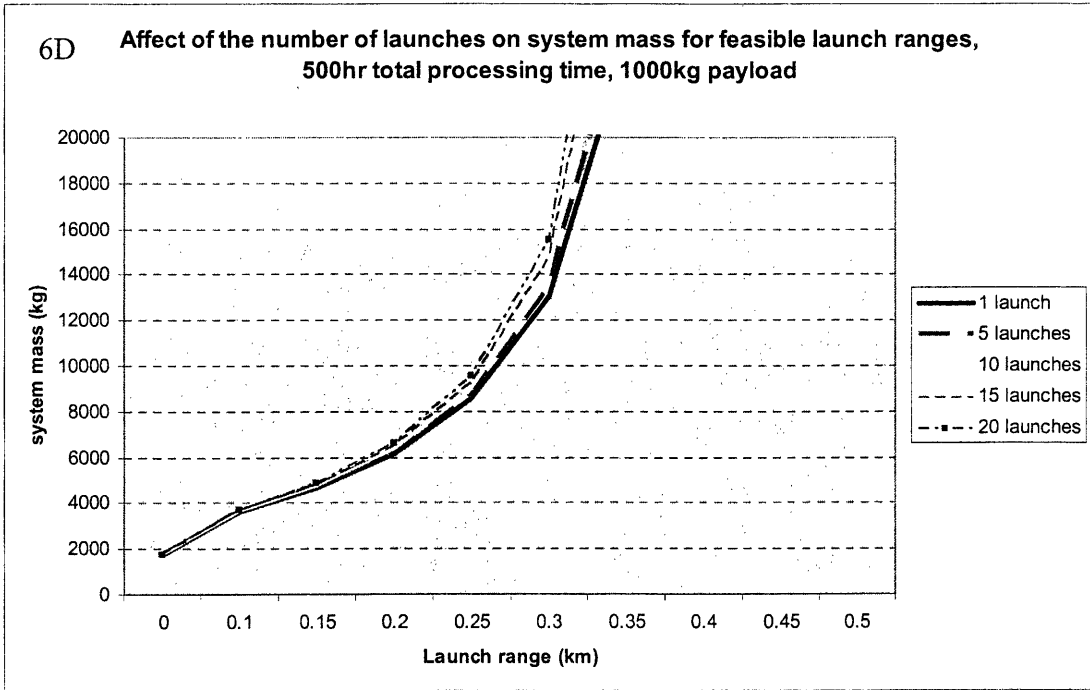
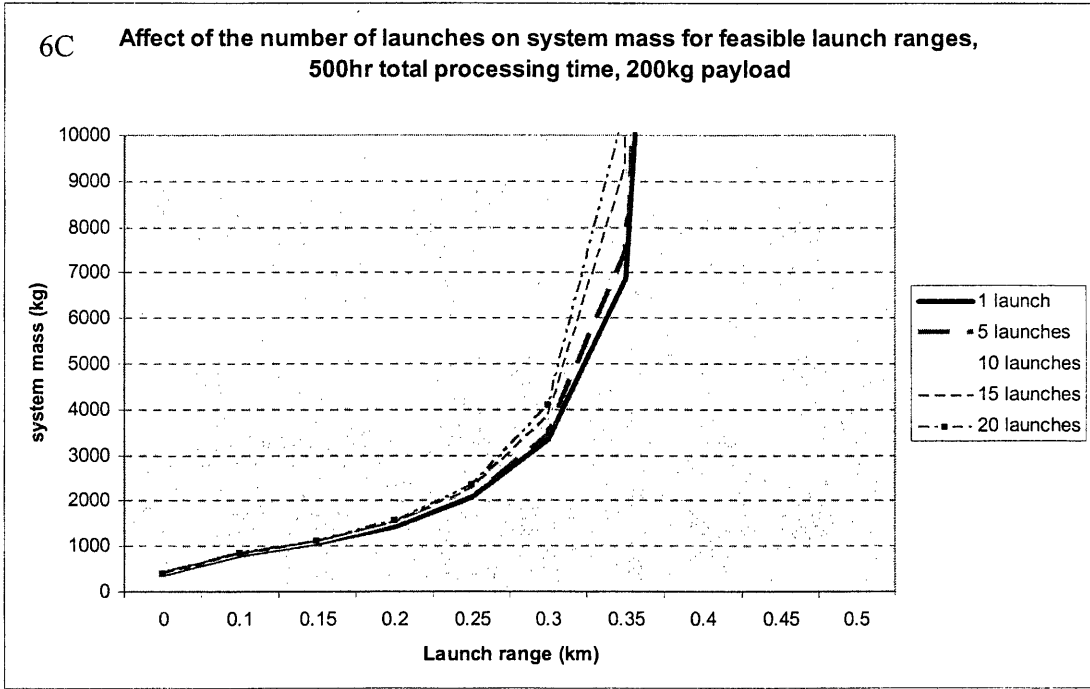


Figure 6A-6D: Highland feedstock launch number comparisons. The number of launches is varied between 1 and 20 over the all feasible launch ranges to show the affect of launch number on system mass.

Figures 6A through 6D demonstrate how the system mass is affected by increasing the number of launches for these 4 scenarios. The graphs display the scenarios with the number of launches set to: 1, 5, 10, 15, and 20. The same general trends are shown for all cases. The distance that the system is capable of reaching with the same system mass decreases with more lunar launches, and the system mass increases exponentially with increasing launch range. The system mass for all scenarios is very large for even extremely short launch ranges.

6.1.5 Mass benefit and system feasibility

The change in the overall processing system mass created from increasing the number of launches is important to note in itself; however, the information necessary to determine if this system is feasible or not is in the mass benefit of the processing architecture over the other two possible architecture.

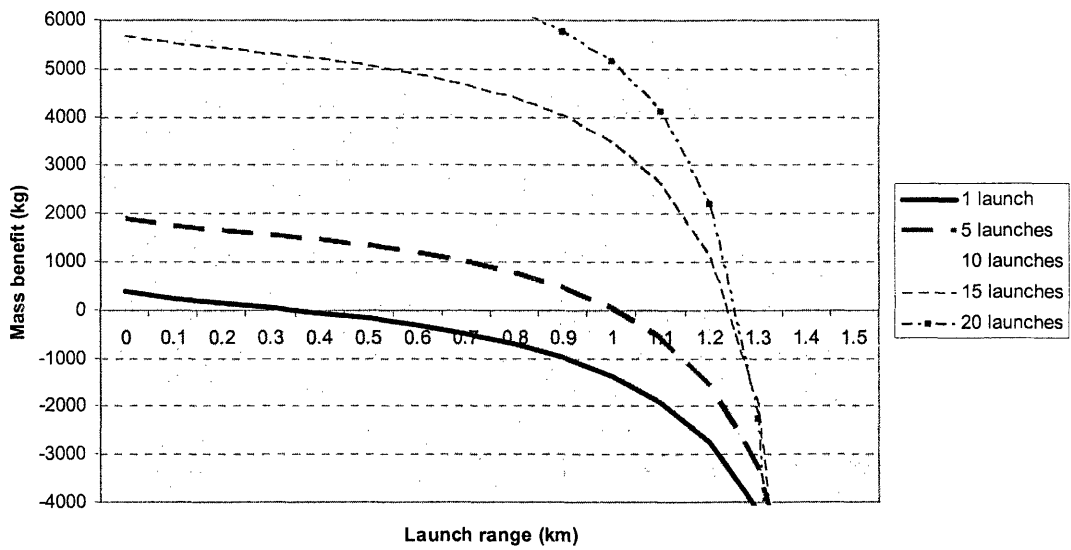
6.1.5.1 *Benefit vs. multiple mission architecture*

The multiple mission architecture's mass only increases with an increase in the number of launches. The number of missions that the multiple mission architecture must launch from the Earth is the number of lunar launches of the processing system mission plus one.

Figures 7A through 7D show the mass benefit of the processing plant architecture over the multiple mission architecture for the feasible launch ranges. Each data series in the graphs represents the scenario with a different number of launches. The point where each series crosses the x-axis is defined as the "maximum beneficial range" for the given scenario.

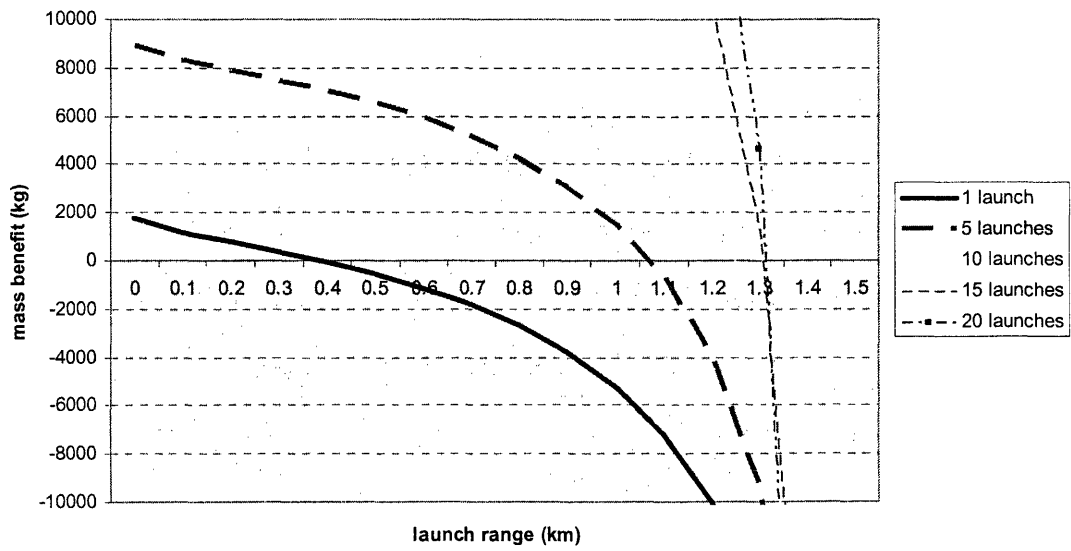
7A

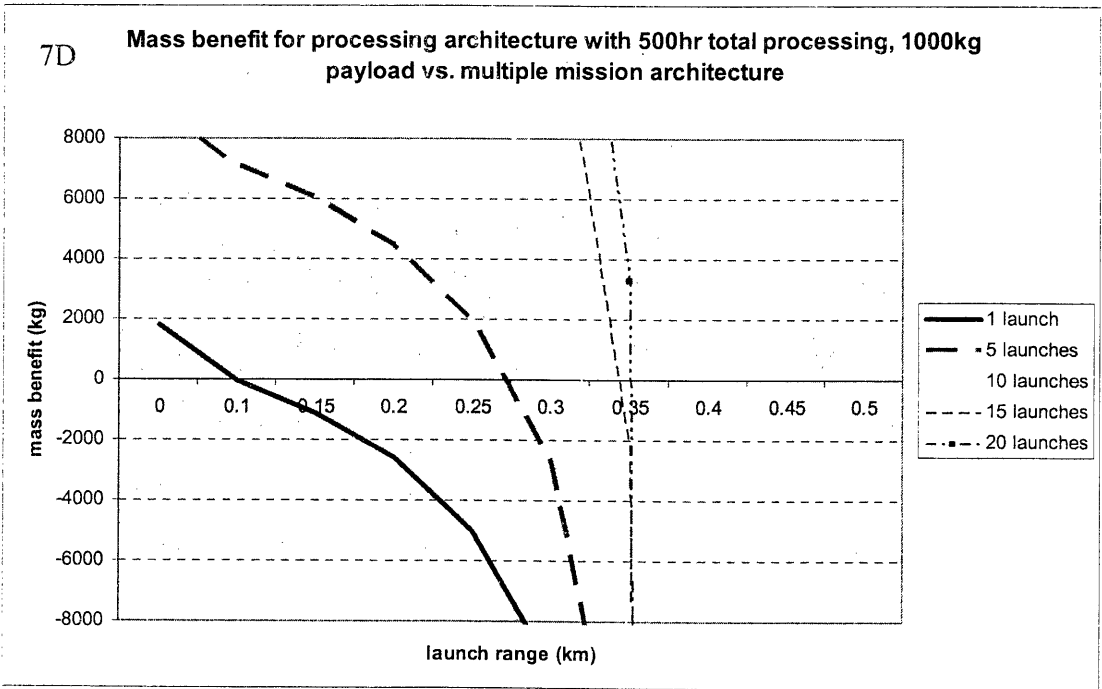
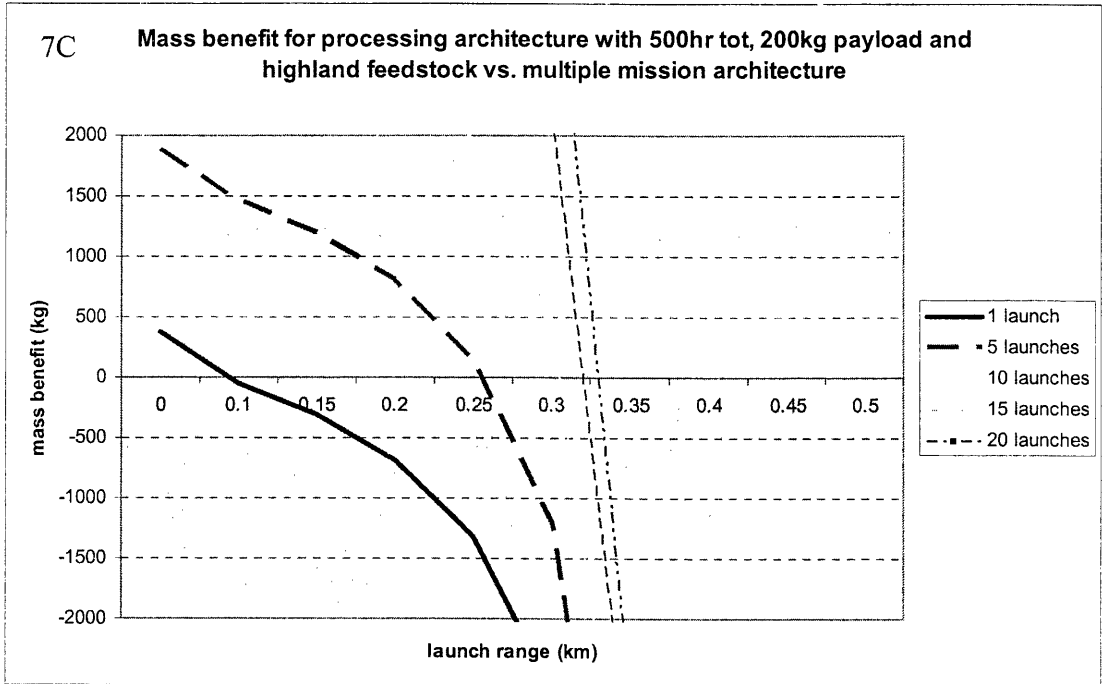
Mass benefit of Processing plant architecture 1000hr tot, 200kg payload and highland feedstock vs. Multiple mission architecture



7B

Mass benefit for processing architecture with 1000hr tot, 1000kg payload vs. Multiple mission architecture





Figures 7A-7D: Highland Feedstock mass benefit vs. multiple mission architecture. The four scenarios are displayed with launch numbers between 1 and 20 in order to show the affect of each scenario at a different number of launches on the overall system mass benefit. Scales on the axes are not the same for each figure.

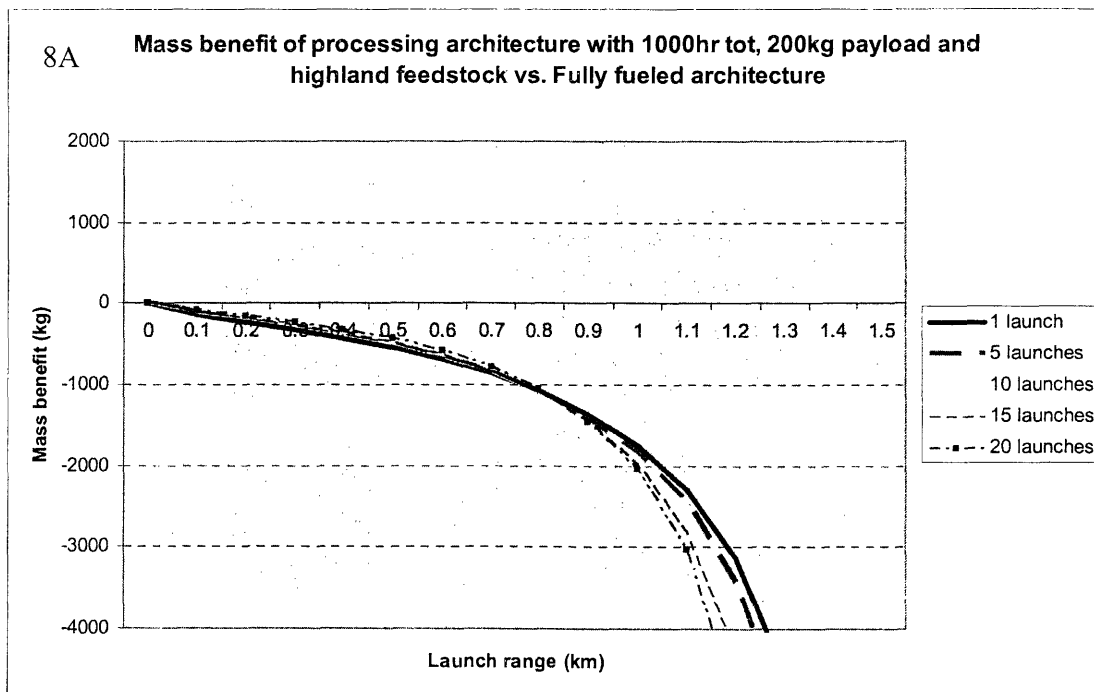
A positive mass benefit is when the overall processing architecture mass is lower than the multiple mission architecture mass. The exact distance of the maximum beneficial launch range varies depending on the total processing time and the payload mass as well as the number of launches. Both the preheating time and the batch processing time have been set to their optimal values.

It is immediately noticeable that when the number of launches is small, any increase in the number of launches significantly increases the maximum beneficial launch range for the processing plant system. However, there is a maximum number of launches beyond which additional launches will lower the maximum beneficial range. At a high number of lunar launches the processing plant architecture's beneficial range approaches the range of feasibility. At launches above this range the mass of the processing system blows up. Therefore, the benefit versus the multiple mission architecture goes immediately negative. With every additional launch, the range of feasibility is slightly decreased due to the added hydrogen and tank mass. Therefore, once the number of launches is large enough so that the beneficial range has nearly reached the range of feasibility, there will not be any further increase in launch range capability due to increasing the number of launches. Instead, adding more launches will only serve to decrease the launch capability due to the decrease in the range of feasibility.

6.1.5.2 *Benefit vs. fully fueled architecture*

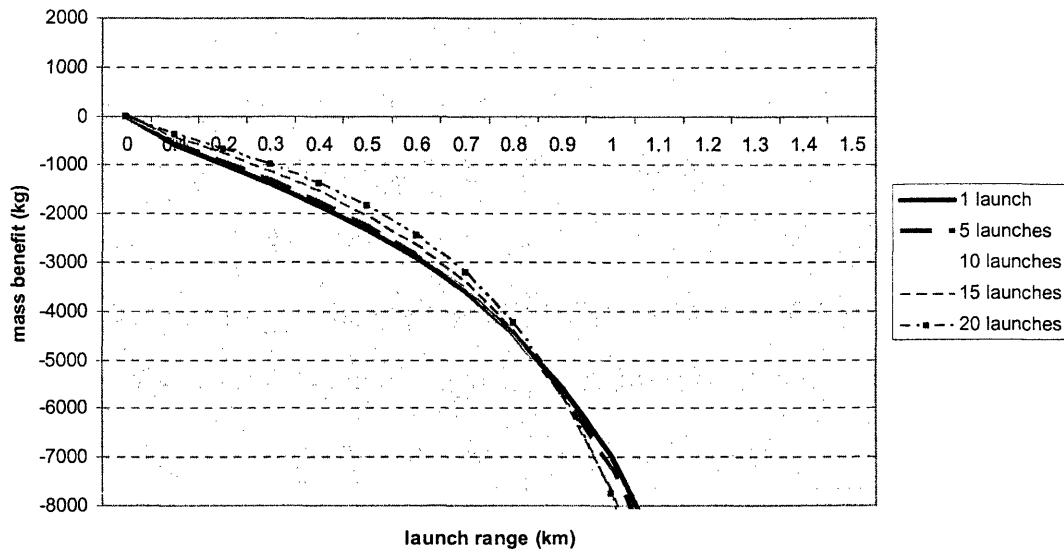
The second possible exploration architecture for comparison with the processing plant mission is a single fully fueled mission. This produces a fairly different mass benefit

analysis. For a highland feedstock system, the mass benefit between these architectures is negative for all four parameter scenarios with any number of launches. However, the behavior of the mass benefit curve over launch range is interesting to analyze. These mass benefit curves are displayed in figures 8A-8D. By examining these graphs it is noticed that the mass benefit curves change shape with a different number of launches. Trials of each scenario run with a high number of launches have a higher mass benefit at small launch ranges than trial runs with a low number of launches. However, the opposite is true at large launch ranges, runs with a high number of launches result in lower mass benefits than runs with a small number of launches. This is most prominently shown in figure 8B, but occurs in all cases.



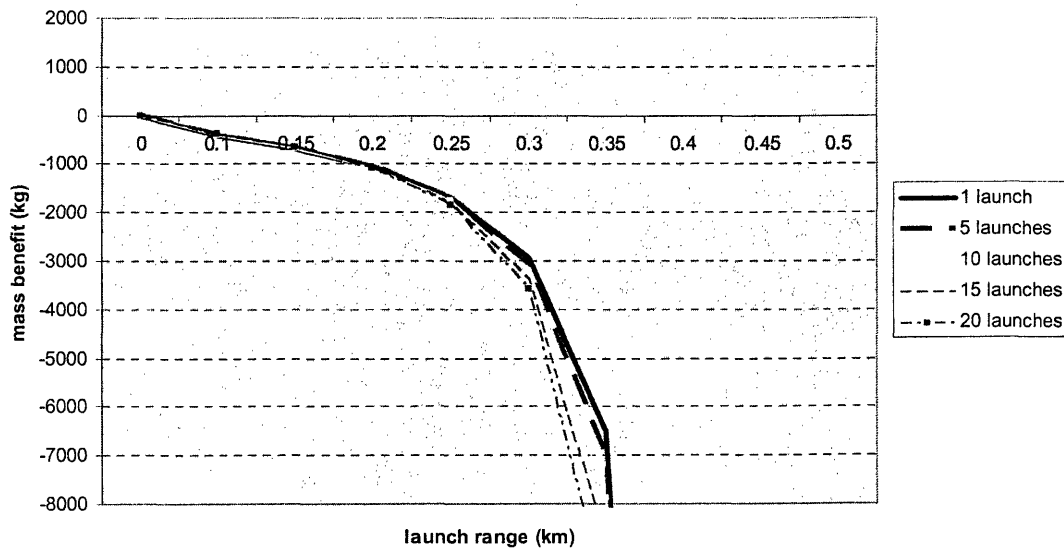
8B

Mass benefit of Processing architecture with a 1000hr tot, 1000kg payload, vs. Fully fueled architecture



8C

Mass benefit of processing architecture with a 500hr tot, 200kg payload and highland feedstock vs. fully fueled architecture



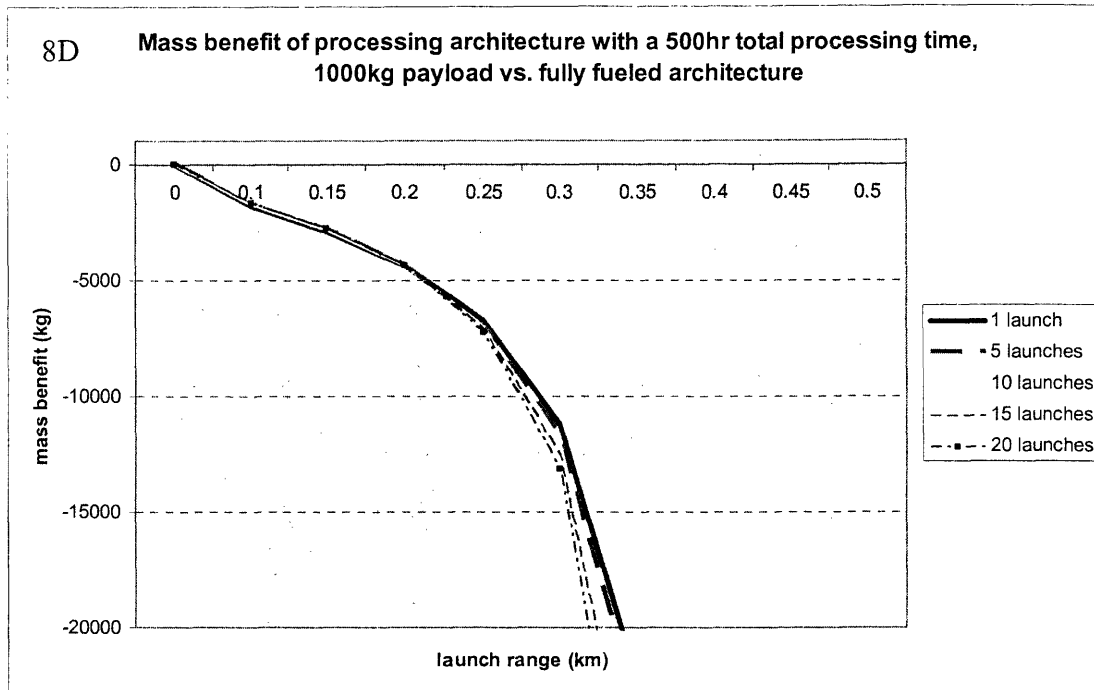


Figure 8A-8D: Highland feedstock mass benefit vs. fully fueled architecture. Each of the four analysis scenarios' mass benefit vs. the fully fueled architecture is displayed with launch numbers between 1 and 20 to show the system mass benefit. The X-axis is the launch range up to the range of feasibility, and the Y-axis is the mass difference between the two architectures (not on the same scale for each figure).

The change in benefit from changing the number of launches can be analyzed by studying the components of the system masses of each architecture. The mass benefit of the processing plant architecture over the fully fueled architecture is described by the equation:

$$B = M_{\text{fueled}} - M_{\text{processing}} \quad (12)$$

To analyze how the mass benefit changes by adding more lunar launches to the system two scenario runs can be compared, a first with a small number of launches and the second with some number of launches greater than the first. The change in benefit from the first run to the second can be expressed as,

$$\Delta B = B_N - B_{init} \quad (13)$$

where B_{init} is equal to the benefit of the first trial run and B_N is equal to the benefit of the second trial run with N number of launches above the first run's number of launches. The first run's mass benefit, B_{init} , can be written as the difference between the total system masses of the fully fueled and processing plant architectures. Each total system mass is the initial payload mass plus the masses of each component being added to the payload mass through the model's iterations. B_{init} is expressed as an equation below.

$$B_{init} = [M_{fueled(0)} + M_{H,land}^F + \sum M_{H,launch}^F + M_{Ox,land}^F + \sum M_{Ox,launch}^F + M_{Htank}^F + M_{OxTank}^F] \\ - [M_{processing(0)} + M_{H,land}^P + \sum M_{H,launch}^P + M_{Ox,land}^P + M_{Htank}^P + M_{OxTank}^P + M_f + M_{RTG}]$$

The superscript "F" is adopted to note masses of the fully fueled architecture, and the superscript "P" notes masses of the processing plant architecture. The benefit of the second trial run, B_N , can be written as,

$$B_N = B_{init} + \Delta B$$

Changing the number of launches directly increases the amount of propellant required for launching the spacecraft. By approximating the system masses to their values after only one iteration the additional system mass due to the added mass of other components can be neglected. Therefore, ΔB will only affect those components which are dependent upon the launch propellant. This approximation eliminates several terms from the equation for B_{init} .

$M_{H,land}$, $\Sigma M_{H,launch}$, $M_{Ox,land}$, and M_{Htank} can all be eliminated because they have the same value for both the fully fueled and processing plant architectures. $M_{fueled(0)}$ is equal to $M_{processing(0)}$ by definition. This leaves the equation for the first run's benefit to be,

$$B_{init} = [\Sigma M_{Ox,launch}^F + M_{OxTank}^F] - [M_{OxTank}^P + M_f + M_{RTG}] \quad (13)$$

All of the terms in equation 13 are functions of the launch propellant except for M_{OxTank}^P , which only depends on the propellant needed to land the craft, $M_{Ox,land}$. Therefore, in this approximation, changing the number of launches will not affect the M_{OxTank}^P and this term will cancel out in the equation for ΔB leaving:

$$\Delta B = \delta \Sigma M_{Ox,launch}^F + \delta M_{OxTank}^F - [\delta M_f + \delta M_{RTG}] \quad (14)$$

where the “ δ ” indicates the difference between the value of the first trial run and the second trial run with an increase in the number of launches.

This equation is not exact because the masses are taken at only one iteration; however, it is a good first order approximation to understand the behavior of the mass benefit between these two architectures. All four terms in equation 14 are functions of the propellant required for a lunar launch. The propellant is a function of the launch range by the exponential: $1 - e^{(-\text{sqrt}(\text{Range}))}$. As launch propellant requirements increase, the mass of the furnace and oxygen tank increase by a factor of the propellant^(2/3), while the RTG increases linearly with the mass of oxygen required for the initial lunar launch. Figure 9 shows the

behavior of the change in benefit with additional launches obtained from this approximate calculation. These are very close to the values taken directly from the model calculations (displayed in the mass benefit graphs of figure 8) showing that this approximation is sufficient for analyzing the mass benefit. The graph displays the change in benefit between the processing plant architecture and the fully fueled architecture using a 1000hr total processing time, a 200kg payload, 3 hr batch, and changing the number of launches from 1 to 10.

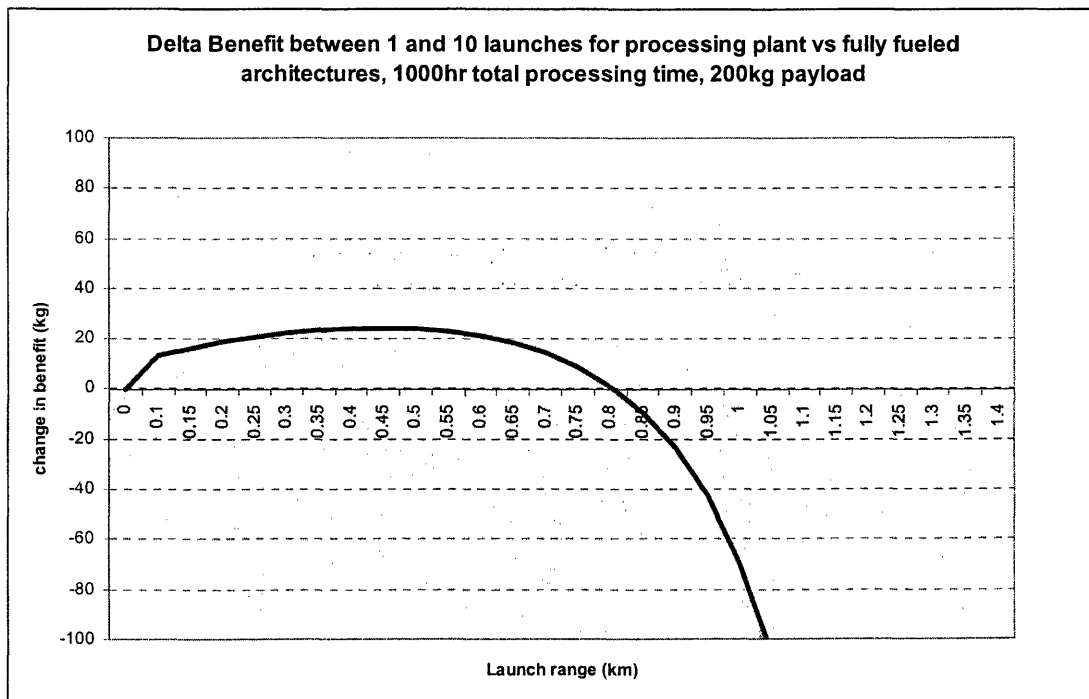


Figure 9: Highland delta benefit vs. fully fueled architecture. The change in benefit between 1 and 10 launch is shown to display how the benefit is changed with additional launches.

From this analysis it is noted that over relatively short ranges for the system, increasing the number of launches improves the benefit of the processing architecture over the fully

fueled architecture, while at large ranges the benefit is decreased by increasing the number of launches. Therefore, as the number of launches is increased the benefit will eventually become positive over a certain value of launch ranges. From figure 8A it can be seen that the mass benefit for this scenario is between -500kg and -1000kg on the range of 0.1km to 1km. From figure 9, the change in mass benefit is approximately 20kg after increasing the number of launches by 10. However, the rate of change is not constant as the number of launches is increased; in other words, the ΔB from a 1 launch scenario to a 20 launch scenario is not equal to twice the ΔB from a 1 launch scenario to a 10 launch scenario. As the number of launches increases, the change in benefit also increases. So the ΔB from 10 to 20 launches will be greater than the ΔB from 1 to 10 launches. However, as an approximation using a constant ΔB of 20kg per additional 10 launches this system will have to undertake a minimum of 250 launches to achieve a positive benefit over the fully fueled system. This translates to a time of approximately 42 years of operation on the lunar surface. In reality these values will be somewhat smaller, but they still remain far out of the bounds of feasibility for this type of exploration mission.

As a final test of feasibility for the highland processing system, the model was run with one a scenario using a 2000hr total processing time. With a 200kg payload and using a 3hr batch cycle the optimal heating time for this system is 5.45 hours at the maximum beneficial range. The mass benefit for this scenario versus the multiple mission architecture is shown in figure 10.

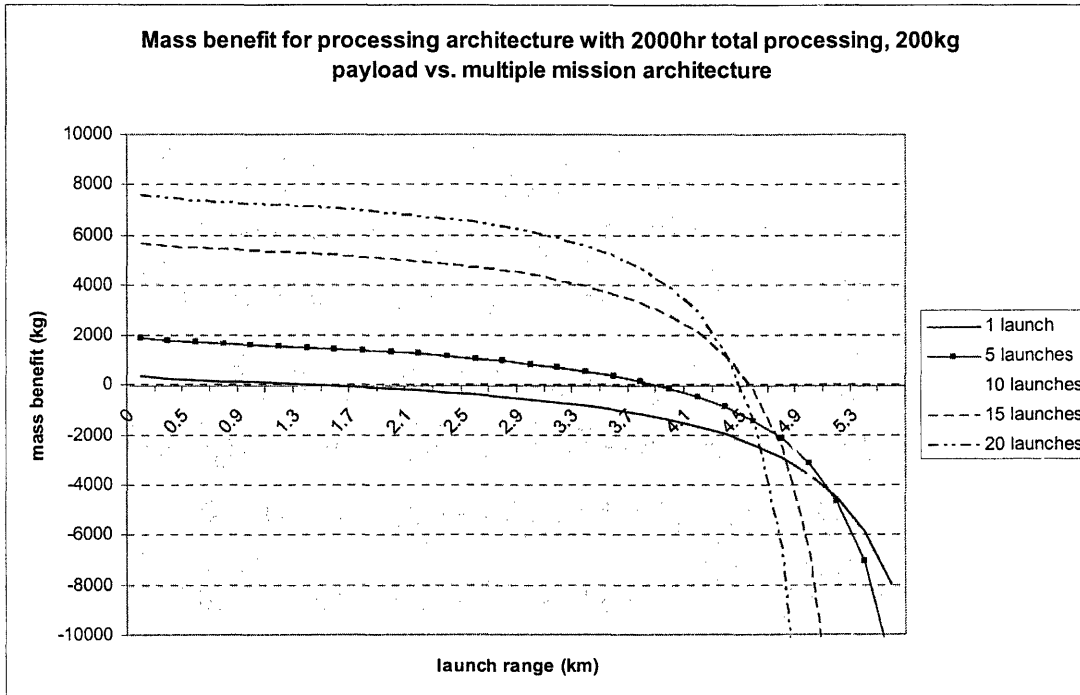


Figure 10: 2000hr total highland system mass benefit vs. multiple mission architecture. A number of launches are displayed over the feasible launch ranges to show the range of benefits available with the increased total processing time.

This is similar to the mass benefit graphs for the previous scenarios; however, the drop in the maximum beneficial range is more clearly show from the 15 to 20 launch data sets. If the number of launches is increased beyond twenty, the maximum beneficial range would continue to drop. Figure 11 shows the mass benefit versus the fully fueled architecture. This shows the same negative mass benefit trends for low launch numbers as in the previous scenarios. However, between launch numbers of 17 and 18, the system completely switches around from a negative mass benefit to a positive mass benefit.

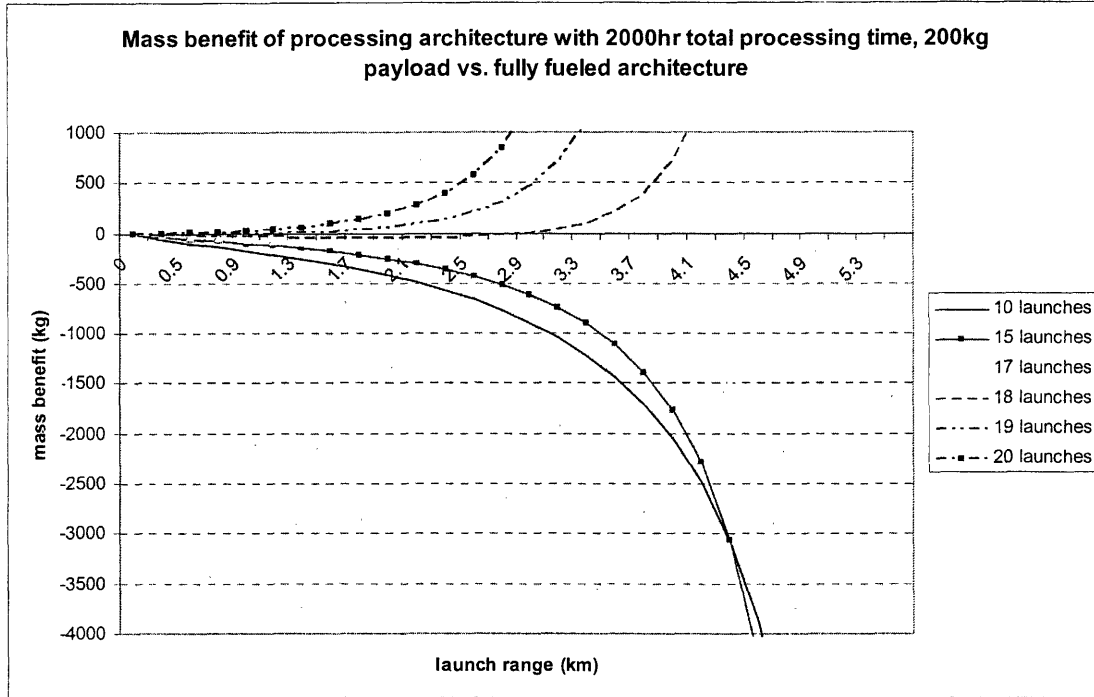


Figure 11: 2000hr total time highland system mass benefit vs. fully fueled architecture. Large launch numbers are shown to produce a positive mass benefit with this increased total processing time.

This switch from a negative to positive mass benefit can be explained by examining the components of the system mass again. In the above approximation, the two components of the fully fueled architecture that contribute to the change in mass benefit with an increased number of launches are the total amount of oxygen required for all the launches and the mass of the oxygen tank. The two components contributing from the processing plant architecture are the mass of the furnace and the mass of the RTG. Both of the fully fueled components depend upon the sum of the oxygen mass of all launches. The processing system components both depend upon the oxygen mass of only one lunar launch. Therefore the change in benefit equation can be written as:

$$\Delta B = [\Delta \sum M_{Ox,launch(i)}^F + \Delta M_{OxTank}^F (\Delta M_{Ox,landing}^F + \Delta \sum M_{Ox,launch(i)}^F)] \quad (15)$$

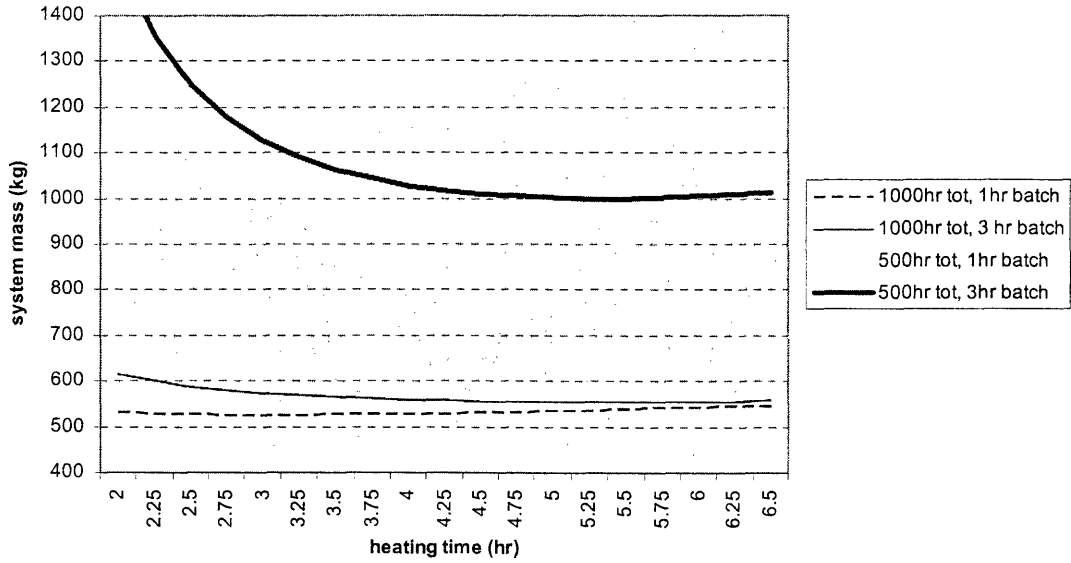
$$- [\Delta M_f(M_{Ox,launch}) + \Delta M_{RTG}(M_{Ox,launch})]$$

The RTG mass is a linear function of the oxygen needed for one lunar launch. The furnace mass is a function raised to the 2/3 power of the oxygen needed for one lunar launch.

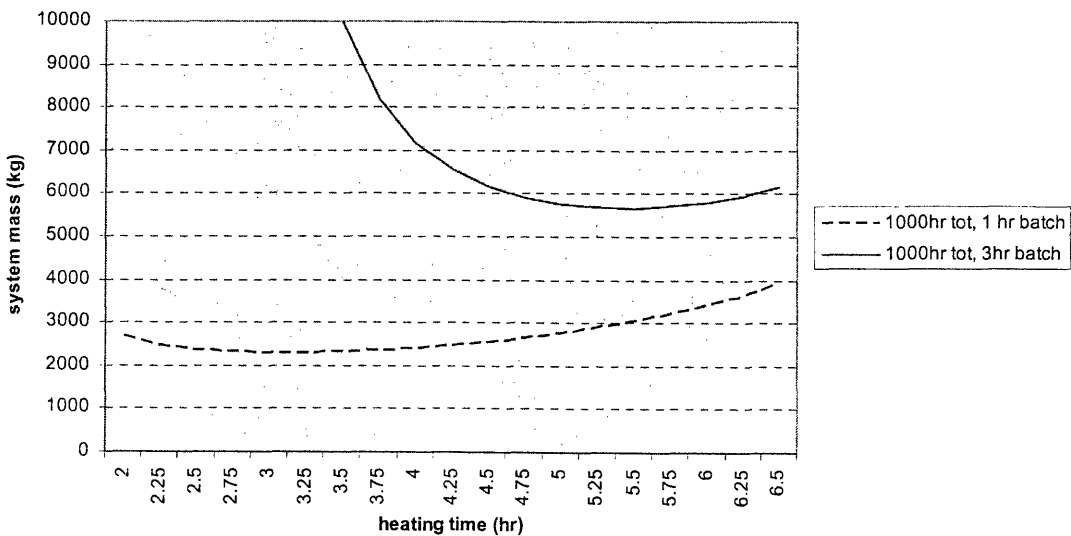
Therefore, in this approximation these masses are only changed by increasing the range of the launch, because the oxygen required is a function of the range, and will not change with the addition of launches to the system. However, in reality the masses will increase slowly with additional launches due to the increased system mass iterated into the system from the added hydrogen mass required for each launch that must be carried.

Therefore, it can be noted that the two processing components, $\Delta M_f(M_{\text{ox,launch}})$ and $\Delta M_{\text{RTG}}(M_{\text{ox,launch}})$ are slightly dependant upon the number of launches, but heavily dependant upon the launch range while the two fully fueled components, $\Delta \Sigma M_{\text{Ox,launch}(i)}^F$ and $\Delta M_{\text{OxTank}}^F (\Delta M_{\text{Ox,landing}}^F + \Delta \Sigma M_{\text{Ox,launch}(i)}^F)$, depend heavily upon both the launch range and the number of launches. If the number of launches is held at a small value (less than 18 for this scenario) and the range is increased, the mass benefit becomes more negative because the processing masses increase more quickly with range than the fully fueled components creating a negative ΔB . Above a certain number of launches the mass of the oxygen tank and the added mass of oxygen for another launch of the fully fueled architecture vary with the launch range by a larger amount than the processing system terms. At this launch range the system switches around to having an increasing benefit with range. This switch would also occur in the previous scenarios; however, it occurs well above the maximum number of launches that the model is designed to analyze. Therefore, it is not shown in those graphs.

12A Mare feedstock system mass vs. heating time for a 200kg payload at 1km launch range



12B Mare feedstock system mass vs. heating time for a 200kg payload at 10km range



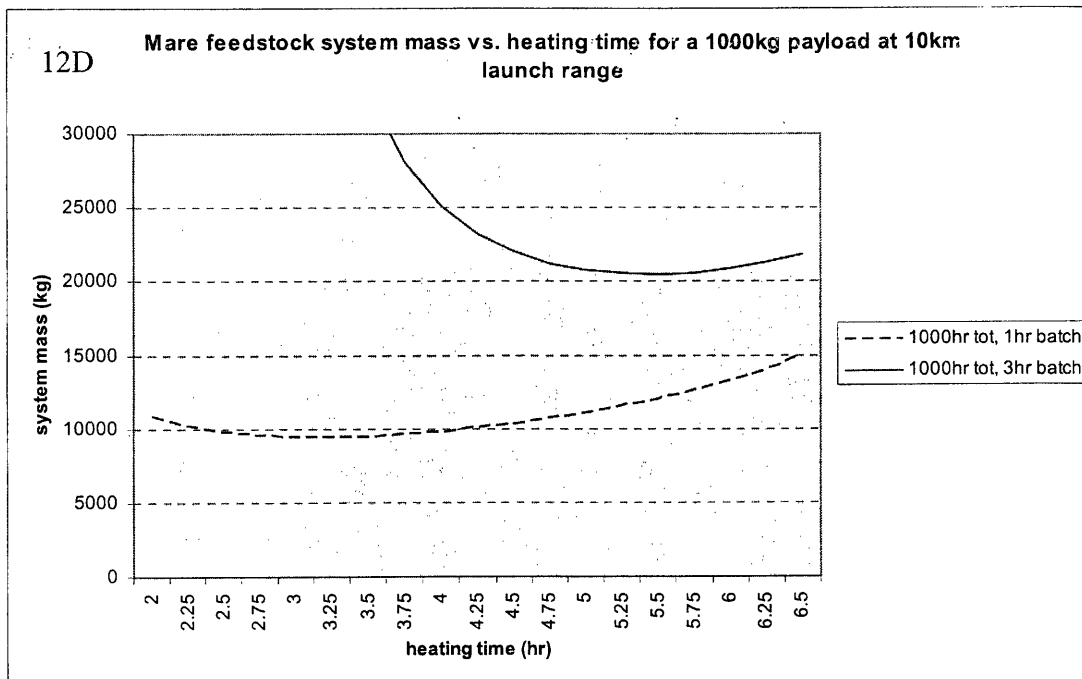
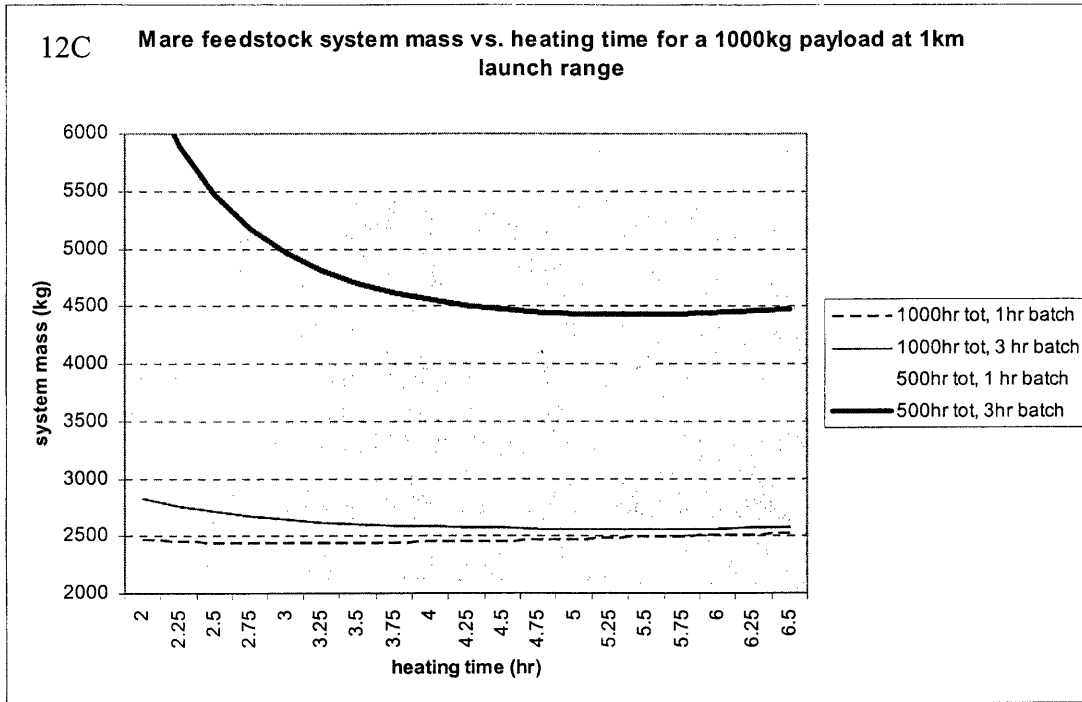


Figure 12A-12D: Mare feedstock system mass vs. heating time. System masses of the parameter scenarios are shown at a 1km range and a 10km range.

Using a 2000hr total processing time per launch can produce positive mass benefits over both the other exploration architectures. However the system remains unrealistic for an actual exploration mission. A minimum of 18 launches is required to produce a mass benefit over the fully fueled system. At approximately 4 months per launch this amounts to a lifetime of 6 years of lunar processing. With a maximum range of approximately 4.5 kilometers per launch the system could cover a total of 81km within 6 years. Theoretically, if a rover could continue operating for six years it would only need to traverse at a speed of approximately 1.6 meters per hour to cover this distance. The MER Rovers cover greater than 10 meters per hour, and advances in technology are expected to increase this number in future years. Therefore with both lifetime considerations and rover architectures taken into account, a processing plant mission utilizing highland regolith as the feedstock will not be beneficial unless significant advances in the processing system components are developed.

6.2 Equatorial mare feedstocks

In contrast to highland soils, the mare regions have a relatively high iron content. This increased iron content leads to a higher expected oxygen yield of 3 to 3.6 wt% from the hydrothermal production method. As with the highland regolith, it was determined by McKay and Allen that the reduction of mare soil with hydrogen is not highly temperature dependant over the 900C to 1050C range [McKay]. Therefore, to reduce the power requirements of the system, all mare scenarios are conducted at 900C. The length of processing time for each batch contributes to the oxygen yield. At a 3 hour batch the

reduction is assumed to be complete, yielding 3.6 wt%, and with a 1 hour batch processing time the reduction has completed the majority of the oxygen extraction achieving a 3 wt% yield. At a processing temperature of 900C and a water content of 0% there are again the same six parameters on which the overall system benefit depends: batch processing time, preheating time, payload mass, total processing time, number of launches, and launch range. The batch processing time and preheating time can both be optimized leaving the remaining four parameters for further system analysis.

6.2.1 Preheating time

The preheating times are calculated for launch ranges up to 10km and varied between 2 to 6 hours for each scenario. The system masses for each scenario with different preheating times are shown at high and low launch range values of 1 and 10km in figures 12A through 12D. Each data series in the graphs represents a different parameter scenario. The variables that define each scenario are the total processing time, payload mass, and the batch processing time. Each of these parameters has 2 possible values which gives 2^3 scenarios for comparison, as was used in the highland feedstock scenarios. Figures 12A and 12B display data for the four scenarios using a 200kg payload; figures 12C and 12D show the 1000kg payload data sets. Figures 12B and 12D only display two data series because at the 10 kilometer range a 500hr total processing time yields system masses that have blown up to extremely large values over the entire range of preheating times. From the analysis of these graphs the minimum heating times are shown for each scenario. It can also be noted that the 1 hour batch has a significantly lower overall system mass than the 3 hour batch in all cases.

This is in contrast to the highland soil feedstock systems where the opposite was true. The optimal heating times for each scenario are again defined as the preheating time at which the system mass is minimized. These values are listed in table 7. As was seen with the highland type feedstock data, the number of launches has a very small affect on the optimal heating time due to the small amount of additional hydrogen and tank mass iterated into the system. This amounts to an optimal heating time change of less than 0.05 hours, which is not significant in this model's calculations.

Mare type feedstock Optimal Heating times									
	Total Time (hr)	Payload Mass (kg)	Batch Time (hr)	# of launches	Launch Range of Optimization (km)				
					0.1	0.5	1	5	10
					Optimal heating times (hrs)				
Scenario 1	1000	200	1	1	2.9	3.0	3.0	3.1	3.1
				5	2.9	3.0	3.0	3.1	3.1
				10	2.9	3.0	3.0	3.1	3.1
Scenario 2	1000	200	3	1	5.1	5.2	5.3	5.4	5.4
				5	5.1	5.2	5.3	5.4	5.4
				10	5.1	5.2	5.3	5.4	5.4
Scenario 3	1000	1000	1	1	3.0	3.1	3.1	3.1	3.1
				5	3.0	3.1	3.1	3.1	3.1
				10	3.0	3.1	3.1	3.1	3.1
Scenario 4	1000	1000	3	1	5.3	5.3	5.3	5.4	5.4
				5	5.3	5.3	5.3	5.4	5.4
				10	5.3	5.3	5.3	5.4	5.4
Scenario 5	500	200	1	1	3.0	3.0	3.1	N/A	N/A
				5	3.0	3.0	3.1	N/A	N/A
				10	3.0	3.0	3.1	N/A	N/A
Scenario 6	500	200	3	1	5.2	5.3	5.3	N/A	N/A
				5	5.2	5.3	5.3	N/A	N/A
				10	5.2	5.3	5.3	N/A	N/A
Scenario 7	500	1000	1	1	3.1	3.1	3.1	N/A	N/A
				5	3.1	3.1	3.1	N/A	N/A
				10	3.1	3.1	3.1	N/A	N/A
Scenario 8	500	1000	3	1	5.3	5.4	5.4	N/A	N/A
				5	5.3	5.4	5.4	N/A	N/A
				10	5.3	5.4	5.4	N/A	N/A

Table 7: Mare feedstock optimal heating times

The optimal heating time varies over a 10 kilometer launch range by several 10ths of an hour. This difference produces a maximum change in system mass of approximately 1 kilogram at the 10 kilometer launch range. Preheating times can be optimized at each launch range. Launch ranges much above 10km are shown to be unrealistic for this system, so the maximum values for the preheating times that are used are the optimal heating times for the 10km launch range. Using preheating times less than the 1 kilometer optimal value produces a significant rise in system mass at all launch ranges that is proportional to the launch range. The total mass for a system using a preheating time optimized at a 1 kilometer range is contrasted with the overall mass of a system using a heating time of 50% the optimal value at 1 kilometer in figure 13.

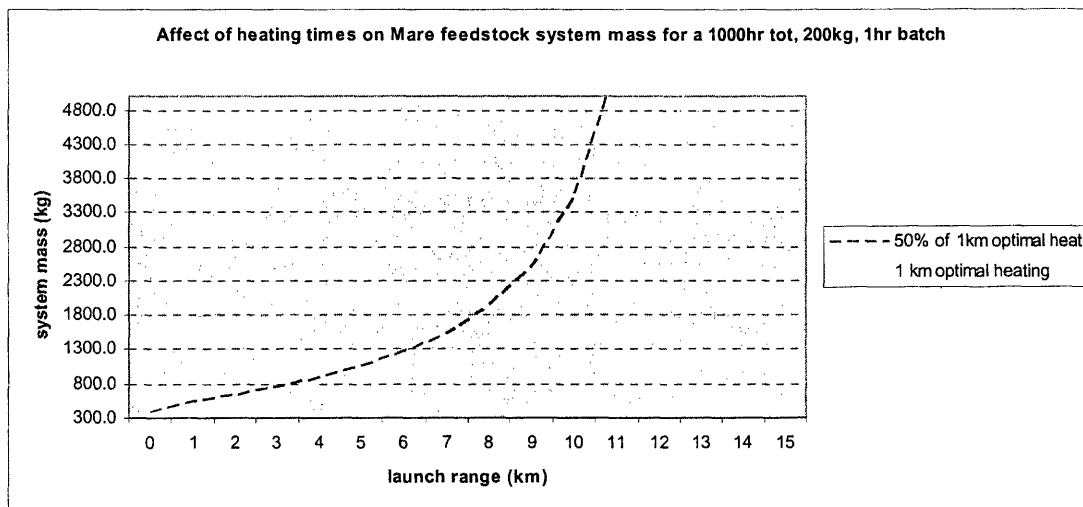


Figure 13: Optimal heating time affects on system mass. Two data series are shown, one for a short range optimal heating time and one for half that time to display the affect of using heating times below the optimal values.

The benefit of using optimal heating times is clear. Similar trends are shown in each scenario. In an actual mission design there may be constraints on the preheating times that can be used. The batch size or volume may have physical limitations from the spacecraft. Several parameters can be changed to lower the batch size: batch processing time, preheating time, and total processing time. Using a preheating time below the optimal values will decrease the batch size at the expense of the overall system mass. The affect of using a shorter preheating time on the batch size is shown in figure 14. Data for a scenario using the 1km optimal heating time is contrasted with the data for a preheating time of 50% the 1km optimal value.

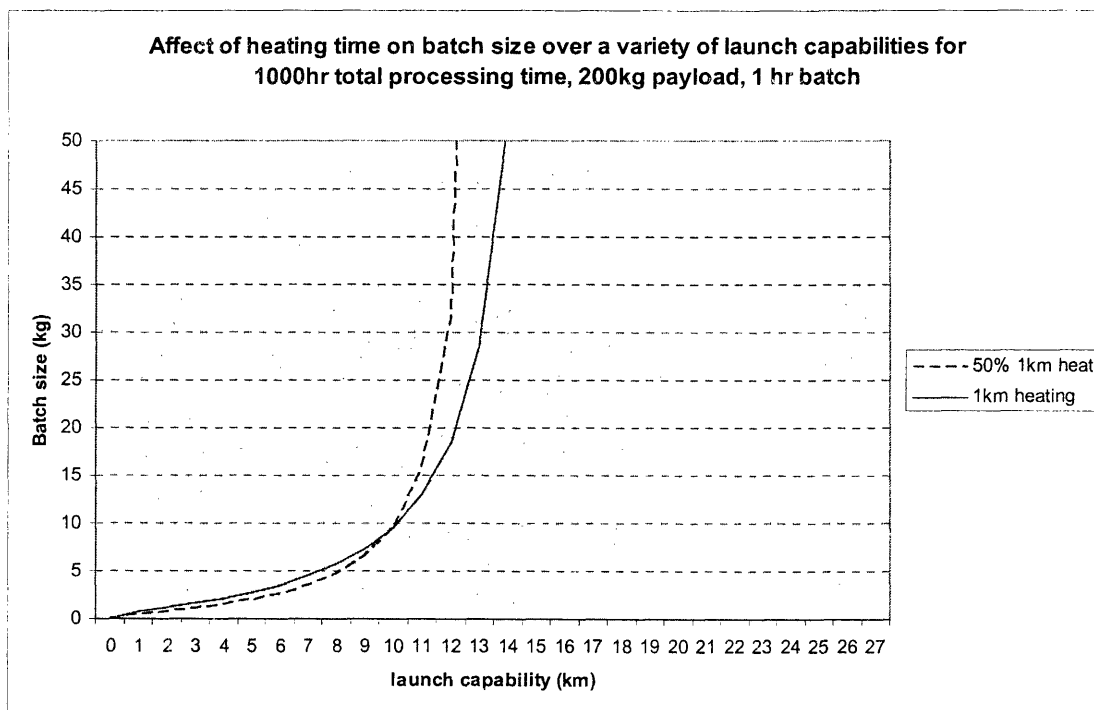


Figure 14: Affect of heating time on batch size. Two data series from one parameter scenario are shown to display the affect of shortening the heating time on the batch size of the processing system.

The overall affect of using lower preheating times does not have a large affect on the batch size. Therefore increasing the total processing time, or reducing the batch processing time may be better ways of reducing the batch size. The total processing time has a much larger effect on the entire system. It can be recommended that the preheating times optimized for each range be utilized in any mission to minimize the overall system mass unless there are significant restraints on the batch size.

6.2.2 Maximum range of feasibility

The optimal heating times found in table 7 are used to determine the maximum range of feasibility for the mare feedstock scenarios. Any range above the range of feasibility causes the system mass to blow up because on the first iteration, the masses added required to launch the spacecraft are greater than the payload mass. The range of feasibility for each of the eight scenarios using a mare type feedstock is listed in table 8. It was noted from the highland feedstock system analysis that doubling the total processing time increases the range of feasibility by a factor of 4. Tests with total processing times of 2000hr were also conducted which yield the same dynamic. Doubling the total processing time cuts the batch size in half which therefore cuts the power requirement and RTG mass in half. The propellant mass required to launch the spacecraft is a linear function of the mass of the craft but a function of the square root of the range. Therefore, this mass savings from changing the total processing time amounts to an increase in the range of feasibility by a factor of the square of the change in the total processing time.

Mare type feedstock range of feasibility				
Total Time (hr)	Payload Mass (kg)	Batch Time (hr)	# of launches	Range of Feasibility (km)
1000	200	1	1	14.58
			5	13.37
			10	12.05
			15	10.91
			20	9.91
1000	200	3	1	11.10
			5	10.29
			10	9.40
			15	8.60
			20	7.90
1000	1000	1	1	16.29
			5	15.04
			10	13.65
			15	12.42
			20	11.32
1000	1000	3	1	12.48
			5	11.64
			10	10.68
			15	9.83
			20	9.06
500	200	1	1	3.62
			5	3.47
			10	3.29
			15	3.12
			20	2.96
500	200	3	1	2.76
			5	2.66
			10	2.54
			15	2.42
			20	2.31
500	1000	1	1	4.04
			5	3.88
			10	3.69
			15	3.52
			20	3.35
500	1000	3	1	3.10
			5	2.99
			10	2.86
			15	2.74
			20	2.63

Table 8: Mare feedstock range of feasibility

Increasing the total processing time to 2000hrs creates a range of feasibility of approximately 59km for a scenario with a 200kg payload, 1hr batch processing time, and 1 launch. A 2000 hour total processing time is four times larger than the 500 hour total processing time, and 59km is approximately 16 times larger than the 3.6km range of

feasibility for the 500hr total processing time system. For the remainder of the mare feedstock system analyses each scenario will be analyzed over its range of feasibility. Launch ranges above this value are not considered because the system mass never converges.

6.2.3 Batch processing time

For the mare feedstock systems the batch processing times are again limited to either 1 or 3 hours. Figures 12A-12D above yield valuable information concerning which batch processing time is more beneficial to the overall system. In each scenario graphed, at optimal heating times, the one hour batch yields a much smaller system mass than the 3 hour batch. This is true over the entire range of feasible launches for these systems.

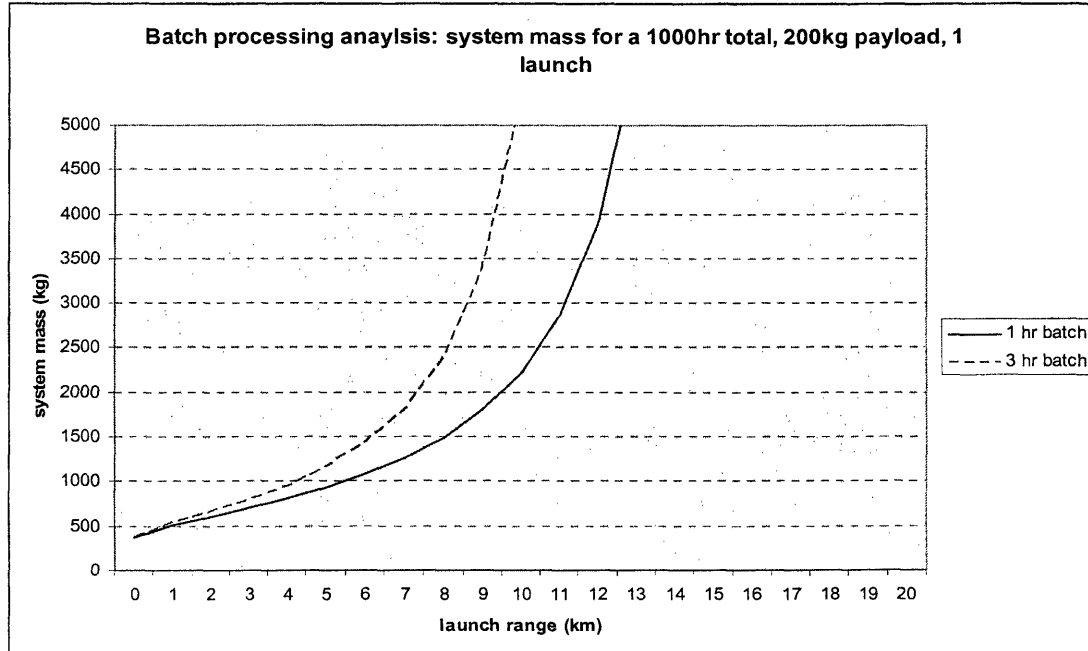


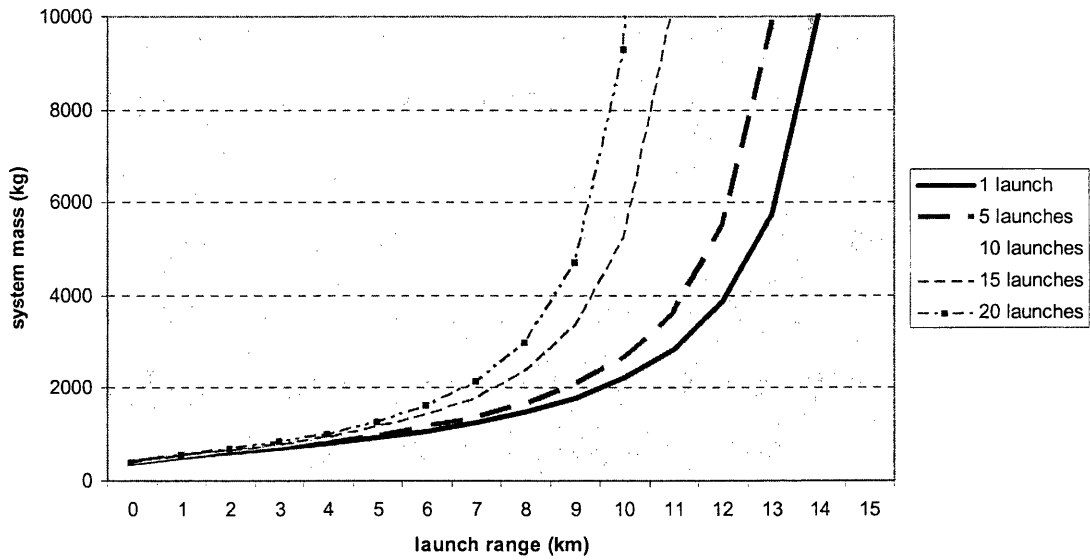
Figure 15: Mare feedstock batch processing time comparisons. Both a one and 3 hr batch processing time are displayed to show the difference in system mass at all feasible launch ranges.

The trend is very similar to the increase in system masses shown by reducing the heating time below the optimal values; however, the magnitude of the increase in system mass by using a 3 hour batch instead of a 1 hour batch is significantly different. Figure 15 shows the system masses for both the 1 and 3 hour batch scenarios over all the feasible launch ranges for a system using a 1000hr total processing time, 200kg payload, and with 1 launch. Similar findings are noted for other parameter scenarios as well. In all cases for the mare feedstock systems, using a 1 hour batch results in a lower overall system mass. The batch processing time and preheating time can both be limited to optimal values. Therefore, the scenarios listed in tables 7 and 8 can now be cut in half by holding the batch processing time to its optimal value of 1hr.

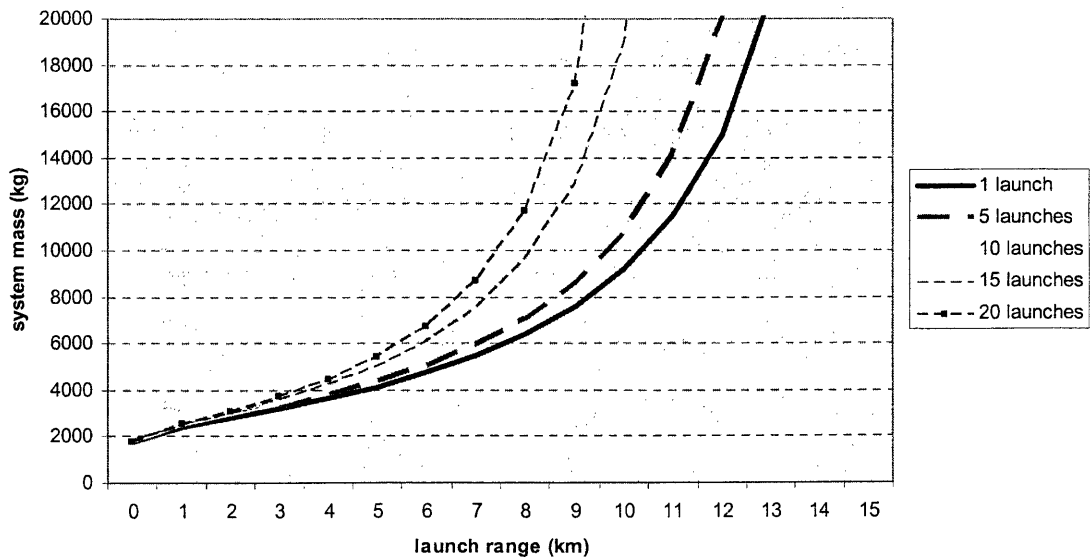
6.2.4 Launch number

The number of launches changes the maximum range of benefit for the mare system in a similar manner to the highland systems. Figures 16A through 16D show the affect of additional launches on the total system mass for each of the four remaining mare feedstock scenarios. The same general trends are noticed in these graphs as were found for the highland type systems. Additional launches increase the overall system mass proportionally by the range of the launch. The magnitude of the system mass is extremely different in graphs 16A and 16C from graphs 16B and 16D because of the different initial payload masses used. Figure 16A and 16C use a 200kg payload while 16B and 16D use a 1000kg payload.

16A Affect of the number of launches on system mass for feasible launch ranges, 1000hr total processing time, 200kg payload



16B Affect of the number of launches on system mass for feasible launch ranges, 1000hr total processing time, 1000kg payload



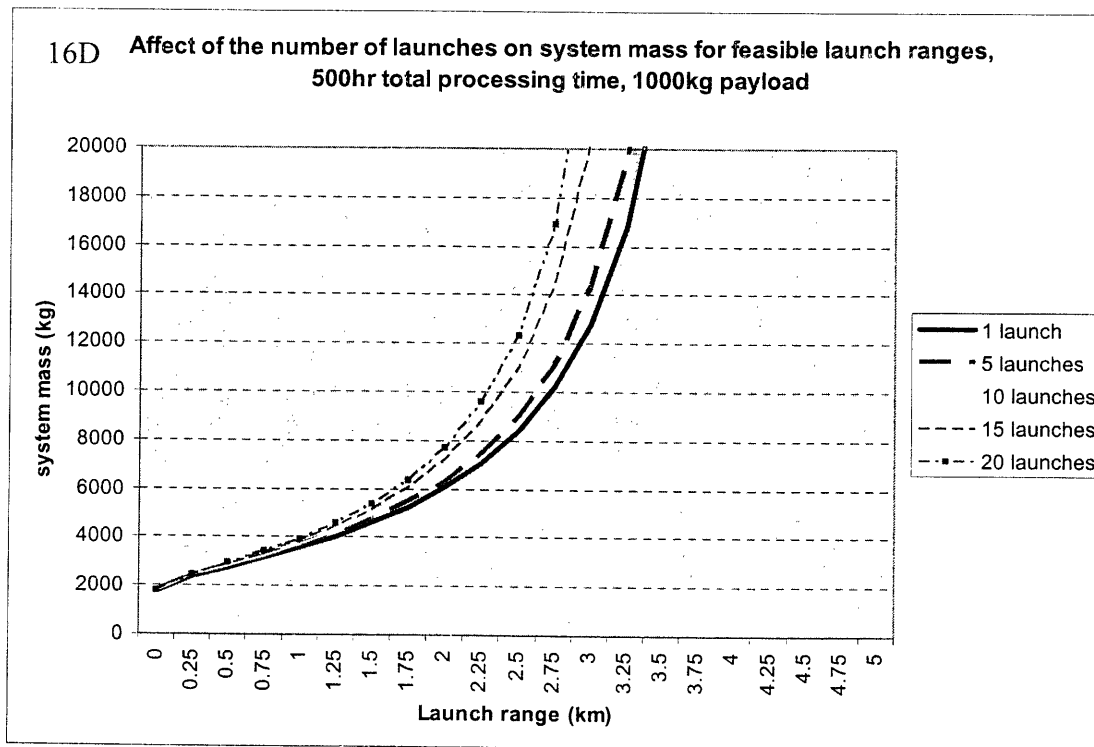
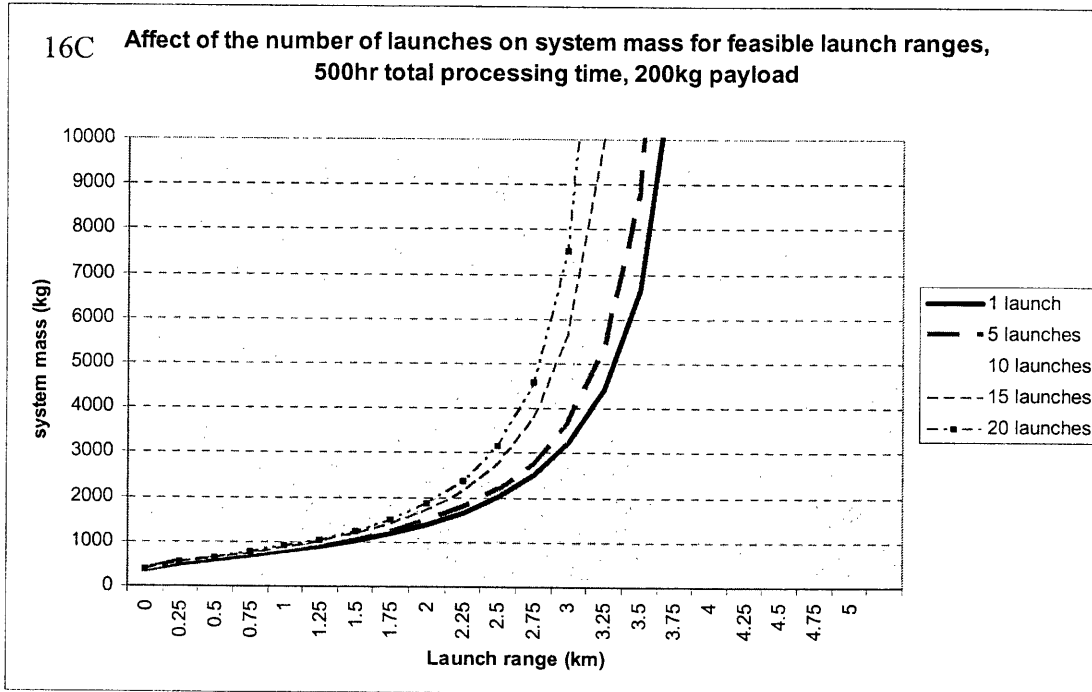


Figure 16A-16D: Mare feedstock launch number comparisons. Four graphs are shown, one for each of the four parameter scenarios, with data series for 1 to 20 launches. The X-axis is over the feasible launch ranges, and the y-axis is the total system mass.

By plotting the data series for two scenarios with different total processing times against each other the relative overall system masses can be seen. Doubling processing times allows a system with the same mass to reach a range 4 times further. This dynamic was explored earlier and is shown in a graphical form in figure 17.

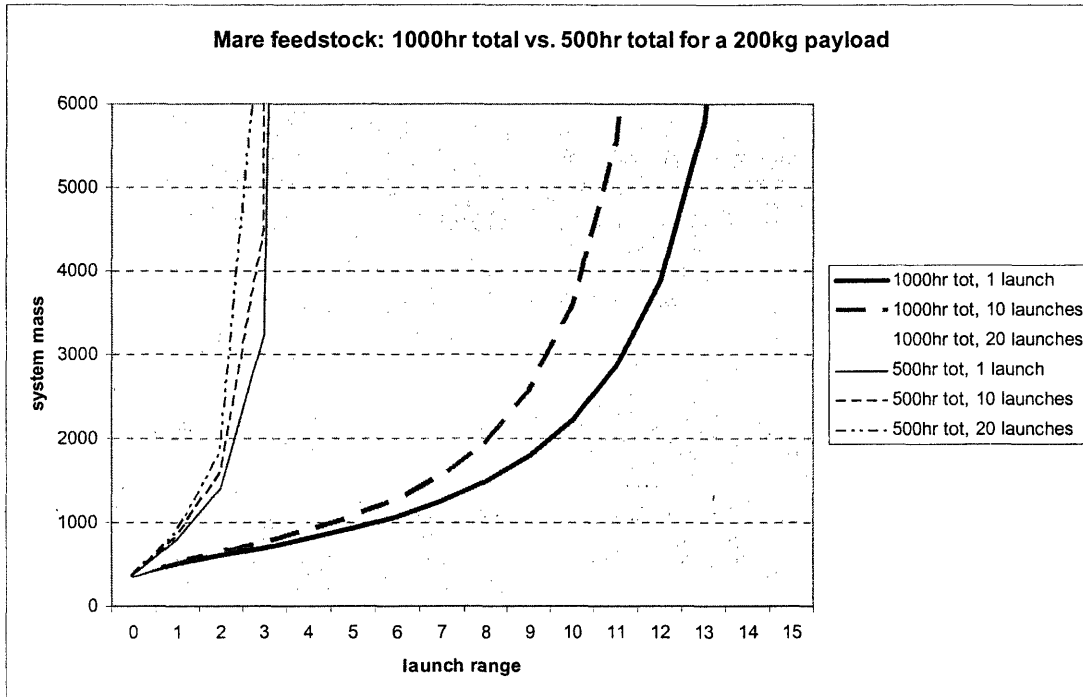


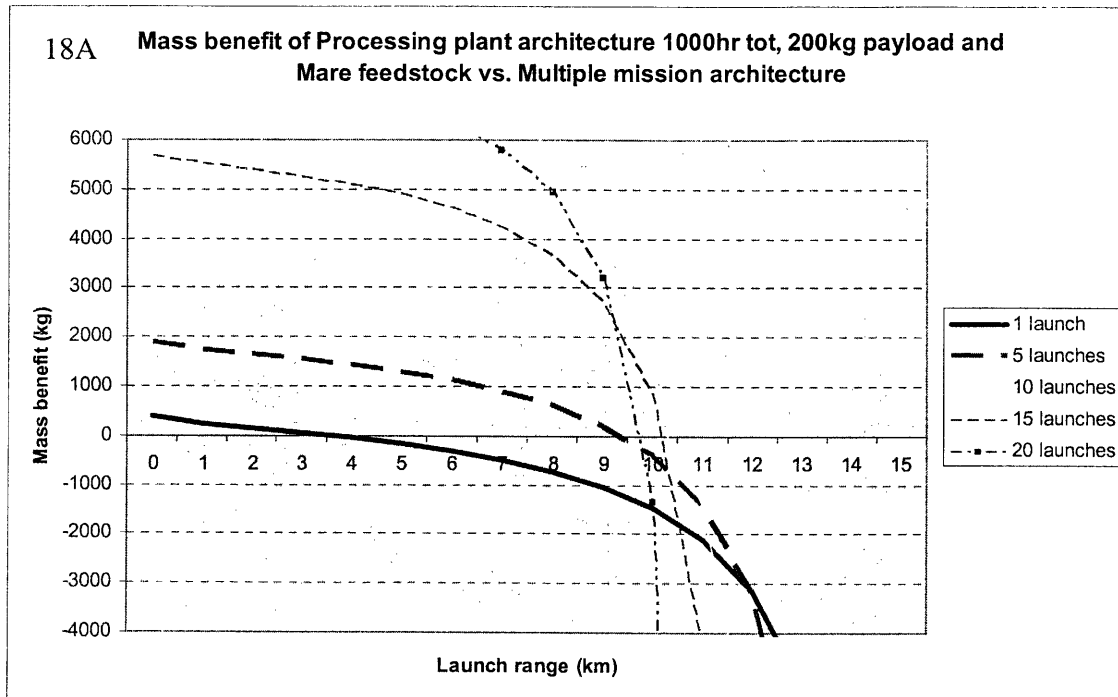
Figure 17: Mare feedstock total time comparisons. This graph takes the system masses of two scenarios with different total times to display the change in system mass for different total processing times per launch.

6.2.5 Mass benefit and system feasibility

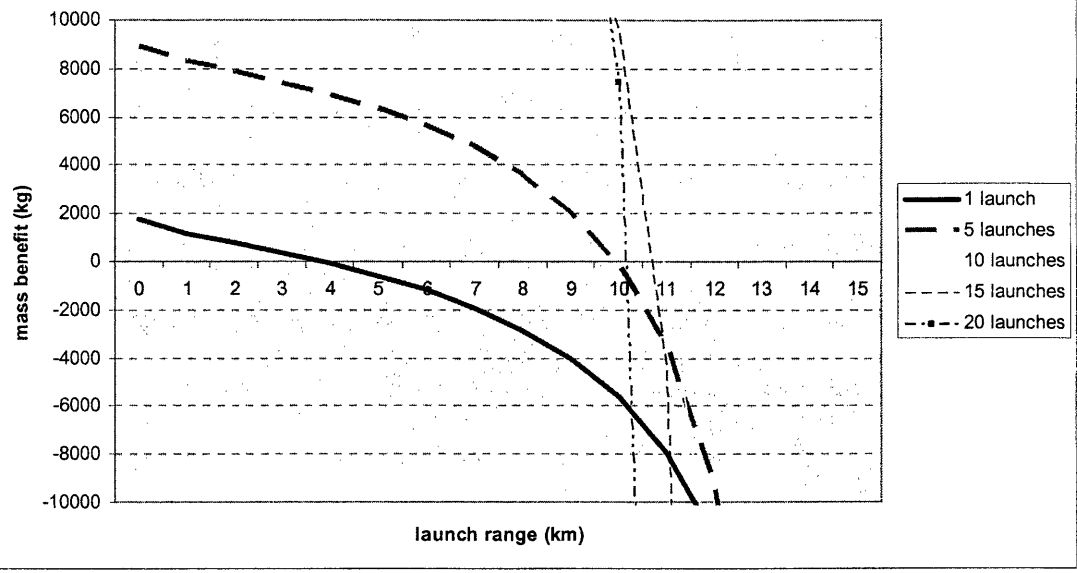
The mass benefit of the processing system versus the two other architectures is the basis for comparison for the processing system with any feedstock type. The mare feedstock processing plant yields a more positive mass benefit than the highland feedstock system due to the higher oxygen yield of the feedstock. The mass benefit values for each architecture are explored below.

6.2.5.1 Benefit vs. multiple mission architecture

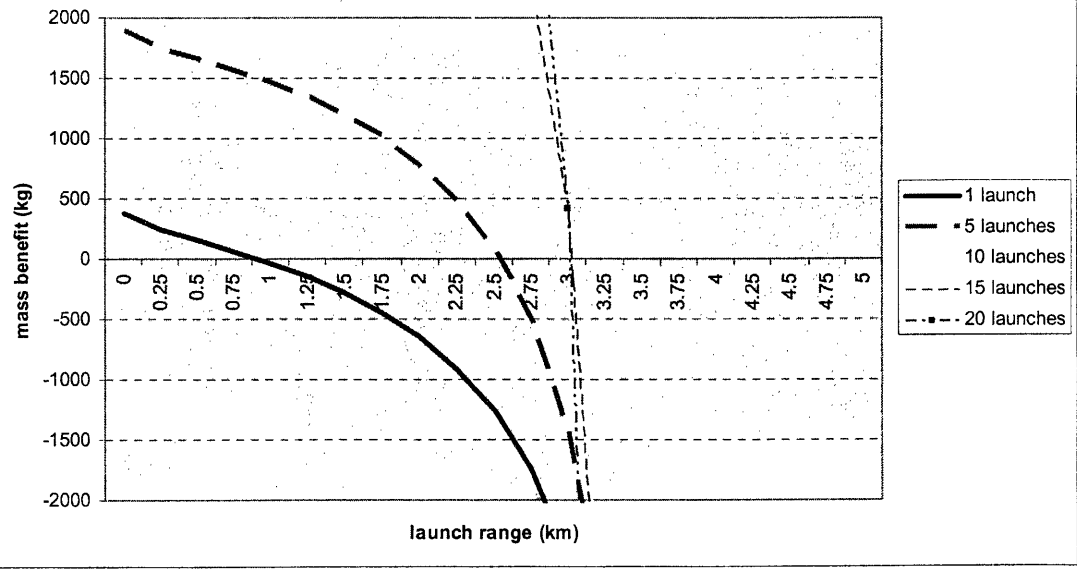
The multiple mission architecture is not affected by any of the processing system parameters other than the number of launches. The same trends in the data sets are visible for the mare system as were seen in the highland system. The only difference is that the maximum range of benefit for the mare system is an order of magnitude larger than for the highland system. Figures 18A through 18D show the mass benefit of the processing plant architecture with a mare feedstock versus the multiple mission architecture.

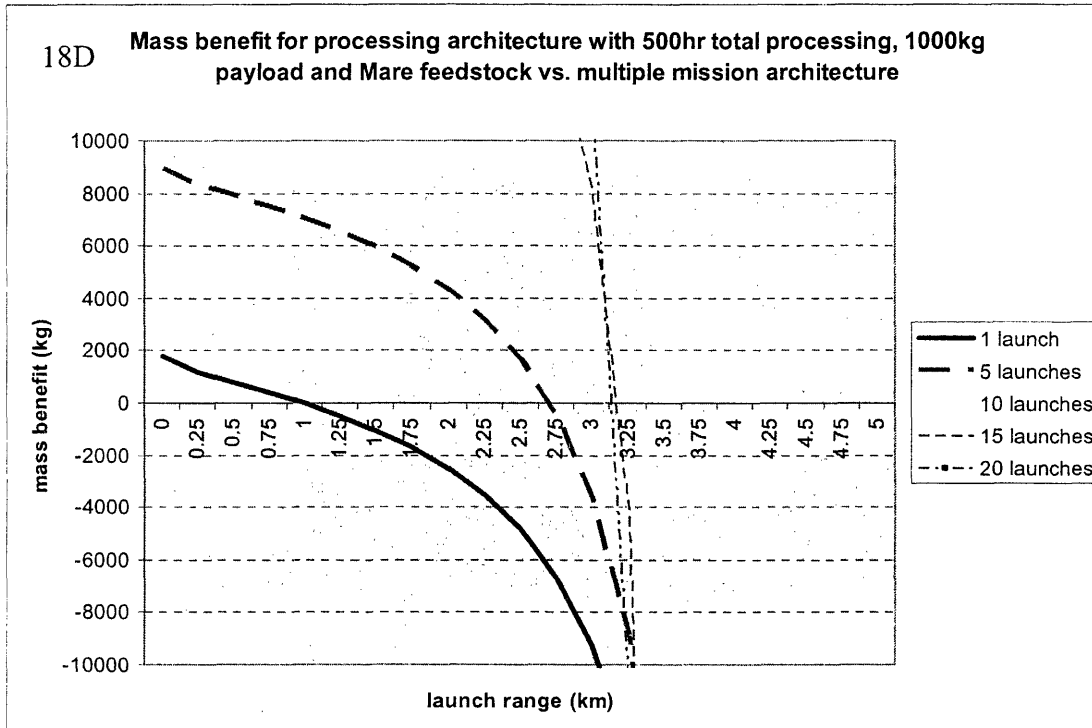


18B Mass benefit for processing architecture with 1000hr tot, 1000kg payload with a Mare feedstock vs. Multiple mission architecture



18C Mass benefit for processing architecture with 500hr tot, 200kg payload and Mare feedstock vs. multiple mission architecture





Figures 18A-18D: Mare feedstock mass benefit vs. multiple mission architecture. Four graphs show the mass benefit for each of the four scenarios with launch numbers between 1 and 20.

The highland feedstock system's maximum range of benefit did not reach the range of feasibility before the 20 launch maximum that this model is design to analyze. However, the mare system reaches that maximum value at 12 launches for a 1000hr total processing time system. Therefore, the addition of launches beyond twelve reduces the maximum beneficial range that the system can achieve. The 500hr total processing time system reaches this point at 18 launches, and is closer to the highland type systems when looking at the mass benefit comparisons. The maximum range of benefit is plotted for each number of beneficial launches in figure 19.

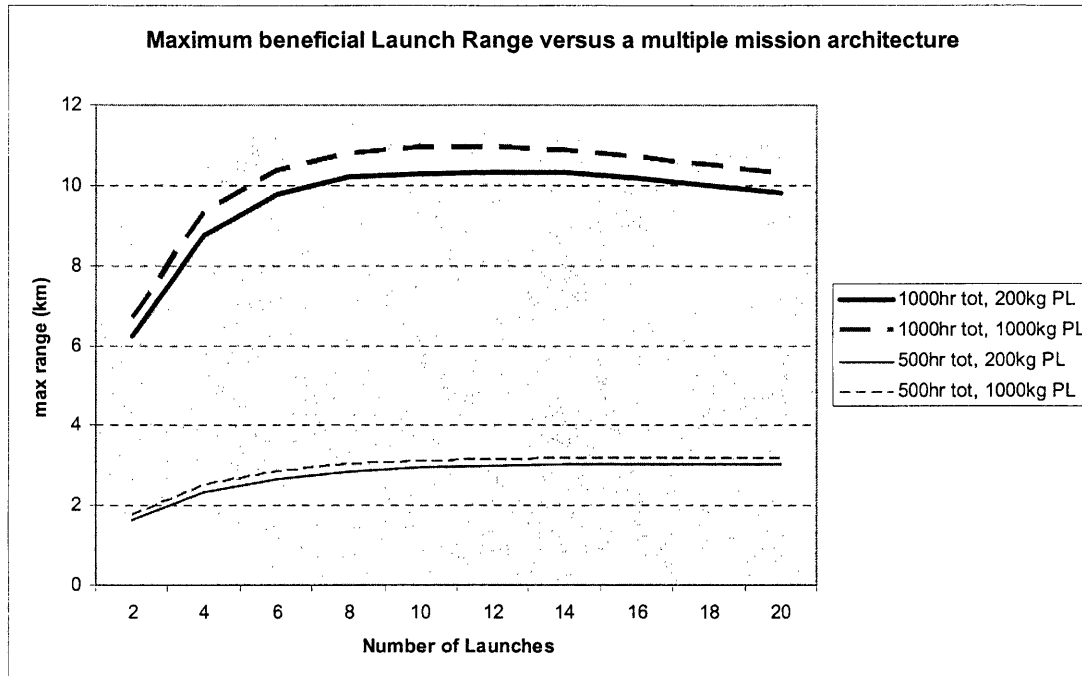
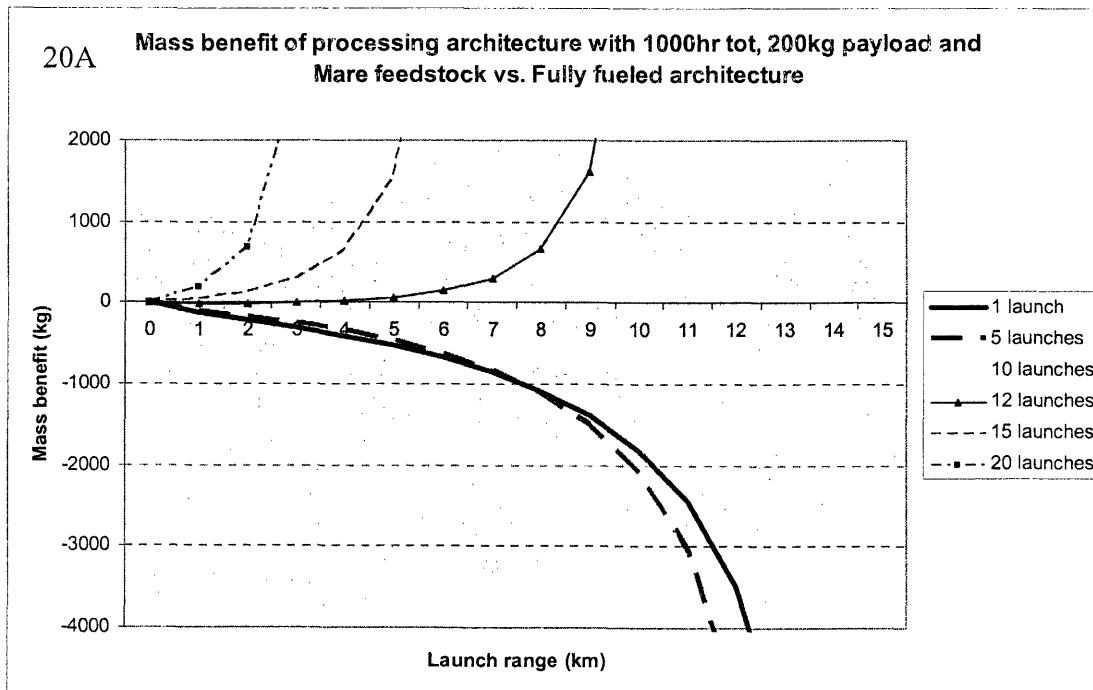


Figure 19: Mare feedstock maximum beneficial range. Four data series display the maximum beneficial range for each scenario over launch numbers between 2 and 20. The maximum beneficial range is found at the peak of each data series.

The number of launches with the maximum range of benefit is shown in this graph where the data series reach a maximum. This is also the point where the range of benefit approaches the range of feasibility of the system. It is important to note that the range of benefit for each number of launches is somewhat less than the range of feasibility. As the processing plant scenario's launch range approaches the range of feasibility, its system mass will begin to blow up. However, it will not diverge until the range is at or above the range of feasibility, it will eventually converge but at very high values. Therefore, because the mass of the multiple mission architecture does not blow up with range, the range of benefit must be somewhat smaller than the range of feasibility.

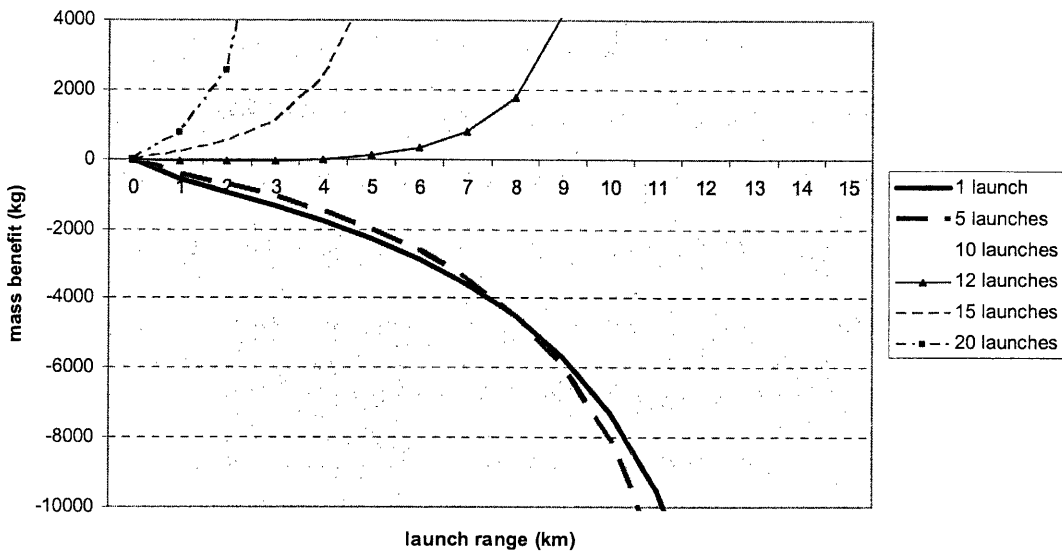
6.2.5.2 Benefit vs. the fully fueled architecture

The fully fueled architecture is dependant upon the launch range as well as the number of launches. The two mare feedstock system scenarios using a 1000hr total processing time yield a slightly different result than the highland systems. For low launch numbers the system still has a negative mass benefit; however, for high launch numbers (12 or greater) the system yields a positive mass benefit. These are shown in figures 20A and 20B below. The two mare feedstock system scenarios using a 500hr processing time yield results very similar to the highland feedstock systems. For all possible launch ranges and number of launches the systems result in a negative mass benefit. This is shown in figures 20C and 20D.



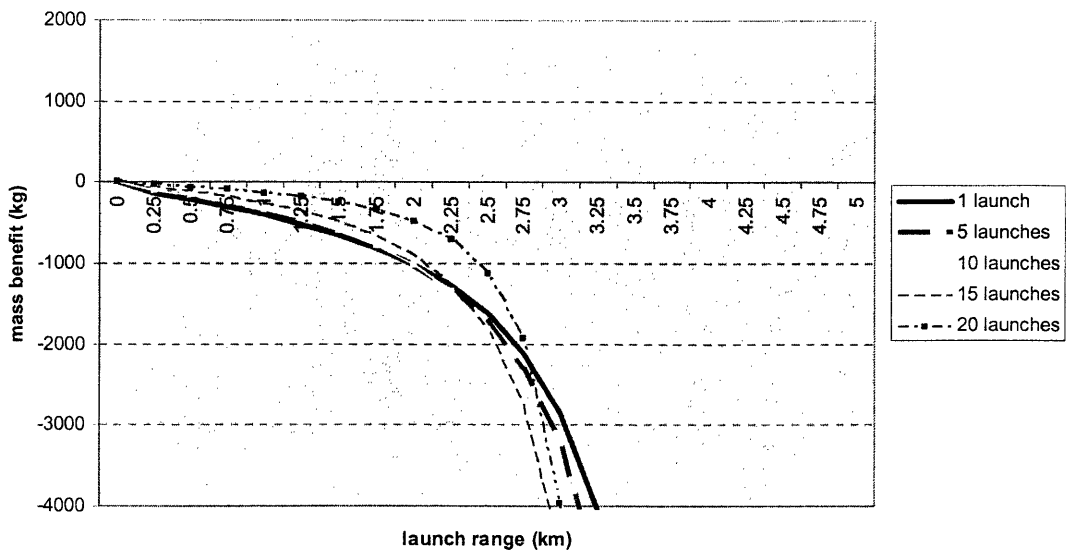
20B

Mass benefit for processing architecture with 1000hr tot, 1000kg payload, with a mare feedstock vs. Fully fueled architecture



20C

Mass benefit of processing architecture with a 500hr tot, 200kg payload and Mare feedstock vs. fully fueled architecture



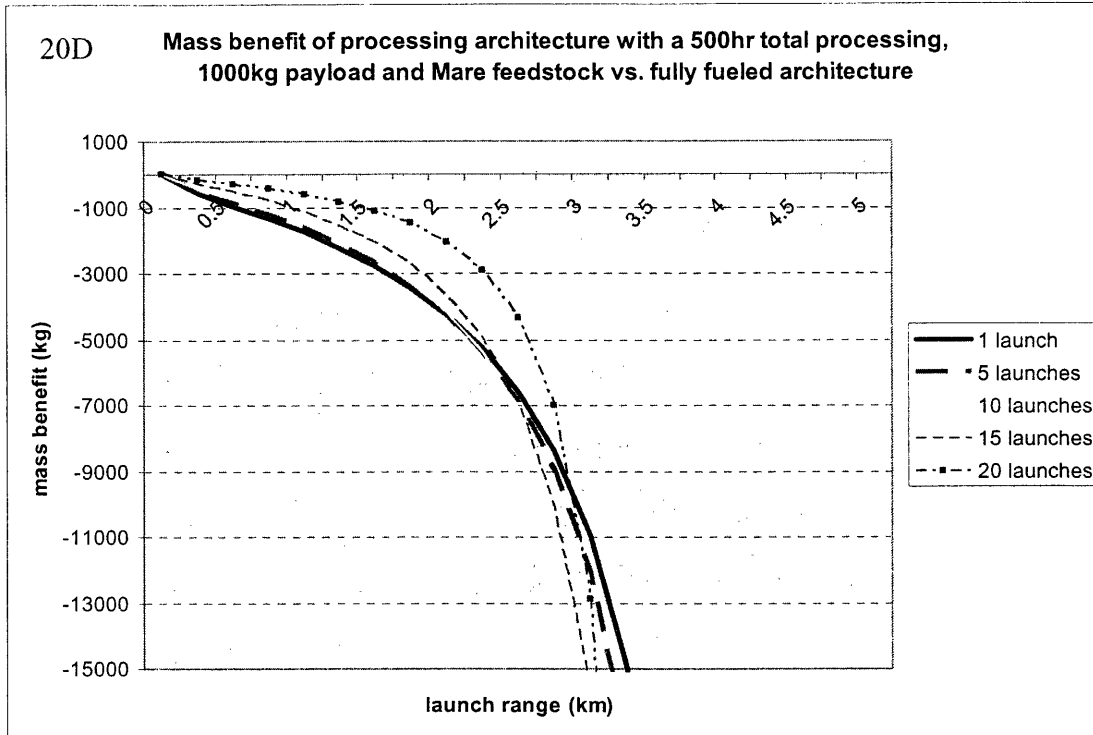


Figure 20A-20D: Mare feedstock mass benefit vs. fully fueled architecture. Each scenario is shown in one graph with launch numbers between 1 and 20. Scenarios with a 1000hr total processing time show some positive mass benefit.

The behavior of the mass benefit curves can again be explained by the approximation developed in section 6.1.5. The switch from a negative mass benefit to a positive benefit, caused by a heavy dependence on range of the fully fueled system components, occurs at 12 launches for the 1000hr total processing time system, but at slightly above the 20 launch number maximum that the model can analyze for the 500hr total processing time systems. Therefore, it can be assumed that a 500hr total processing time system using mare regolith as the feedstock is not a beneficial architecture for lunar exploration. However, if the total processing time is increased to 1000hrs then a positive mass benefit over both architectures is achieved. Figures 20C and 20D show very clearly the change in benefit caused by putting more launches onto any scenario. Larger launch numbers increase the benefit

versus the fully fueled architecture up to a certain range where the furnace and RTG mass outweigh the additional mass components of the fully fueled system.

6.2.5.3 Overall System feasibility

In determining the overall feasibility of a mare type system, both the mission length and the total system mass must be considered. Tables 9a and 9b list the total mass of the system required for a number of launches and the total distance that it can achieve (number of launches multiplied by launch range). A beneficial mission must be designed for a minimum of 12 launches. With each launch requiring approximately 2 months of mission time (processing time is assumed to be $\frac{3}{4}$ the mission time) this makes for a mission length of 2 years (or longer if it is designed for more launches). A two year time frame is not unreasonable. However, there may be stresses on the processing system over such an amount of time. With long duration time periods the processing system as well as the power system will experience some amount of degradation. Further study is needed on the hydrothermal reduction system to properly quantify this degradation. This model does not incorporate any system degradation with time into the processing architecture. To glean further information out of tables 9a and 9b one can compare the masses of systems that achieve the same total distance but with different numbers of launches and launch ranges. For example, a system making 12 lunar launches of 5 kilometers each travels a total distance of 60km over the length of its mission. A system making 15 launches at 4km each and one making 20 launches at 3 km each also travel a total of 60km in their mission lifetime. However, systems with a longer lifetime (making more launches), will experience a greater amount of system degradation which must be taken into account when designing

the missions. Further analysis of this system is required to achieve a more comprehensive view of the processing plant architecture using mare regolith as the feedstock. Additional model runs with longer total processing times need to be analyzed to compare their benefit with the 1000hr total processing time scenarios.

The processing plant architecture must also be compared to rover capabilities. Currently rovers can travel approximately 100 meters a day. For the processing plant's lunar launch period of 1000hr, or approximately 2 months of mission time, this amounts to a total distance of 5.6km. The maximum distance of benefit for the processing plant architecture is approximately 10.5km. Therefore the processing plant architecture is a beneficial exploration architecture compared to today's rover capabilities.

Mare total launch masses and distances

Table 9-A range per launch (Km)	12 launch capability		13 launch capability		14 launch capability		15 launch capability		16 launch capability		17 launch capability		18 launch capability		19 launch capability		20 launch capability	
	Total Range (km)	Lunar Orbit Mass (kg)	Total Range (km)	Lunar Orbit Mass (kg)	Total Range (km)	Lunar Orbit Mass (kg)	Total Range (km)	Lunar Orbit Mass (kg)	Total Range (km)	Lunar Orbit Mass (kg)	Total Range (km)	Lunar Orbit Mass (kg)	Total Range (km)	Lunar Orbit Mass (kg)	Total Range (km)	Lunar Orbit Mass (kg)	Total Range (km)	Lunar Orbit Mass (kg)
0	0	377.6	0	377.6	0	377.6	0	377.6	0	377.6	0	377.6	0	377.6	0	377.6	0	377.6
1	12	536.8	13	538.9	14	541.0	15	543.1	16	545.2	17	547.3	18	549.4	19	551.6	20	553.8
1.5	18	592.3	19.5	595.4	21	598.5	22.5	601.6	24	604.7	25.5	607.8	27	611.1	28.5	614.4	30	617.7
2	24	648.7	26	652.9	28	657.2	30	661.5	32	665.9	34	670.3	36	674.8	38	679.4	40	684.0
2.5	30	707.9	32.5	713.5	35	719.1	37.5	724.9	40	730.8	42.5	736.7	45	742.8	47.5	749.0	50	755.2
3	36	771.3	39	778.6	42	785.9	45	793.4	48	801.1	51	808.9	54	816.9	57	825.0	60	833.3
3.5	42	840.4	45.5	849.6	49	859.0	52.5	868.7	56	878.5	59.5	888.6	63	899.0	66.5	909.6	70	920.5
4	48	916.4	52	928.1	56	940.1	60	952.4	64	965.0	68	978.0	72	991.3	76	1005.0	80	1019
4.5	54	1001.2	58.5	1015.9	63	1031.0	67.5	1046.6	72	1062.7	76.5	1079.3	81	1096.4	85.5	1114.1	90	1132
5	60	1096.6	65	1115.1	70	1134.2	75	1154.0	80	1174.5	85	1195.7	90	1217.7	95	1240.6	100	1264
5.5	66	1205.3	71.5	1228.6	77	1252.7	82.5	1277.9	88	1304.0	93.5	1331.3	99	1359.8	104.5	1389.5	110	1420
6	72	1330.5	78	1359.9	84	1390.6	90	1422.7	96	1456.3	102	1491.6	108	1528.6	114	1567.5	120	1608
6.5	78	1476.5	84.5	1513.9	91	1553.2	97.5	1594.6	104	1638.2	110.5	1684.2	117	1732.9	123.5	1784.4	130	1839
7	84	1649.2	91	1697.2	98	1747.9	105	1801.8	112	1859.1	119	1920.0	126	1984.9	133	2054.3	140	2128
7.5	90	1856.6	97.5	1918.9	105	1985.4	112.5	2056.6	120	2133.0	127.5	2215.0	135	2305.4	142.5	2398.9	150	2502
8	96	2110.3	104	2192.5	112	2281.2	120	2377.0	128	2481.0	136	2594.1	144	2717.5	152	2852.7	160	3001
8.5	102	2427.2	110.5	2537.9	119	2658.7	127.5	2791.1	136	2936.6	144.5	3097.3	153	3275.4	161.5	3474.1	170	3696
9	108	2833.5	117	2986.4	126	3155.9	135	3344.4	144	3555.5	153	3793.1	162	4062.1	171	4369.1	180	4721
9.5	114	3370.9	123.5	3589.4	133	3836.1	142.5	4116.4	152	4437.5	161.5	4808.3	171	5240.1	180.5	5748.8	190	6354
10	120	4101.6	130	4496.8	140	4814.5	150	5255.5	160	5777.6	170	6402.0	180	7156.2	190	N/A	200	N/A
10.5	126	N/A	136.5	N/A	147	N/A	157.5	N/A	168	N/A	178.5	N/A	189	N/A	199.5	N/A	210	N/A

Table 9-B	12 launch capability	13 launch capability	14 launch capability	15 launch capability	16 launch capability	17 launch capability	18 launch capability	19 launch capability	20 launch capability	
range per launch (km)	Total Range (km)	Lunar Orbit Mass (kg)	Total Range (km)	Lunar Orbit Mass (kg)	Total Range (km)	Lunar Orbit Mass (kg)	Total Range (km)	Lunar Orbit Mass (kg)	Total Range (km)	Lunar Orbit Mass (kg)
0	0	1782.2	0	1782.2	0	1782.2	0	1782.2	0	1782.2
1	12	2479.6	13	2488.0	14	2496.5	15	2505.1	16	2513.7
1.5	18	2748.5	19.5	2731.0	21	2743.8	22.5	2756.3	24	2769.1
2	24	2959.2	26	2976.3	28	2993.6	30	3011.1	32	3028.3
2.5	30	3209.8	32.5	3222.2	35	3235.0	37.5	3247.8	40	3260.7
3	36	3475.9	39	3504.7	42	3534.1	45	3564.0	48	3593.5
3.5	42	3762.8	45.5	3799.3	49	3834.7	52.5	3874.7	56	3919.6
4	48	4057.7	52	4121.5	56	4165.4	60	4216.6	64	4265.8
4.5	54	4420.8	58.5	4477.9	63	4536.6	67.5	4597.0	72	4669.1
5	60	4805.1	65	4876.2	70	4949.5	75	5025.2	80	5103.5
5.5	66	5237.6	71.5	5326.0	77	5411.6	82.5	5492.7	88	5571.0
6	72	5729.1	78	5839.5	84	5953.5	90	6071.1	96	6199.4
6.5	78	6294.3	84.5	6432.8	91	6577.8	97.5	6729.9	104	6888.1
7	84	6952.2	91	7121.2	98	7311.6	105	7467.2	112	7614.3
7.5	90	7728.6	97.5	7852.0	105	8189.1	112.5	8441.2	120	8719.7
8	96	8659.3	104	8848.3	112	9257.6	120	9589.4	128	9946.3
8.5	102	9796.3	110.5	10176.2	119	10587.1	127.5	11035.0	136	11518.6
9	108	11215.6	117	11726.2	126	12285.6	135	12901.0	144	13681.0
9.5	114	13056.0	123.5	13741.7	133	14521.5	142.5	15407.2	152	16399.5
10	120	15450.6	130	16482.6	140	17613.5	150	18932.5	160	20453.3
10.5	126	18795.4	136.5	20320.5	147	21103.8	157.5	24218.3	168	26756.2
11	132	23706.9	143	N/A	154	N/A	165	N/A	176	N/A
11.5	138	N/A	149.5	N/A	161	N/A	172.5	N/A	184	N/A
12	144	N/A	156	N/A	168	N/A	180	N/A	192	N/A

Table 9: Mare total system masses and distances. Values for all beneficial launch numbers and ranges are shown for a Mare feedstock system using a 1000hr total processing time.

It is stated that the future Mars Science Laboratory (MSL) rover will travel a total of 30km in its 280 day lifetime. If driving continuously this amounts to a range of approximately 3 kilometers per month, or about 6 kilometers in the time that the processing plant system could launch to a new site. Again the processing plant architecture still exhibits a significant benefit compared to this rover capability. There are several scientific considerations to take into account when considering rovers versus the processing plant architecture; however, these are not addressed here. Different scientific goals may require a rover mission while for others it may be beneficial to utilize this architecture.

The masses of the spacecraft in lunar orbit required for both the 200kg and 1000kg payload systems are not unachievable. A 200kg payload mission could be launched to the moon using today's heavy lift boosters. To send a 1000kg processing mission would require the development of a larger rocket. Because of the feasible system masses and the benefit of the processing system over the multiple mission architecture and the fully fueled architecture as well as possible rover capabilities, it is concluded that for proper scientific goals a processing plant architecture could be a feasible and beneficial exploration system if using mare regolith as a feedstock and system degradation over time is not extreme.

6.3 Equatorial glassy feedstock

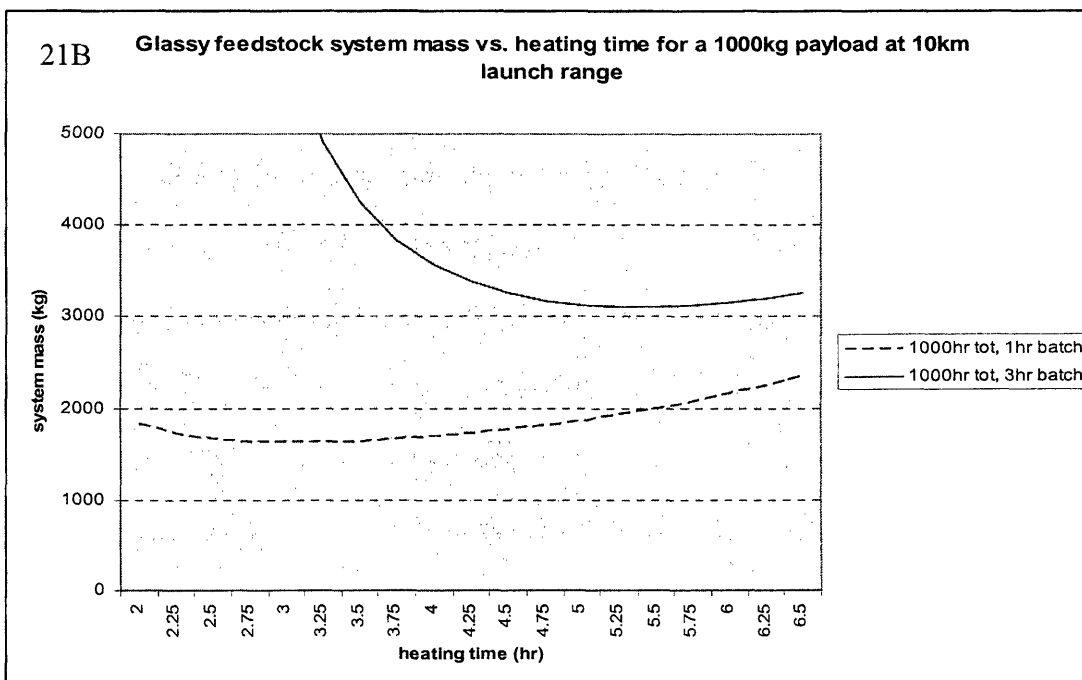
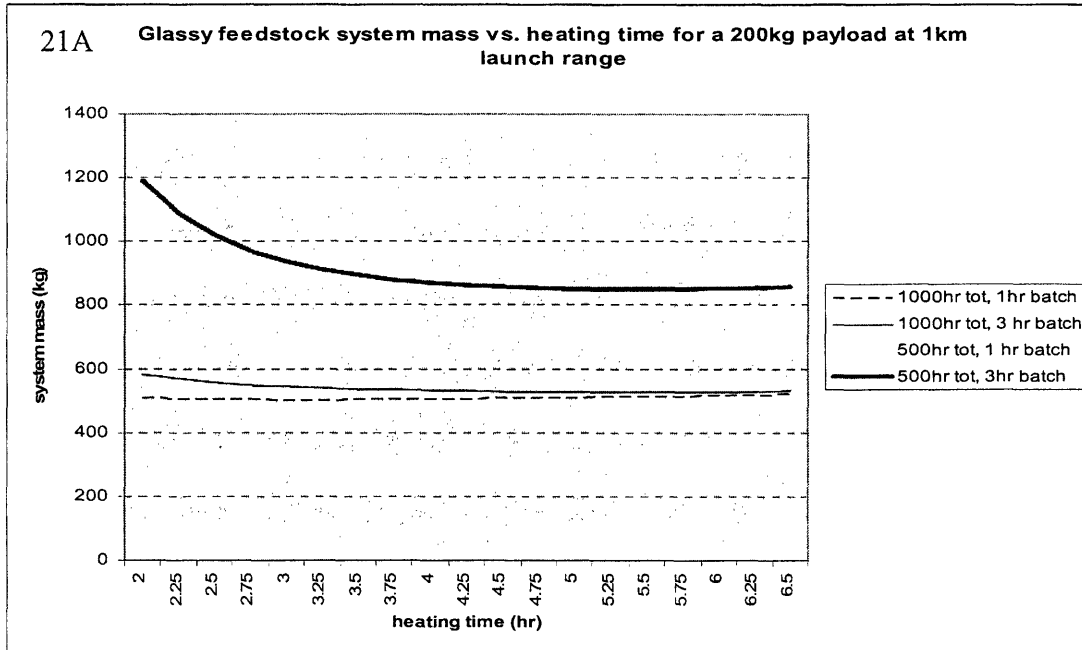
The pyroclastic glasses on the moon are not found in vast deposits covering large regions like the mare or highlands. So when considering them as a feedstock for this process it is

important to realize that a much more detailed knowledge is needed of where and to what extent pyroclastic glasses cover the lunar surface. The reduction of lunar glasses with hydrogen was found to be highly dependant upon the temperature of the process over the 900C to 1050C range. Higher temperatures yielded a significantly higher oxygen percent. The oxygen yield achieved at 900C from an Apollo glass sample in laboratory tests conducted by Carleton Allen was 1.75 wt% after 1 hour of processing and 2 wt% after 3 hours. At 1050C the oxygen yield was 3.6 wt% after 1 hour and 4.3 wt% after 3 hrs. Using glassy feedstock at a 900C processing temperature is little different than using a low yield mare feedstock. Therefore, in order to test the difference in system feasibility between mare and glassy feedstocks, the processing temperature is held at 1050C for all model runs. This will maximize the oxygen yield to values larger than those achieved by the general mare regolith feedstocks considered in the previous section.

6.3.1 Preheating time

The optimal heating times for all three feedstock types are very similar. The same system dynamics apply to all scenarios. Small deviations in the additional masses cause small deviations in the optimal heating times. The major source of difference in the optimal heating times from one scenario to the next is the change in batch size. The same eight scenarios are again used for analyzing the system parameters. Figures 21A through 21D show the system mass values for all eight scenarios at launch ranges of 1km and 10km. These graphs are very similar to graphs 12A-12D describing the mare system scenario preheating times. The only difference in the graphs is the scale of the system mass and a very slight change in where the minimum of each curve occurs. This shows that the

oxygen yield obtained from the type of feedstock has little affect on the optimal heating times.



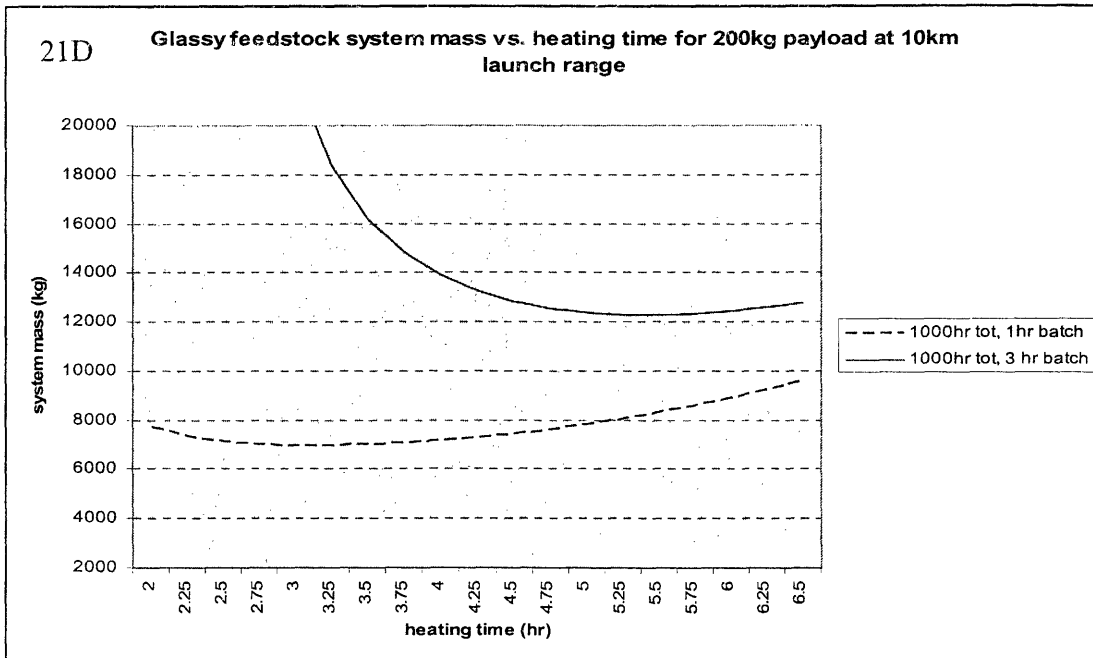
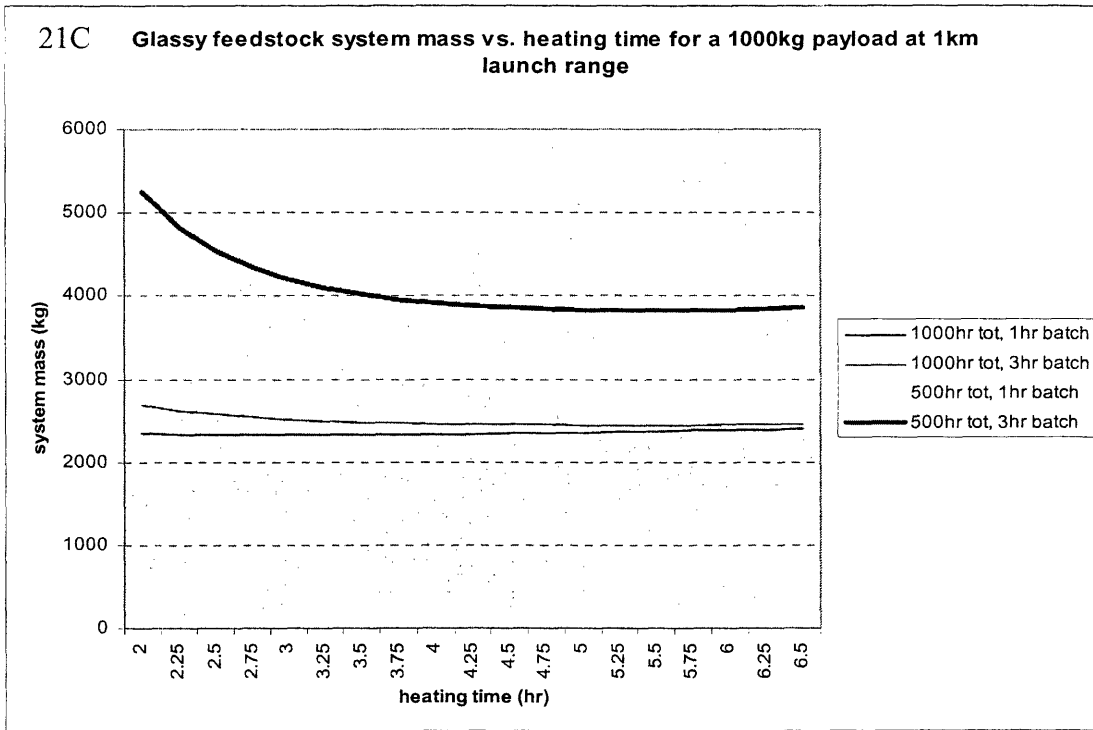


Figure 21A-21D: Glassy feedstock system mass vs. heating times. Four scenarios are shown at both a 1km and 10km launch range. The optimal heating time is shown at the minimum of each data series.

Figures 21B and 21D only show the data series for the 1000hr total processing time scenarios because the 500hr scenarios caused the system mass at both a 1 and 10km range to blow up.

Glassy type feedstock Optimal Heating times							
	Total Time (hr)	Payload Mass (kg)	Batch Time (hr)	# of launches	Launch Range of Optimization (km)		
					1	5	10
					Optimal heating times (hrs)		
Scenario 1	1000	200	1	1	3.03	3.07	3.07
				5	3.03	3.07	3.07
				10	3.03	3.07	3.07
Scenario 2	1000	200	3	1	5.28	5.36	5.40
				5	5.28	5.36	5.40
				10	5.28	5.36	5.40
Scenario 3	1000	1000	1	1	3.08	3.11	3.12
				5	3.08	3.11	3.12
				10	3.08	3.11	3.12
Scenario 4	1000	1000	3	1	5.36	5.40	5.43
				5	5.36	5.40	5.43
				10	5.36	5.40	5.43
Scenario 5	500	200	1	1	3.07	N/A	N/A
				5	3.07	N/A	N/A
				10	3.07	N/A	N/A
Scenario 6	500	200	3	1	5.34	N/A	N/A
				5	5.34	N/A	N/A
				10	5.34	N/A	N/A
Scenario 7	500	1000	1	1	3.10	N/A	N/A
				5	3.10	N/A	N/A
				10	3.10	N/A	N/A
Scenario 8	500	1000	3	1	5.40	N/A	N/A
				5	5.40	N/A	N/A
				10	5.40	N/A	N/A

Table 10: Glassy feedstock optimal heating times. Times are listed for each of the eight scenarios at 1,5,and 10km launch ranges, with 1,5, and 10 launches.

Table 10 shows the optimal heating times for the glassy feedstock scenarios. These are only slightly higher than the optimal times for the mare feedstock scenarios – on the

order of 0.01 hours, which is not a significant factor in this model. These preheating times are again used to analyze the remaining parameter values. The same increase in system mass is demonstrated when preheating times are dropped below their optimal values. For short launch distances this is not a large factor, but as the launch range is increased the difference in system mass becomes substantial. Optimal heating times are used for all further analyses.

6.3.2 Maximum range of feasibility

The maximum range possibly achieved by the glassy feedstock scenarios is higher than the bare scenarios. The increase in oxygen yield from the glassy feedstock creates this added benefit to the system. Doubling the total processing time again quadruples the maximum range of feasibility. This effect is also slightly dependent upon the number of launches. For a 1 launch system the range of feasibility for a 1000hr total processing time is almost exactly 4 times the range of feasibility for a 500hr total processing time.

However, as more launches are added to the system the range of feasibility drops faster for the systems with larger total processing times. The range of feasibility for a 1000hr total processing time, 200kg payload, and 1 hr batch system with 20 launches is less than 4 times the maximum range for the 500hr total processing time system with the same payload and heating time. This stems from the added mass going into the hydrogen tank for each launch. At the shorter ranges that are feasible for the 500hr total system, less hydrogen and tank mass are needed for each launch. Therefore, less mass is added to the system for each launch, and the range of feasibility does not decrease as fast with each

additional launch as it does when each launch has a greater range. The maximum range of feasibilities for glassy feedstock systems are listed in table 11.

Glassy type feedstock range of feasibility				
Total Time (hr)	Payload Mass (kg)	Batch Time (hr)	# of launches	Range of Feasibility (km)
1000	200	1	1	17.37
			5	15.81
			10	14.13
			15	12.68
			20	11.43
1000	200	3	1	12.76
			5	11.76
			10	10.67
			15	9.72
			20	8.87
1000	1000	1	1	19.39
			5	17.77
			10	15.99
			15	14.43
			20	13.07
1000	1000	3	1	14.32
			5	13.28
			10	12.12
			15	11.09
			20	10.17
500	200	1	1	4.31
			5	4.11
			10	3.88
			15	3.67
			20	3.47
500	200	3	1	3.17
			5	3.04
			10	2.89
			15	2.76
			20	2.63
500	1000	1	1	4.80
			5	4.60
			10	4.36
			15	4.13
			20	2.92
500	1000	3	1	3.55
			5	3.42
			10	3.27
			15	3.12
			20	2.98

Table 11: Glassy feedstock range of feasibility

6.3.3 Batch processing time

The preheating time graphs, figures 21A-21D, again yield a significant amount of information for the batch processing time as well. In all scenarios the 1 hour batch produces an overall lower system mass when optimal heating times are used. The mass benefit from using the 1 hour batch over the 3 hour batch is proportional to the range at which the system is launching, the size of the payload, and the preheating time. Taking a 1000hr total processing time, and a 200kg payload with just 1 launch we can analyze the affect of the two batch times over all feasible launch ranges.

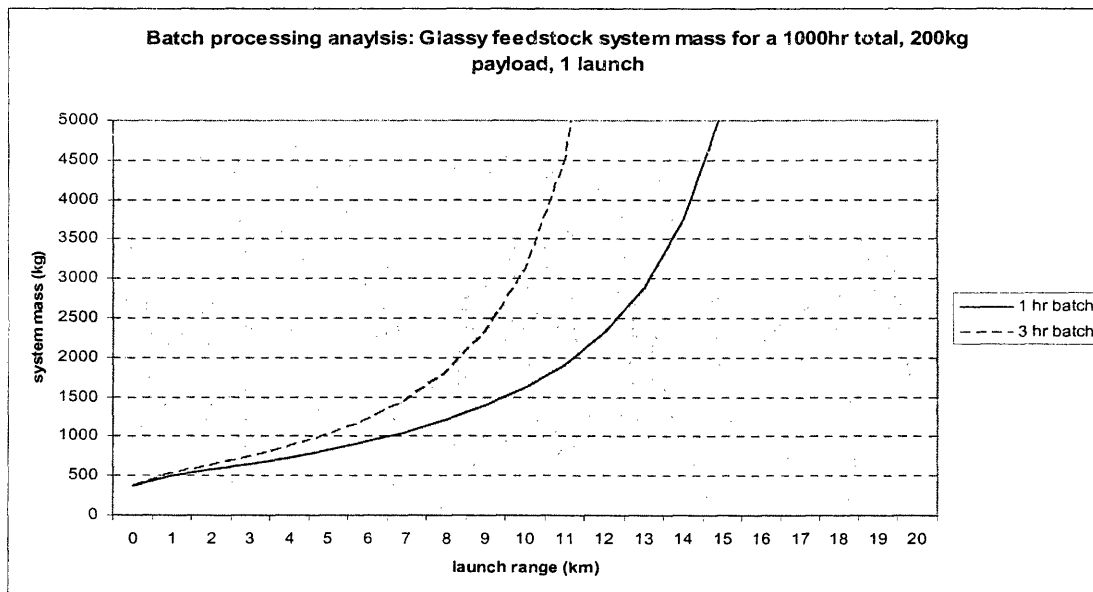


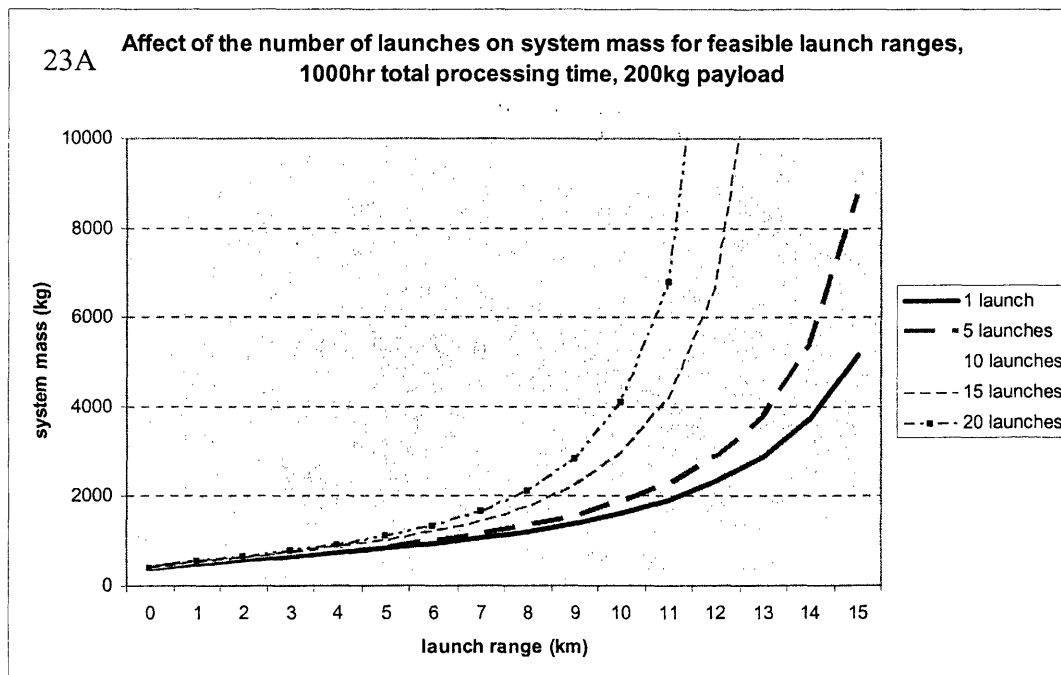
Figure 22: Glassy feedstock batch processing time comparisons. Both the 1 and 3 hr batch scenarios are shown in one parameter case using 1000hr total processing time and a 200kg launch, to show the difference in total system mass.

Comparing this graph to figure 15 displaying the same data for the mare system it is seen that for the same amount of system mass the glassy system can reach a larger launch

capability. This data also exhibits a similar trend to the mare graph but with different values for the system mass. The one hour batch processing time is utilized in the remaining glassy feedstock analysis.

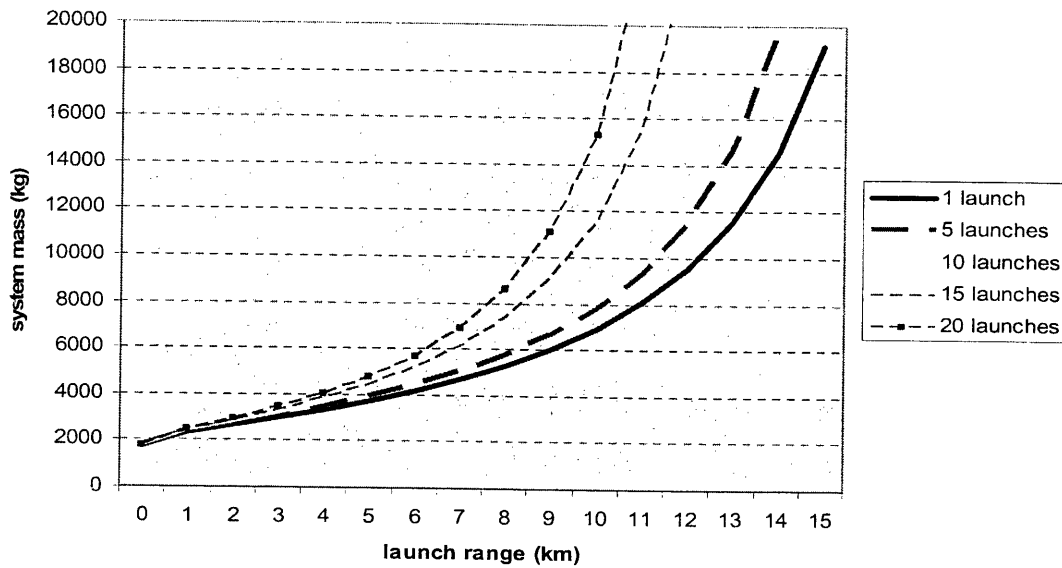
6.3.4 Launch number

The four scenarios using a 1 hr batch processing time that have been analyzed for the highland and mare systems will also be analyzed for the glassy feedstock systems. Figures 23A through 23D display the system mass for cases using launch numbers between 1 and 20 over all feasible launch ranges.



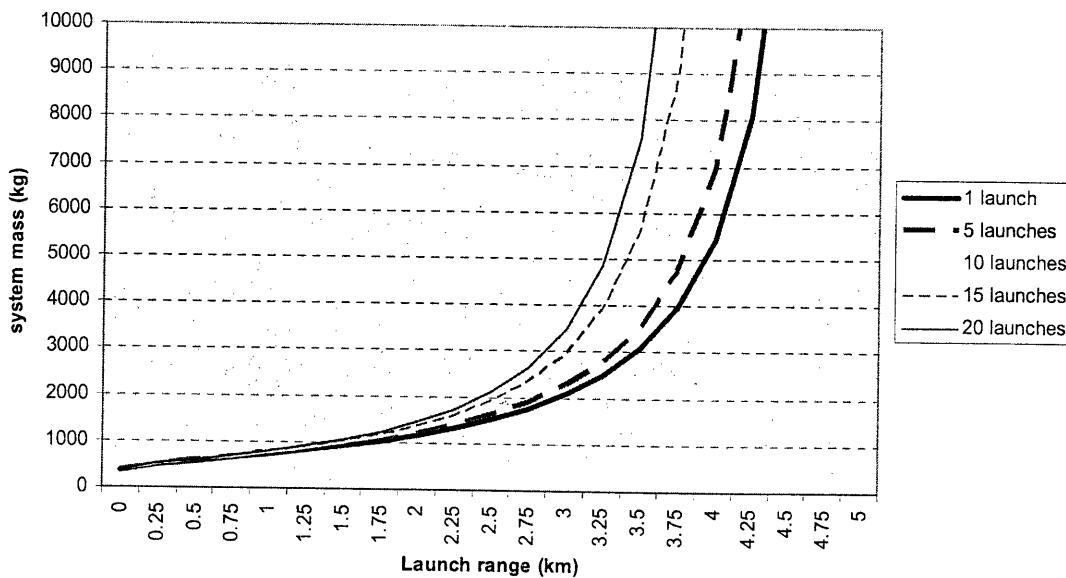
23B

Affect of the number of launches on system mass for feasible launch ranges, 1000hr total processing time, 1000kg payload



23C

Affect of the number of launches on system mass for feasible launch ranges, 500hr total processing time, 200kg payload



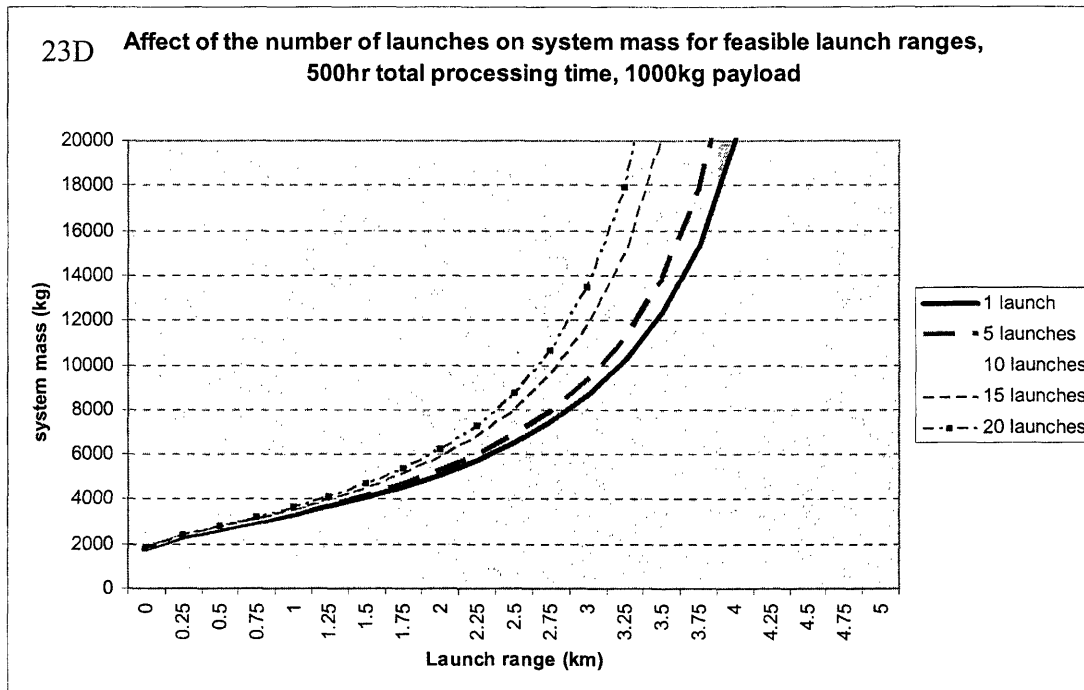


Figure 23A-23D: Glassy feedstock launch number comparisons. The four 1 hour batch processing time scenarios are shown with 1 through 20 launches. The system mass is displayed versus launch range to show how masses change with the number of launches for different ranges.

The scenarios using a 500hr total processing time reach the same system mass at much shorter ranges than the 1000hr scenarios, again following the rule that the increase in the range is a factor of the square of the increase in total processing time. The same difference is seen between launch numbers as was noted with the highland and mare feedstocks. Increasing the number of launches shortens the launch range that any mission can reach with the same overall system mass.

An additional scenario is created for comparisons using a 2000hr total processing time with a 200kg payload and an optimal heating time of 3.13hrs. This scenario is graphed against both the 1000hr and 500hr total processing time scenarios in figure 24 below.

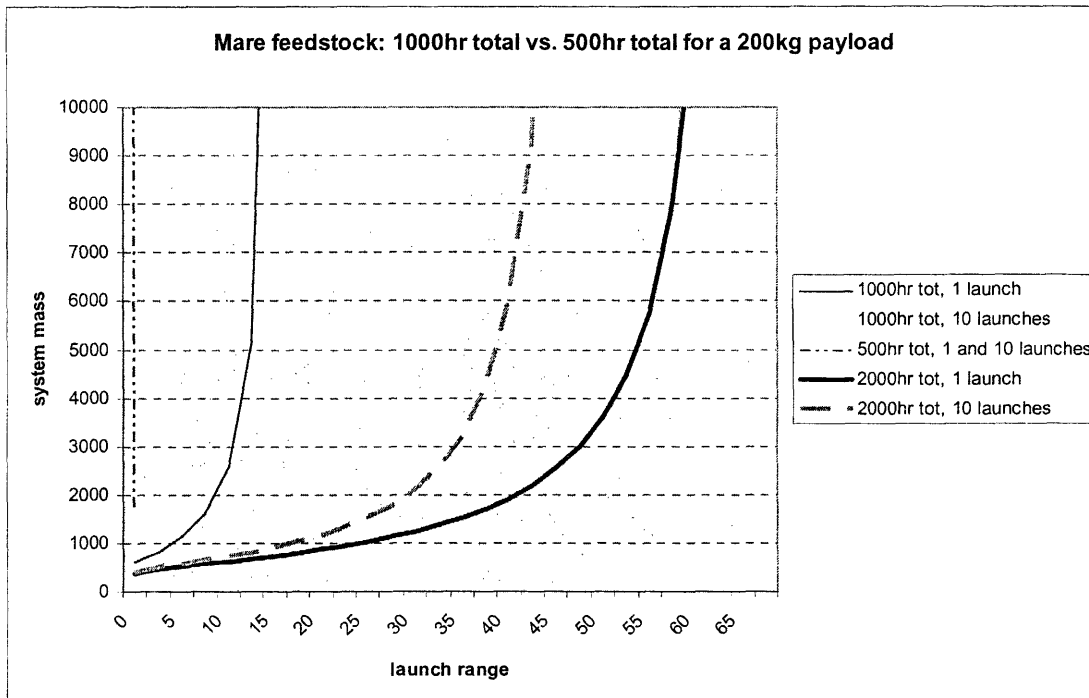


Figure 24: Glassy feedstock total processing time comparison. Comparisons are made between a 2000hr , 1000hr, and 500hr total processing time, to show the affect of different total times on the launch ranges that can be reached.

The difference in launch capabilities is clearly shown. Using longer total processing times is obviously very beneficial because the launch distance is increased by the square of the increase in total processing time. Longer processing times lead to other system complications as mentioned before. A 2000hr total processing time per launch will require further information on the processing system mechanics and system degradation that is not yet known to determine how long the total processing time can feasibly be.

6.3.5 Mass benefit and system feasibility

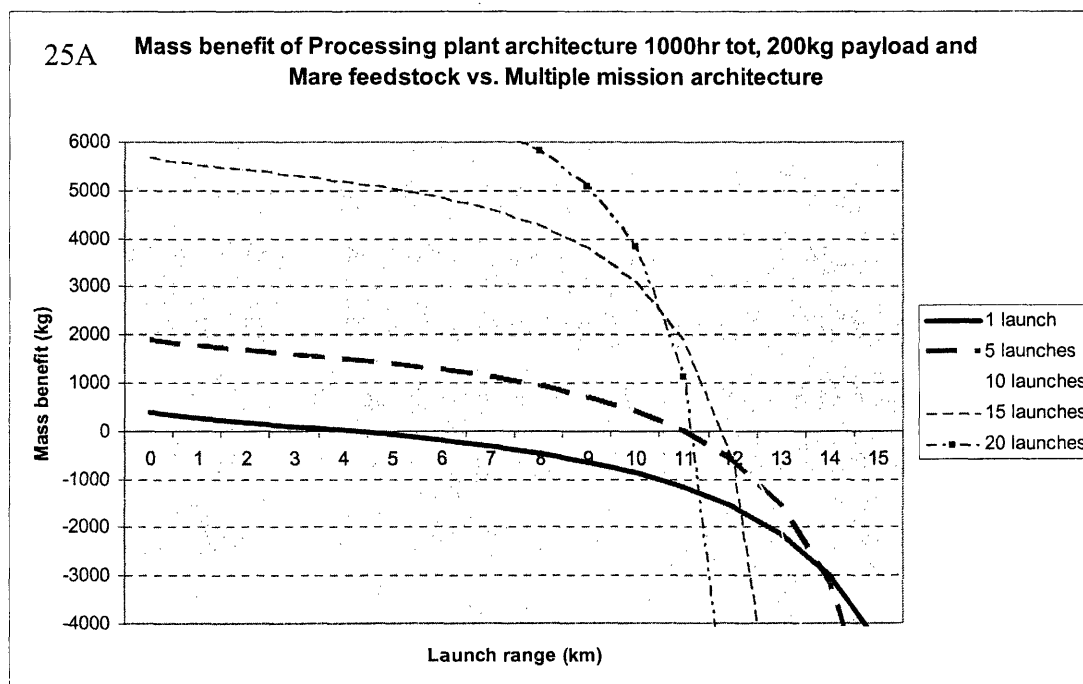
The mass benefit analysis for the glassy feedstock systems exhibit the same trends as the mare systems, but with increased benefits over the other architectures. The glassy system

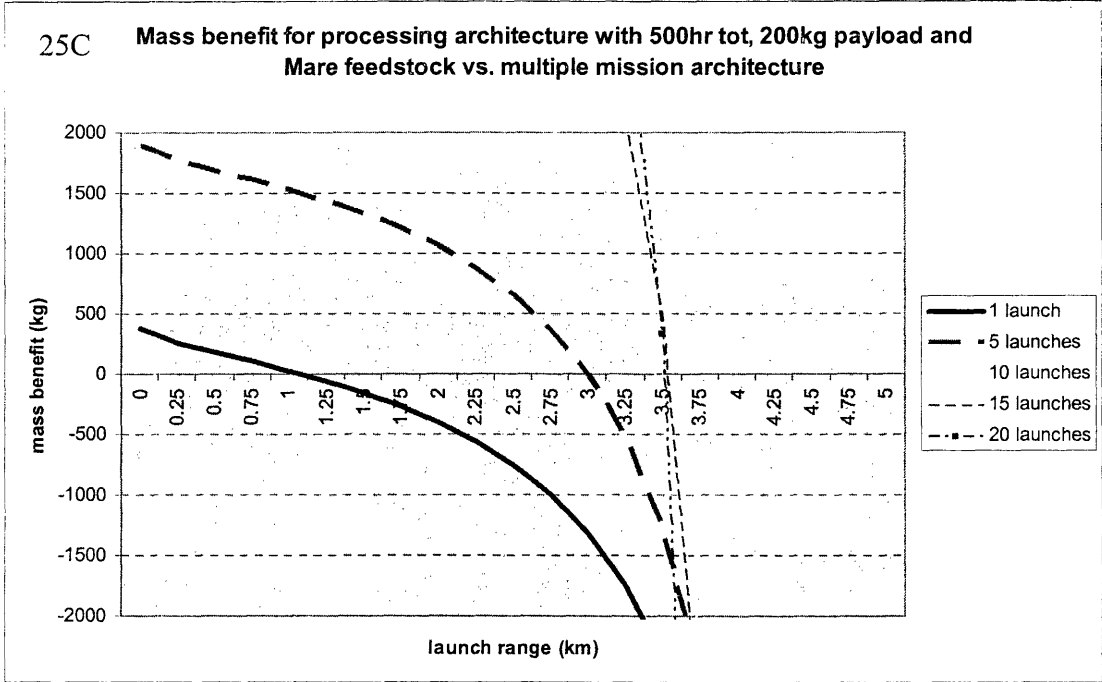
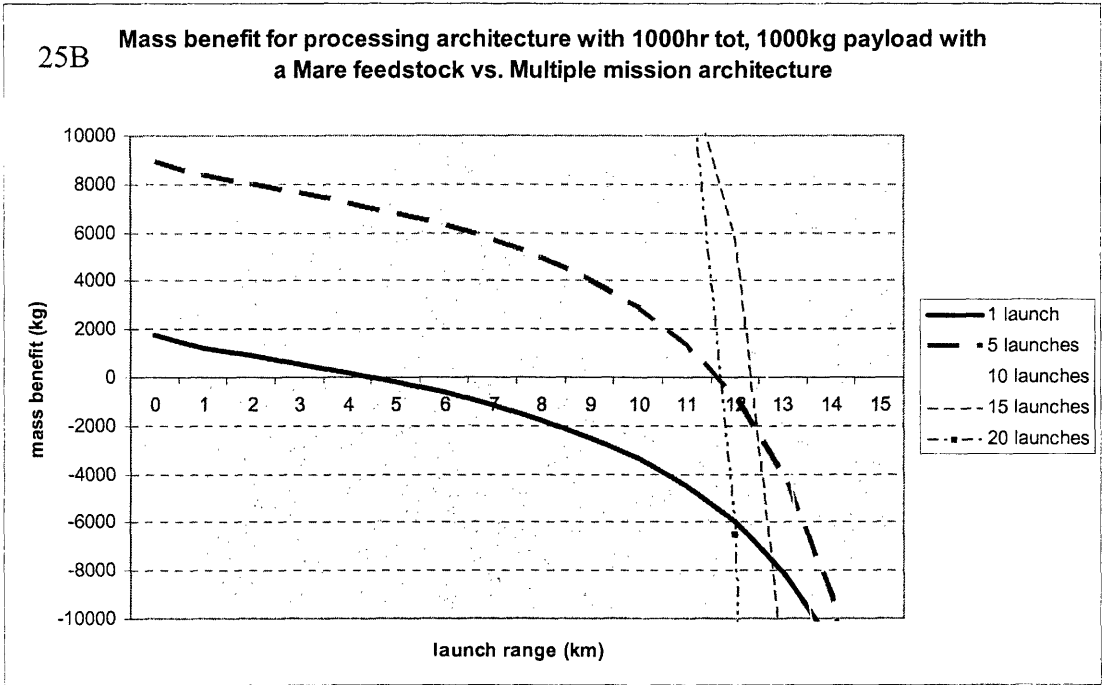
has longer beneficial launch ranges versus the multiple mission system and reaches a positive mass benefit versus the fully fueled architecture at lower launch numbers.

6.3.5.1 Benefit vs. Multiple Mission architecture

Figures 25A through 25E show the mass benefit versus the multiple mission architecture.

Figure 25E shows the mass benefit for the 2000hr total processing scenario. All 5 of these scenarios exhibit the same trends seen before. Increasing the number of launches increases the maximum range of benefit for the system until the range of benefit nears the range of feasibility of the system as a whole. At this point, additional launches reduce the maximum range of benefit.





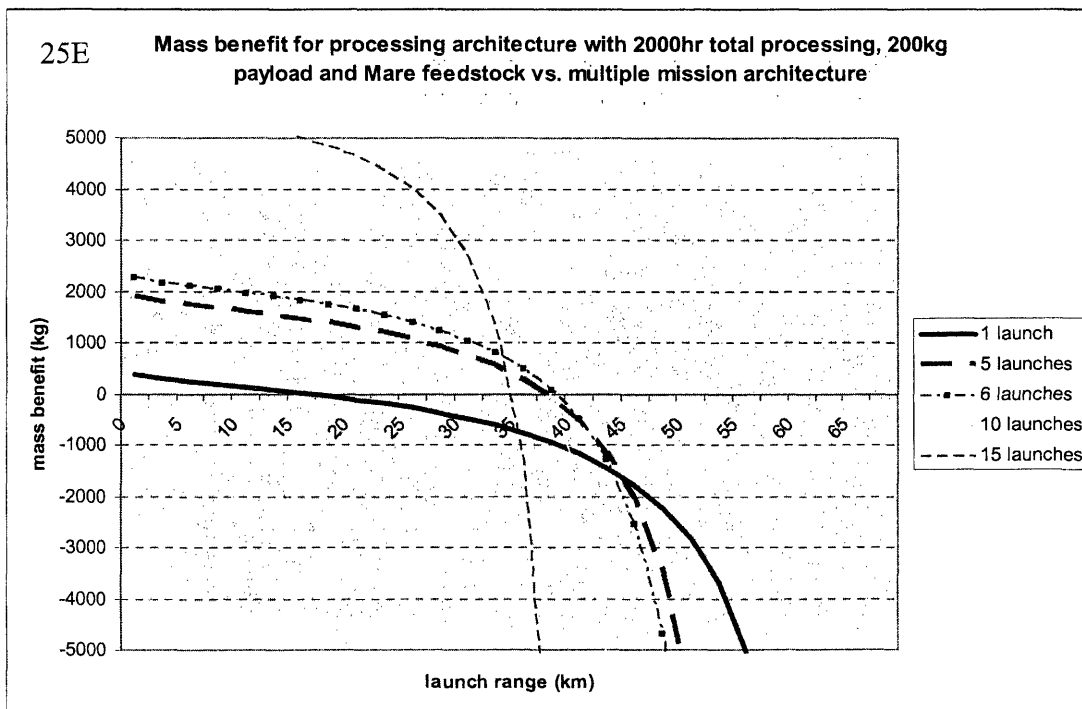
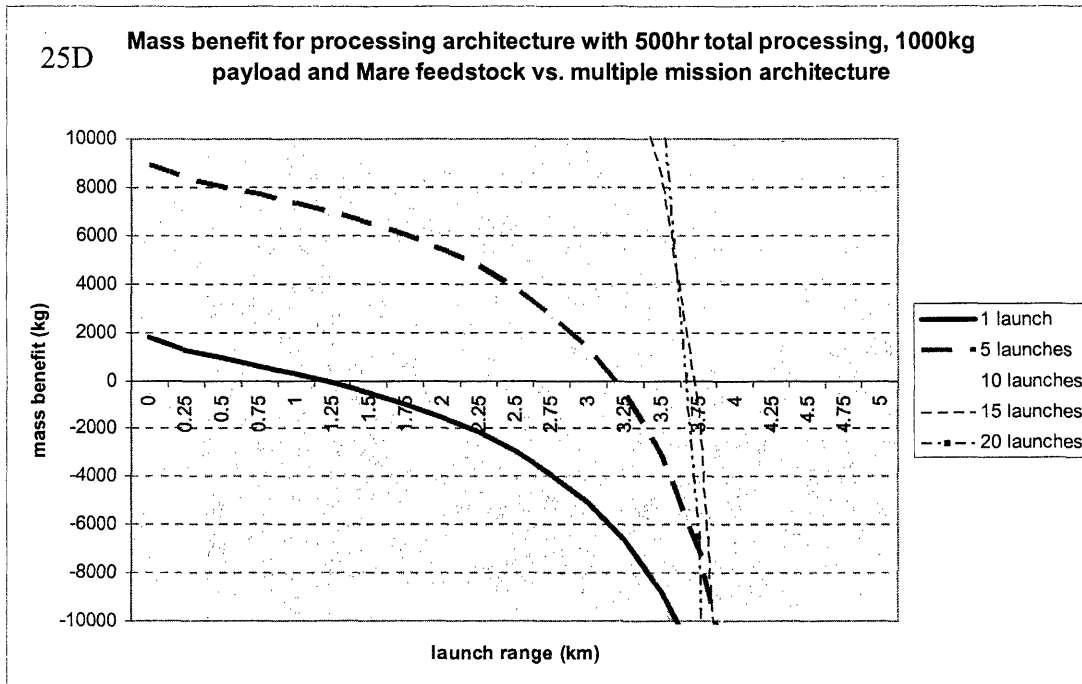


Figure 25A-25E: Glassy feedstock mass benefit vs. multiple mission architecture. Each graph shows one parameter scenario with data series for launch numbers between 1 and 20.

The maximum ranges of benefit are plotted in figure 26 for each of the four original scenarios. The fifth test scenario using a 2000hr total processing time and 200kg payload has a peak launch range of 38.1km at 8 lunar launches.

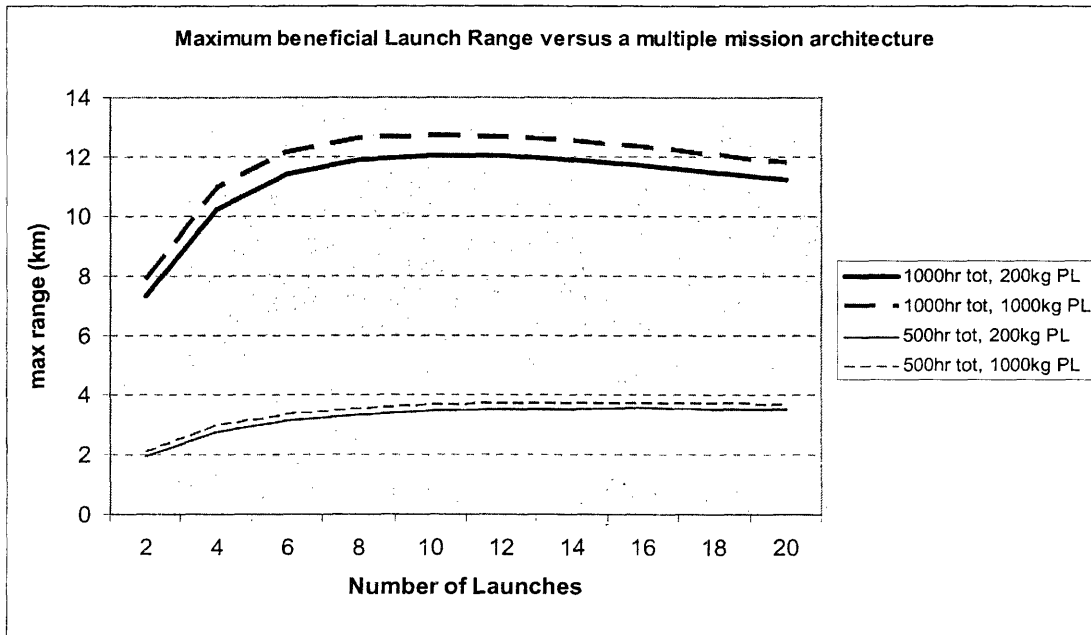
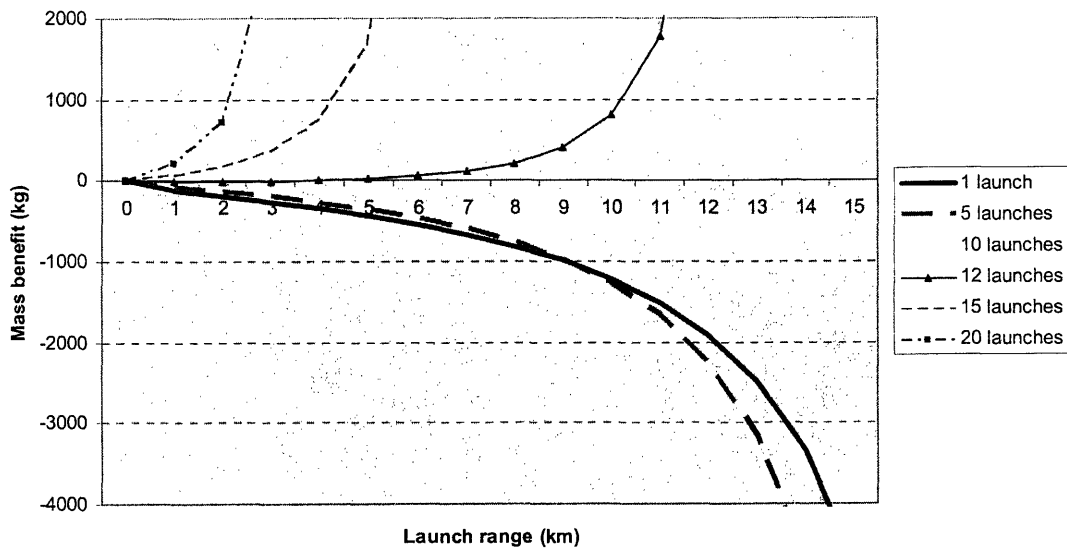


Figure 26: Glassy feedstock maximum beneficial range. The range of benefit is shown for 4 scenarios. The maximum range of benefit can be found at the launch range where the data series peaks.

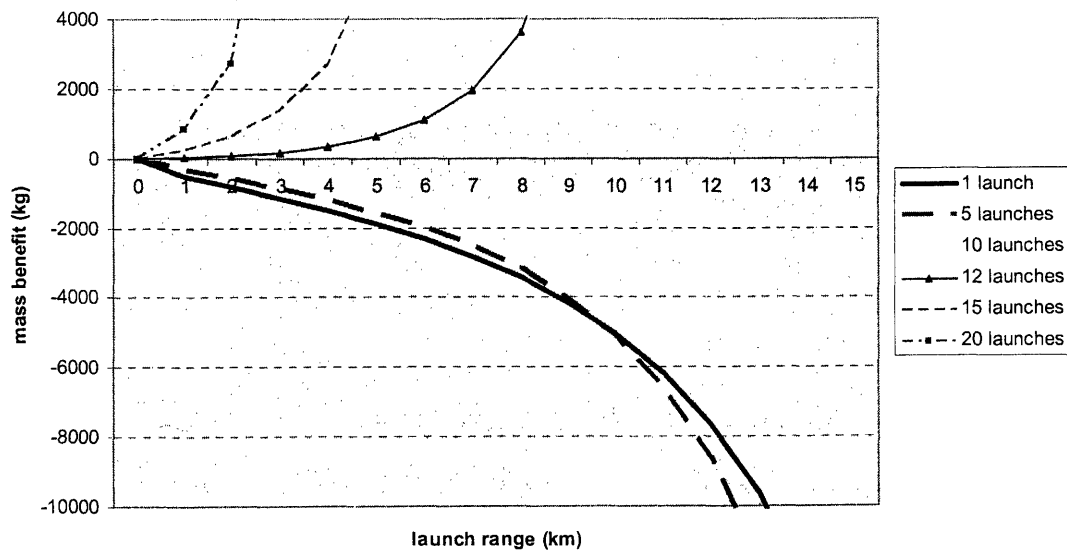
6.3.5.2 Benefit vs. fully fueled architecture

Figures 27A through 27E show the mass benefit of the 5 scenarios (four original 1000hr and 500hr total processing times plus a fifth with a 2000hr total processing time for comparison) versus the fully fueled architecture.

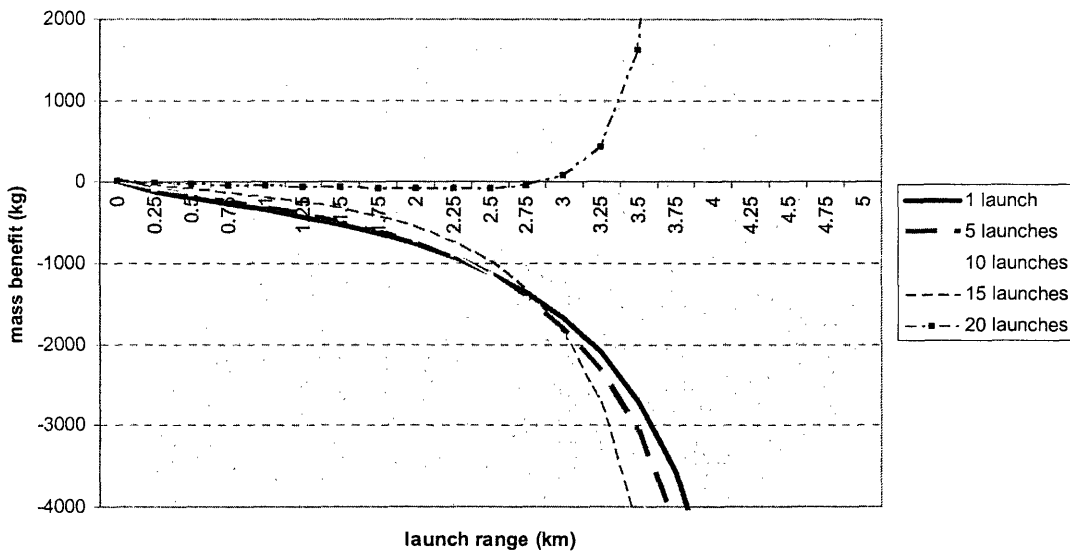
27A Mass benefit of processing architecture with 1000hr tot, 200kg payload and Mare feedstock vs. Fully fueled architecture



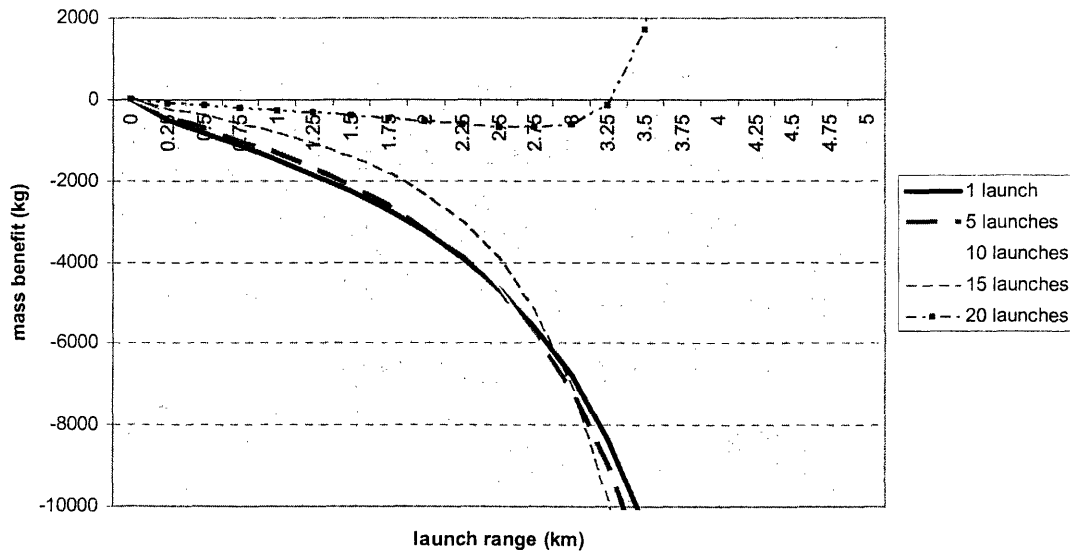
27B Mass benefit for processing architecture with 1000hr tot, 1000kg payload, with a mare feedstock vs. Fully fueled architecture



27C Mass benefit of processing architecture with a 500hr tot, 200kg payload and Mare feedstock vs. fully fueled architecture



27D Mass benefit of processing architecture with a 500hr total processing, 1000kg payload and Mare feedstock vs. fully fueled architecture



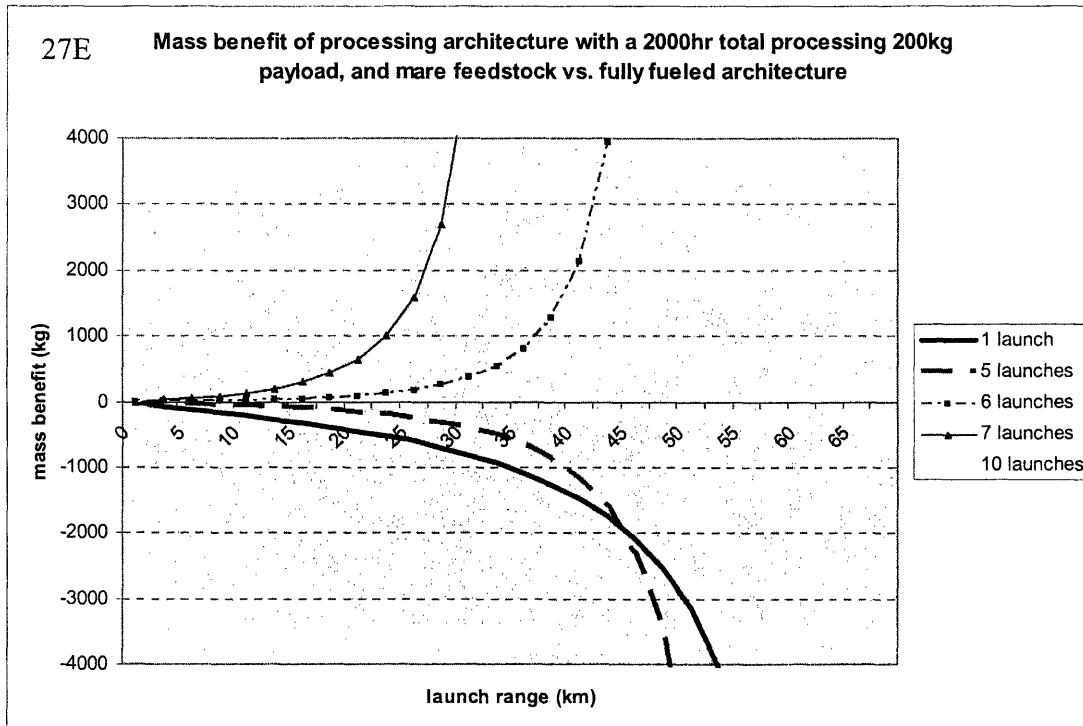


Figure 27A-27E: Glassy feedstock mass benefit vs. fully fueled architecture. Each graph shows one parameter scenario with between 1 and 20 launches.

These graphs show the affect of the change in benefit approximation developed in the highland section, 6.1.5 very clearly. The number of launches at which the system yields a positive mass benefit versus the fully fueled architecture is slightly less than the number of launches of the maximal launch range capability versus the multiple mission architecture. Figures 27C and 27D elucidate another fact of the behavior of the system as the launch number is increased. The benefit of the system switches from a negative value to a positive value at launch ranges nearest the range of feasibility first. The data series for 20 lunar launches in figures 27C and 27D show a negative mass benefit at low ranges and a positive mass benefit at ranges approaching the upper limit of what is feasible. This is because at short ranges, the fully fueled system mass has not reached its range of

feasibility yet, while at higher launch ranges the fully fueled system mass blows up to infinity because these ranges are beyond it's range of feasibility. The addition of more launches makes the fully fueled system mass blow up at all ranges because it is compounding the mass of fuel and tanks for each launch. The positive mass benefit alone does not mean that higher ranges are better, because both system masses are extremely large. It is just that the fully fueled system mass has reached the point where it blows up while the processing plant mass eventually converges to a very large number. In order to have a feasible system the total mass of the spacecraft must also be considered.

6.3.5.3 Overall system feasibility

Four items are primary factors in determining the feasibility of using glassy soils as a feedstock: mass of the system, total launch range it can achieve, total time of the mission, and the availability of lunar pyroclastic glasses. This analysis has not examined in detail the availability of pyroclastic glasses, and therefore assumes that greater knowledge of the composition and extent of pyroclastic glass deposits will be known by the time this mission is designed. Tables 11A, 11B, and 11C have been created to analyze the mission mass, total range, and total time. Table 11A lists the ranges and mass values for a glassy feedstock system with 1000hr total processing time and 200kg payload. Table B lists the same values for a system with 1000hr total processing time and a 1000kg payload, and table C lists these values for a comparison scenario with a 2000hr total processing time, and a 200kg payload. Each table lists the values only for the number of launches and launch ranges that are beneficial over both other exploration architectures. Glassy feedstock scenarios using 500hr total processing times did have a result with positive

benefits over both architectures at 20 launches. However, only launch ranges between 2.75km and 3.5km provided this positive mass benefit. Within this narrow range a processing plant system is a beneficial means of exploration and could be used. A total range of 55 to 70 kilometers could be achieved at a 500hr total processing time per launch, which also results in a 20 month mission (20 launches multiplied by one month per launch). The model predicts a total system mass between 2660kg and 7560kg for a mission using these parameters. These masses are not above the feasible range to deliver to lunar orbit. By utilizing a shorter processing time it may also lessen the system degradation. Therefore, total processing times less than 1000hrs can be considered although they are not graphed or tabulated below.

Analyzing the data displayed in tables 11A, 11B, and 11C provides much more information about the feasibility of a glassy feedstock system. Each column provides either the system mass for the scenario at the given number of launches, or the total mission distance. The scenarios with various numbers of launches can be plotted against each other to compare the system masses required to reach the same total mission range. The total mission range is simply the launch range multiplied by the number of launches.

Table 12-A Glassy total launch masses and distances for 1000hr total processing per launch and 200kg payload

Table range per launch (km)	12 launch capability			13 launch capability			14 launch capability			15 launch capability			16 launch capability			17 launch capability			18 launch capability			19 launch capability			20 launch capability		
	Total Range (km)	Orbit Mass (kg)	Lunar Orbit Mass (kg)	Total Range (km)	Orbit Mass (kg)	Lunar Orbit Mass (kg)	Total Range (km)	Orbit Mass (kg)	Lunar Orbit Mass (kg)	Total Range (km)	Orbit Mass (kg)	Lunar Orbit Mass (kg)	Total Range (km)	Orbit Mass (kg)	Lunar Orbit Mass (kg)	Total Range (km)	Orbit Mass (kg)	Lunar Orbit Mass (kg)	Total Range (km)	Orbit Mass (kg)	Lunar Orbit Mass (kg)	Total Range (km)	Orbit Mass (kg)	Lunar Orbit Mass (kg)	Total Range (km)	Orbit Mass (kg)	Lunar Orbit Mass (kg)
0	0	378	0	378	0	378	0	378	0	378	0	378	0	378	0	378	0	378	0	378	0	378	0	378	0	378	0
1	12	521	13	523	15	527	16	529	17	531	18	533	19	535	20	537	19	535	19	535	19	535	19	535	20	537	19
2	24	617	26	620	30	626	32	632	34	636	36	640	38	645	40	649	36	640	38	645	38	645	38	645	40	649	38
3	36	713	39	724	45	737	48	744	51	750	54	757	57	764	60	771	51	750	57	764	57	764	57	764	60	771	57
4	48	832	52	842	60	862	64	872	68	882	72	894	76	905	80	917	68	894	76	905	76	905	76	905	80	917	76
5	60	967	65	981	75	1012	80	1028	85	1044	90	1061	95	1079	100	1097	85	1044	95	1079	95	1079	95	1079	100	1097	95
6	72	1131	78	1153	90	1199	96	1223	102	1249	108	1275	114	1303	120	1331	102	1249	114	1303	114	1303	114	1303	120	1331	114
7	84	1339	91	1371	105	1441	112	1479	119	1518	126	1560	133	1604	140	1650	119	1518	133	1604	133	1604	133	1604	140	1650	133
8	96	1611	104	1660	120	1768	128	1828	136	1892	144	1960	152	2038	160	2112	136	1892	152	2038	152	2038	152	2038	160	2112	152
9	108	1982	117	2060	135	2286	144	2386	153	2494	162	2561	171	2691	180	2833	153	2494	171	2691	171	2691	171	2691	180	2833	171
10	120	2520	130	2650	150	2854	160	3132	170	3311	180	3556	190	3811	200	4103	170	3311	190	3811	190	3811	190	3811	200	4103	190
11	132	3261	143	3598	165	4178	176	4539	187	4967	198	5462	209	6064	220	6798	187	4967	209	6064	209	6064	209	6064	220	6798	209
12	144	4324	156	5326	180	6178	192	7104	204	8112	216	9204	228	10392	240	11688	204	8112	228	10392	228	10392	228	10392	240	11688	228
13	156	N/A	169	N/A	195	N/A	208	N/A	221	N/A	234	N/A	247	N/A	260	N/A	221	N/A	247	234	N/A	247	234	N/A	260	N/A	247

Table 12-B Glassy total launch masses and distances for 1000hr total processing per launch and 1000kg payload

range per launch (Km)	12 launch capability		13 launch capability		14 launch capability		15 launch capability		16 launch capability		17 launch capability		18 launch capability		19 launch capability		20 launch capability	
	Total Range (km)	Lunar Orbit Mass (kg)	Total Range (km)	Lunar Orbit Mass (kg)	Total Range (km)	Lunar Orbit Mass (kg)	Total Range (km)	Lunar Orbit Mass (kg)	Total Range (km)	Lunar Orbit Mass (kg)	Total Range (km)	Lunar Orbit Mass (kg)	Total Range (km)	Lunar Orbit Mass (kg)	Total Range (km)	Lunar Orbit Mass (kg)	Total Range (km)	Lunar Orbit Mass (kg)
0	0	1782	0	1782	0	1782	0	1782	0	1782	0	1782	0	1782	0	1782	0	1782
1	12	2410	13	2418	14	2426	15	2434	16	2443	17	2451	18	2459	19	2468	20	2476
2	24	2823	26	2839	28	2854	30	2870	32	2886	34	2903	36	2919	38	2936	40	2953
3	36	3251	39	3276	42	3302	45	3328	48	3355	51	3382	54	3410	57	3438	60	3467
4	48	3728	52	3767	56	3806	60	3846	64	3888	68	3930	72	3973	76	4017	80	4063
5	60	4282	65	4339	70	4397	75	4457	80	4519	85	4583	90	4649	95	4717	100	4787
6	72	4945	78	5027	84	5113	90	5203	96	5295	102	5391	108	5491	114	5595	120	5704
7	84	5768	91	5883	98	6011	105	6144	112	6284	119	6430	126	6583	133	6745	140	6915
8	96	6807	104	6988	112	7179	120	7382	128	7595	136	7821	144	8057	152	8325	160	8602
9	108	8199	117	8479	126	8767	135	9066	144	9376	153	9697	162	10029	171	10392	180	11118
10	120	10126	130	10570	140	11035	150	11538	160	12075	170	12654	180	13247	190	13855	200	14526
11	132	13604	143	14295	154	14998	165	15601	176	16209	187	16833	198	17462	209	18116	220	23256
12	144	1725	156	19199	168	20931	180	22897	192	24887	204	26911	216	32908	228	34975	240	N/A
13	156	N/A	169	N/A	182	N/A	195	N/A	208	N/A	221	N/A	234	N/A	247	N/A	260	N/A

Table 12-C range per launch (Km)	6 launch capability			7 launch capability			8 launch capability			9 launch capability			10 launch capability			11 launch capability			12 launch capability		
	Total Range (km)	Lunar Orbit Mass (kg)	Total Range (km)	Lunar Orbit Mass (kg)	Total Range (km)	Lunar Orbit Mass (kg)	Total Range (km)	Lunar Orbit Mass (kg)	Total Range (km)	Lunar Orbit Mass (kg)	Total Range (km)	Lunar Orbit Mass (kg)	Total Range (km)	Lunar Orbit Mass (kg)	Total Range (km)	Lunar Orbit Mass (kg)	Total Range (km)	Lunar Orbit Mass (kg)	Total Range (km)	Lunar Orbit Mass (kg)	
0	0	378	0	378	0	378	0	378	0	378	0	378	0	378	0	378	0	378	0	378	
2	12	470	14	472	16	475	18	477	20	479	22	482	24	484	26	486	28	488	30	490	
4	24	523	28	527	32	531	36	535	40	539	44	543	48	547	52	551	56	555	60	559	
6	36	573	42	579	48	585	54	591	60	597	66	603	72	609	78	615	84	621	90	627	
8	48	623	56	631	64	639	72	648	80	656	88	665	96	674	104	683	112	692	120	701	
10	60	675	70	686	80	697	90	708	100	719	110	731	120	744	132	757	144	770	156	783	
12	72	731	84	744	96	758	108	773	120	788	132	803	144	818	156	833	168	848	180	863	
14	84	791	98	808	112	825	126	844	140	863	154	884	168	905	182	927	196	949	210	971	
16	96	856	112	877	128	899	144	923	160	948	176	974	192	1001	208	1029	224	1057	240	1085	
18	108	927	126	954	144	982	162	1011	180	1043	198	1077	216	1118	234	1155	252	1195	270	1233	
20	120	1007	140	1040	160	1075	180	1112	200	1153	220	1196	240	1243	264	1293	288	1341	312	1389	
22	132	1097	154	1138	176	1181	198	1229	220	1280	242	1336	264	1397	288	1453	312	1511	336	1569	
24	144	1199	168	1249	192	1304	216	1364	240	1430	264	1503	288	1583	312	1657	336	1727	360	1791	
26	156	1315	182	1378	208	1448	234	1525	260	1610	286	1706	312	1813	336	1897	360	1983	384	2067	
28	168	1450	196	1530	224	1618	252	1718	280	1830	308	1957	336	2044	360	2177	384	2261	408	2349	
30	180	1608	210	1709	240	1824	270	1954	300	2104	330	2277	360	2481	384	2619	408	2769	432	2861	
32	192	1797	224	1927	256	2076	288	2250	320	2454	352	2697	384	2990	408	3147	432	3297	456	3439	
34	204	2025	238	2194	272	2393	306	2630	340	2916	374	3268	408	3709	432	3987	456	4269	480	4545	
36	216	2307	252	2532	288	2803	324	3165	360	3551	396	4083	432	4786	456	5067	480	5363	504	5665	
38	228	2662	266	2968	304	3249	342	3639	380	4083	418	4683	456	5363	480	5769	504	6081	528	6405	
40	240	N/A	280	N/A	320	N/A	360	N/A	400	N/A	440	N/A	480	N/A	520	N/A	560	N/A	600	N/A	

Table 12-C cont.	13 launch capability			14 launch capability			15 launch capability			16 launch capability			17 launch capability			18 launch capability			19 launch capability			20 launch capability		
	Total Range (km)	Lunar Orbit Mass (kg)	Lunar Orbit Mass (kg)	Total Range (km)	Lunar Orbit Mass (kg)	Lunar Orbit Mass (kg)	Total Range (km)	Lunar Orbit Mass (kg)	Lunar Orbit Mass (kg)	Total Range (km)	Lunar Orbit Mass (kg)	Lunar Orbit Mass (kg)	Total Range (km)	Lunar Orbit Mass (kg)	Lunar Orbit Mass (kg)	Total Range (km)	Lunar Orbit Mass (kg)	Lunar Orbit Mass (kg)	Total Range (km)	Lunar Orbit Mass (kg)	Lunar Orbit Mass (kg)	Total Range (km)	Lunar Orbit Mass (kg)	
0	0	378	378	0	378	378	0	378	378	0	378	378	0	378	378	0	378	378	0	378	378	0	378	
2	26	486	489	28	489	491	32	494	496	34	496	496	36	499	499	38	501	501	38	501	501	40	504	
4	52	552	557	56	557	561	64	566	571	68	571	571	72	575	575	76	580	580	76	580	580	80	585	
6	78	617	623	84	623	630	96	636	645	102	645	645	108	652	652	114	660	660	114	660	660	120	668	
8	104	684	692	112	692	704	128	704	724	136	724	724	144	735	735	152	747	747	152	747	747	160	759	
10	130	756	770	140	770	784	160	784	798	170	798	816	180	828	828	190	845	845	190	845	845	200	861	
12	156	827	855	168	855	873	192	873	893	204	893	916	216	935	935	228	958	958	228	958	958	240	987	
14	182	897	927	196	927	956	224	956	992	238	992	1030	252	1060	1060	266	1091	1091	266	1091	1091	280	1125	
16	208	967	1002	224	1002	1036	256	1036	1084	272	1084	1139	288	1210	1210	304	1253	1253	304	1253	1253	320	1300	
18	234	1037	1076	252	1076	1120	288	1120	1184	306	1184	1267	324	1393	1393	342	1455	1455	342	1455	1455	360	1522	
20	260	1107	1151	280	1151	1200	320	1200	1264	340	1264	1345	360	1624	1624	380	1712	1712	380	1712	1712	400	1809	
22	286	1177	1227	308	1227	1280	352	1280	1349	374	1349	1430	396	1923	1923	418	2052	2052	418	2052	2052	440	2198	
24	312	1247	1303	336	1303	1360	384	1360	1436	408	1436	1538	432	2326	2326	456	2521	2521	456	2521	2521	480	2749	
26	338	1317	1375	364	1375	1436	416	1436	1524	442	1524	1635	468	2694	2694	494	2904	2904	494	2904	2904	520	3085	
28	364	1387	1447	392	1447	1516	448	1516	1616	476	1616	1739	504	3067	3067	532	3279	3279	532	3279	3279	560	3472	
30	390	1457	1519	420	1519	1596	480	1596	1708	510	1708	1844	540	3451	3451	570	3665	3665	570	3665	3665	600	3763	
32	416	1527	1593	448	1593	1680	512	1680	1796	544	1796	1946	576	3835	3835	608	4089	4089	608	4089	4089	640	4171	
34	442	1597	1675	476	1675	1772	544	1772	1900	578	1900	2064	612	4219	4219	646	4363	4363	646	4363	4363	680	4455	
36	468	N/A	N/A	504	N/A	N/A	576	N/A	N/A	612	N/A	N/A	648	N/A	N/A	684	N/A	N/A	684	N/A	N/A	720	N/A	
38	494	N/A	N/A	532	N/A	N/A	608	N/A	N/A	646	N/A	N/A	684	N/A	N/A	722	N/A	N/A	722	N/A	N/A	760	N/A	
40	520	N/A	N/A	560	N/A	N/A	640	N/A	N/A	680	N/A	N/A	720	N/A	N/A	760	N/A	N/A	760	N/A	N/A	800	N/A	

Table 12A-12C: Glassy total system masses and distances. Values for all beneficial launch numbers and ranges are shown for a glassy feedstock system using a 1000hr total processing time per launch (A and B) and a 2000hr total processing time per launch (C).

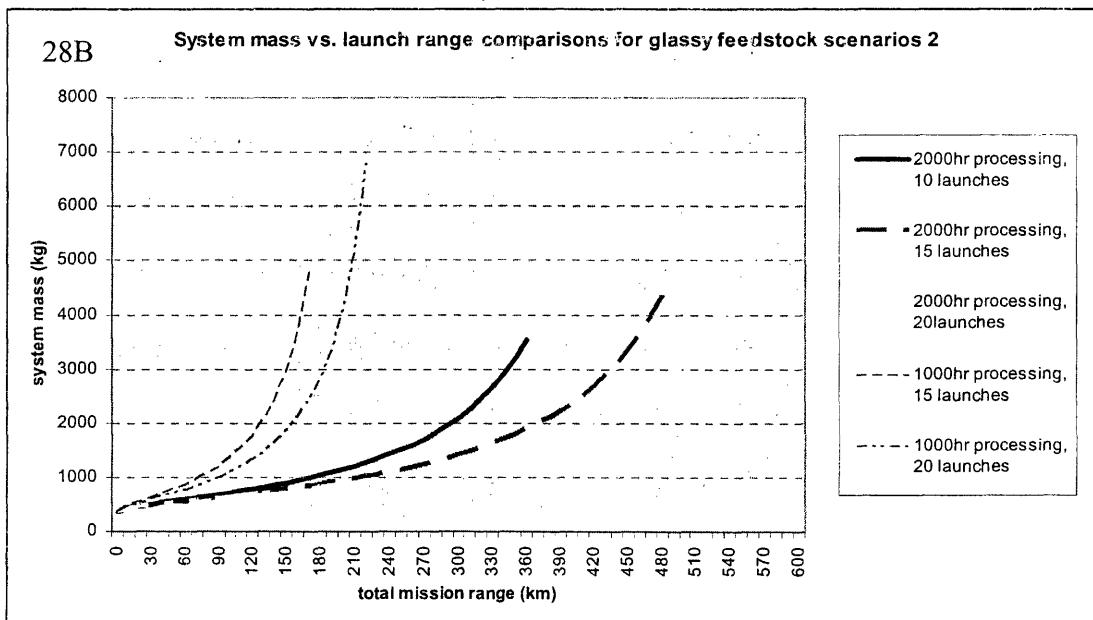
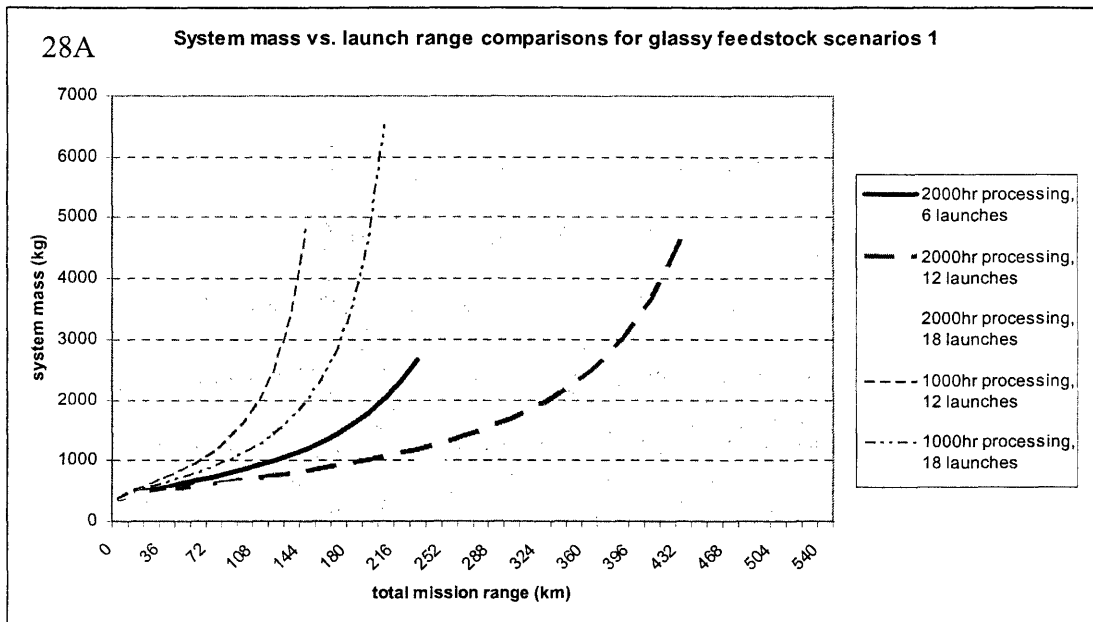


Figure 28A-28B: Glassy feedstock system masses vs. total mission range. Five data series are shown in each graph using either a 2000hr or 1000hr total processing time per launch and beneficial launch numbers. Systems with larger total processing times can reach much longer launch ranges. The 5 data series are truncated at the point where they are no longer beneficial above the other two architectures.

Figures 28A and 28B display the system mass data scenarios using a 200kg payload graphed over the beneficial launch ranges of scenarios with both a 1000hr and 2000hr total processing time per launch. One analysis is to consider missions with the same total mission time. For example, a 2000hr total processing time mission with 10 launches has the same total mission time as a 1000hr total processing time mission with 20 launches. This analysis is important because mission planners may determine that there is a maximum mission time length for any such processing mission that they can conduct, or there may be other constraints on the total mission time. The missions with 2000hr total processing times and less launches require a significantly lower system mass than the 1000hr total processing time missions with the same total mission time. However, this also means that the 2000hr total processing time missions will only be visiting half the lunar sites as the 1000hr total processing time missions. The scientific requirements of the mission may determine that it is more beneficial to use the 1000hr total processing time mission despite the higher overall mass. If a certain number of sites is desired, shorter launch ranges may be used to keep the overall system mass the same. For example, if there is a 2000kg cap on the system mass and a time limit of 2 years, the mission planners could utilize either a 2000hr processing time system with 6 launches or a 1000hr processing time system with 12 launches. The 2000hr processing time per launch with 6 launches system can reach a total range of approximately 220km, while the 1000hr processing time per launch with 12 launches system can only reach a total distance of approximately 140km. Again, science requirements will dictate which set of parameters is better suited for the mission. There are many trades that can be conducted when planning such a mission. Another analysis is simply looking at the total distance traveled. A science requirement of such an exploration mission may be that it must be able to travel a certain

distance on the lunar surface in its lifetime. If this is so, the importance of using long total processing times is apparent. However, there will be engineering constraints that limit the total amount of time and mass for a mission to reach these distances. As was previously mentioned, the system will degrade over time; however, this degradation has yet to be modeled. Trades can be conducted using any combination of total mission time, the number of launch sites, system mass, and total mission distance as constraints. These trades are not explored in further depth in this study because more knowledge about the science goals of any mission are required to make relevant trade studies on these variable.

Overall, the processing plant architecture with a glassy feedstock can provide a significant benefit to lunar exploration. There are limitations to this benefit and uncertainties in its extent. However, using the assumptions and parameter values developed in this model, a substantial increase in our lunar exploration ability can be achieved by utilizing the processing plant architecture with a glassy type feedstock. To determine the exact feasibility of various mission designs, further study and model detail is required. More information about the distribution and concentration of glassy deposits on the lunar surface is also required before missions can be designed to utilize this feedstock for the processing plant architecture.

7. Polar Ice Deposits

This model has not yet been constructed to compute the possibility of increasing the oxygen yield by adding an ice concentration to the feedstock. However, a quick analysis of the relative yields and energy requirements provides a basis for comparison. An ice content of

1.5 wt% estimated by Feldman [Feldman] is adopted for this analysis. The lunar ices will sublimate simply by raising the temperature of the regolith to the ambient temperature of the lunar environment exposed to solar radiation. It could be assumed that solar radiation alone could be used to power this process; however, if there is a design constraint that prevents this, a power source on the spacecraft could provide the needed energy. This energy is over an order of magnitude less than what is required to extract oxygen from the regolith oxides. The energy needed to conduct electrolysis is also less than $1/10^{\text{th}}$ that needed to heat the regolith for hydrothermal reduction (285kJ/mol versus $\sim 3000\text{kJ/mol}$). Taking a power system requirement of $1/10^{\text{th}}$ the power required for hydrothermal reduction yields an estimated mass for the power system that could be required. This is still a high end estimate. Assuming that all the water is released, a simple model can be iterated to determine how much regolith is required to produce the needed propellant, and how far such a spacecraft could be launched. This system would allow a spacecraft to launch itself more than 200 kilometers per launch and still obtain a benefit over both other architectures if using water ice as the source of propellant. Water ice also provides other benefits from such a launch architecture. Hydrogen could be obtained from the ice as well as oxygen. This would allow the system to continue on indefinitely until the system has degraded to a point where it is no longer operational. In other words, the number of launches would not be limited by the amount of hydrogen mass that needs to be carried on the spacecraft. From this extreme improvement in launch range capability it is doubtful that a processing plant architecture utilizing a hydrothermal reduction method for oxygen production will be useful at the poles. At the ice concentrations estimated by Feldman, the added mass of the power system required to extract oxygen from the regolith itself would not provide a benefit above a system that simply processed more regolith to

extract the oxygen from the ice deposits. These numbers are a very rough calculation, and further detailed studies could be useful in determining the exact benefit of polar ice deposits and whether or not a hydrothermal processing plant has any utility at the poles. However, it is clearly apparent that if polar ice deposits exist at concentrations near what Feldman predicts, oxygen extraction from the ice alone is the preferred method of propellant production for a lunar launch exploration mission design.

8. Technological Improvements of Importance

There are many technologies required for the processing plant architecture which have much room for improvement. Three such technologies are vitally important to the design of the processing plant mission – cryogenic liquification and storage of propellants, hydrothermal processing plant designs, and RTG power production. The cryogenic liquification and storage stage of this mission design has not been incorporated into this model yet. It is assumed that there will be further advances in this technology, which could provide significant improvements in the system design. However, until further detail of this system is incorporated into the model any mass savings from possible improvements in cryogenic propellant storage cannot be analyzed.

8.1 The hydrothermal processing system

It is important to note possible improvements in processing system designs. There is not much to consider when looking at future improvements. The reaction will remain the same

reaction with the same power requirements. However, it is possible to create better beneficiation, sorting, and furnace reduction methods which could potentially increase the oxygen yield from any given feedstock. The stoichiometric oxygen yield from feedstock samples is not being achieved from the reduction methods because of grain size complications, possible sintering of the regolith, and other as of yet unforeseen complications in the process. As more research on the actual reduction process is gathered and more information on the lunar regolith properties is known, further advances in furnace design could yield to significant improvements. Several companies and research groups have been looking at other methods of improving the oxygen yield. For example, Carbotec Inc. has developed their fluidized bed reactor design to improve the oxygen yield [Carbotec]. Further research from this group could lead to system design improvements. This model does analyze various production furnace designs, but instead focuses on the feasibility analysis of the exploration architecture as a whole. Therefore, any attempt at analyzing improvements for various processing plant designs will be saved for future analyses.

8.2 Power production systems

The power production system used in this model is from the RTG technology of the Cassini mission. This technology is already several years old and significant improvements for future missions are already underway. Stirling Radioisotope Power Systems (SRPS) are being designed for use in future exploration missions. These are more advanced versions of the RTG technology used on Cassini. It is estimated that SRPS designs will achieve an 8W per kilogram power density well before any lunar processing plant mission would be ready. The Jupiter Icy Moons Orbiter (JIMO) mission under development has estimated that the RTG

power system available for use will be capable of reaching 16W/kg by the 2012 timeframe estimated for its launch. Because the power system is such a large percentage of the total system mass, it is very improvement in the efficiency of RTG technology will greatly benefit the system design. The power system mass is a simple linear function, therefore increasing the power density of the RTG in the model from the 4W/kg currently used to the SRPS design of 8W/kg cuts the power system mass in half. This is nearly equivalent to doubling the total processing time in the model. The total processing time has a direct affect on the number of batches for each launch which in turn has a linear affect on the size and volume of each batch. The mass of each batch has a linear relationship on the power system mass which is equivalent to the effect of changing the power density. However, the volume change of each batch caused by changing the total processing time has an affect on the furnace mass which is also incorporated into the system. The model has shown that the furnace mass is two orders of magnitude less than the RTG mass for processing plant scenarios with feasible parameter values. Therefore the change in overall system mass caused by the changing the total processing time is a very close approximation to changing the power density of the RTG, although at high launch ranges and launch numbers this mass difference can be considered significant. For a first order estimation of the affect that improved RTG systems would have on the overall processing plant system mass, a further analysis of the model runs previously mentioned is sufficient. The previous model runs using a 1000hr total processing time are adequate estimations of a system utilizing SRPS technology (8W/kg) at 500hr total processing times. Similarly, model runs with 2000hr total processing times can be used as estimations for systems with improved SRPS power technology at 1000hr total processing times. In general any change in processing time can be used as an approximation for the

system with the same change in power density. The importance of improving the RTG technologies is clear in comparing these scenarios. The technological advances between the Cassini RTG and the future JIMO RTG estimates cause a significant improvement in the system capabilities of the processing plant architecture. Using the JIMO RTG estimates processing plant missions would be feasible using highland regolith feedstocks, and the maximum beneficial ranges are significantly improved, as seen in the scenarios described in the previous sections.

As an upper bound on the system improvements capable from increased RTG technologies the thermal RTG energy output can be utilized. RTG's create the electrical power required for spacecraft systems by converting thermal energy created by radioactive decay into electrical energy. The thermal power density of the Cassini RTG is approximately 200W/kg. If 100% of this thermal energy could be utilized the processing plant missions would have an extremely improved exploration capability. At such a high RTG efficiency the power system becomes less of a factor in the overall mass determination. The propellant system masses account for a much greater percentage of the total mass. Because of this new dynamic, the 3 hour batch processing time is more beneficial for systems with such a high RTG efficiency. The dependence of the entire system mass on the RTG mass for a theoretical 100% thermal energy conversion RTG and a Cassini type RTG can be compared in figures 29A and 29B. The lower the power densities for the RTG system, the more dependant the total system mass becomes upon the RTG mass. This varies slightly with the launch range.

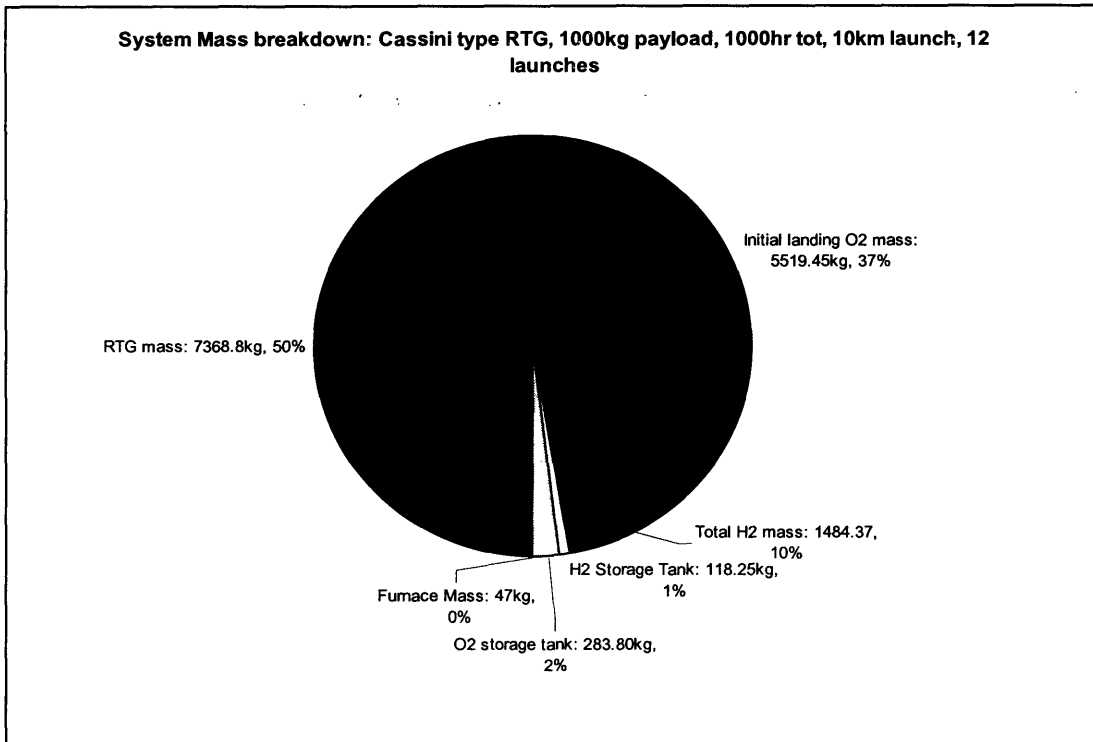
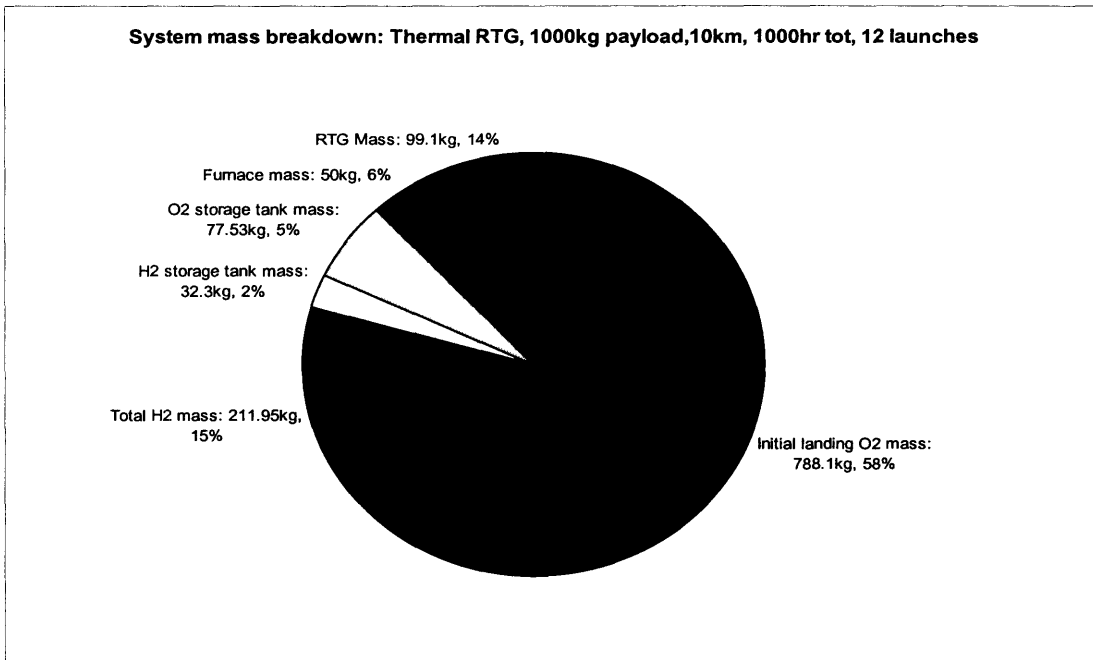


Figure 29A-29B: System mass breakdown. The percentage of the total system mass that each component takes up is displayed for a 100% RTG conversion efficiency system in figure A, and for a Cassini type RTG system in figure B. Both figures are for a mare feedstock system and use the same system parameters for comparison.

Longer distances will create larger propellant system masses. However, the RTG mass also increases with launch range and even at the longest feasible launch ranges for all scenarios the RTG mass still dominates the system for a mission with a Cassini type RTG.

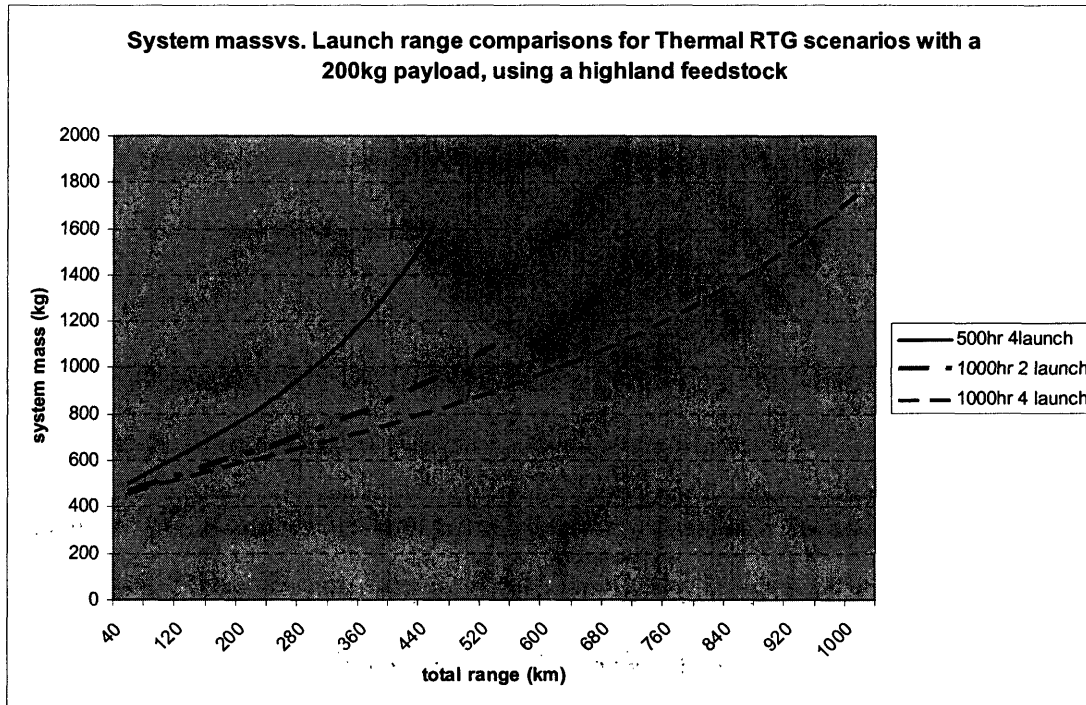
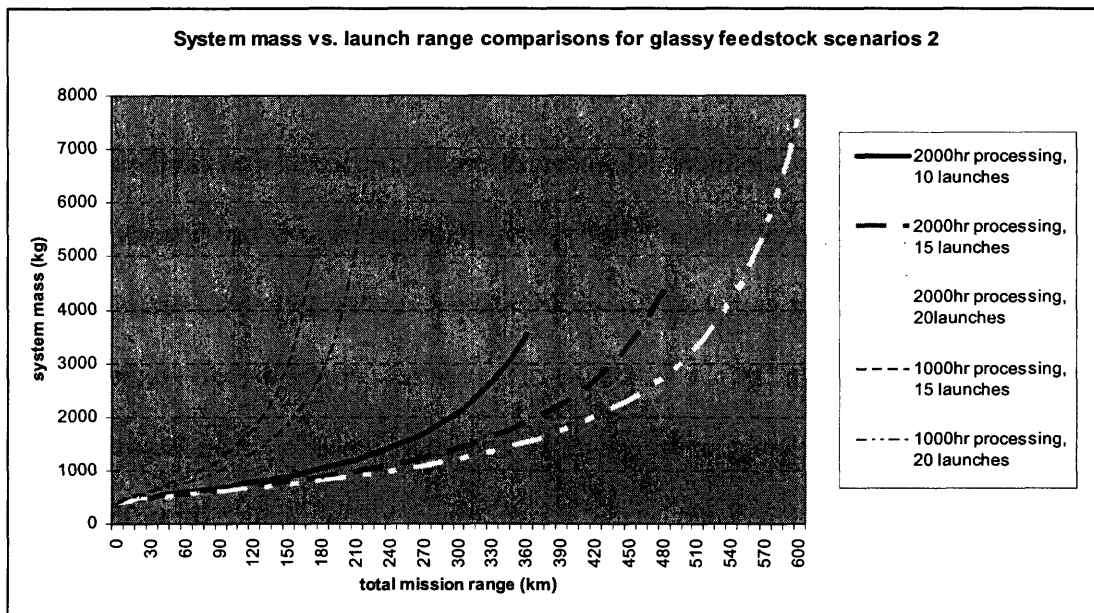


Figure 30: Thermal RTG total mission time comparisons. The system mass vs. launch range for several cases are shown to compare the system mass and launch range obtained for different systems with the same overall mission time.

Figure 30 displays the exploration capability and system masses for several scenarios using a 100% thermal energy conversion for the RTG power system. The difference from today's RTG conversion efficiencies of up to 16W/kg to a theoretical 100% thermal energy use RTG is dramatic. At 100% efficiency the processing plant system would be feasible in all regions of the lunar surface and would be able to nearly travel from the lunar pole to the equator within its lifetime. Again, significant system degradations would somewhat lessen the extent of possible exploration; however, this does not take away from the fact that at 100% RTG

efficiency this type of exploration architecture is by far more beneficial than any other means of exploring the lunar surface. Figure 28B is reprinted here for easy data comparisons. The maximum range of the 100% thermal RTG system using a highland feedstock is almost double the maximum range of a Cassini type RTG system using glassy feedstock, a total processing time twice as long and with five times the number of launches. At these two maximum ranges (~1000km for the 100% thermal RTG, ~600km for the Cassini RTG), the system masses are ~1800kg vs ~7000kg respectively.



9. Error Analysis

A detailed error analysis of the model and scenario systems has not been conducted. The major sources of error are easy to define in this system without an in-depth study. At the low power densities for the RTG systems expected to be available in the near future for use, the

entire system mass of a processing plant mission is largely composed of the power system. Therefore, any error in the power generation capabilities of the RTGs can create a significantly different result. For long missions the RTGs will undergo some amount of degradation that has not been modeled. This could produce significantly lower beneficial ranges for long duration missions (several years in length). At shorter timescales the RTG degradation will not be a large factor. However, the amount of RTG degradation still needs to be incorporated into the model in order to determine the degree that this would change the exploration capabilities of this system.

A second major source of error in this model comes from the neglected mass of the oxygen liquification and storage system. This will be a fairly significant mass in the system. In other system designs for processing plants the liquification and storage system has been on the same order of magnitude as the furnace mass. So in the entire scope of the mission it is not estimated to cause a drastic change in the systems exploration capability. The mass could easily be incorporated into the payload system mass for launch ranges much lower than the range of feasibility of the system.

The last major source of error comes directly from the processing system itself. The uncertainty in the type of material being used for the furnace will cause a small uncertainty in the furnace mass, but again this is not significant on the scale of the entire spacecraft. The major uncertainty in the processing system is in the oxygen yield achieved through the reduction reaction. This has been highly variable in laboratory experiments due to the variation in the composition of the samples. Different grain sizes on the lunar surface may

cause added complications in defining the oxygen yield. Larger grain sizes will reduce the yield from any sample. The processing chamber itself will also undergo degradation overtime. This degradation has not been modeled in this study and has not been analyzed to any level of detail in laboratory experiments. Therefore, missions with long timescales will not be able to reach the launch ranges shown in the scenarios. In reality each successive launch range will be slightly shorter than the one before due to the corrosive elements degrading the processing chamber. At some point in time, the entire system will fail due to the large extent of this degradation. Further studies are needed to determine how long such hydrothermal processing chambers could remain in use.

10. Discussion and conclusions

Although much more detail of the processing apparatus and degradation of the system over time has yet to be implemented, this model serves as a good approximation of the system design for a lunar processing plant exploration architecture. The goal of constructing a model to analyze the benefit of this architecture to lunar exploration has been achieved. The analysis of this version model is not ideally suited to make conclusions on exact ranges of the exploration capabilities that are feasible for such a mission. However, the model is sufficient to determine the general feasibility of this architecture system and to obtain order of magnitude estimates for feasible launch capabilities and associated mission masses. The model can also be used to gain an understanding of the system dynamics of such a mission.

Two major areas of research have been determined to be key for the future development of such an exploration system. These areas, listed in order of importance are:

1. RTG or other power source technological advances
2. Processing plant efficiency advances

The improved RTG efficiency has been shown to be extremely important in increasing the capability of this architecture. The mass of the RTG is the dominant factor in the overall system mass and small increases in efficiency can greatly change the exact beneficial ranges for future missions. Advances in processing efficiency will also be very beneficial to improving the exploration range of any such mission. Increasing the oxygen yield from any feedstock will be very important to increasing the architecture's benefit.

At today's level of RTG efficiency, using this system in the highland regions is not feasible. At the ranges where the system provides a positive benefit over the multiple mission and fully fueled architectures, a rover could easily accomplish the same distance within the mission lifetime. A mission using mare regolith or pyroclastic glasses as its feedstock source could be feasible with today's RTG efficiencies. At RTG efficiencies expected to be reached by the time that any such mission would be launched, it can be concluded with a high level of certainty that this architecture will provide some level of benefit over other possible means of lunar exploration in the mare regions and regions with glass deposits available. Assuming that the system degradation is not severe, this architecture could also be beneficial in highland regions with the increased RTG efficiencies.

Before utilizing this architecture for actual lunar missions further information on the composition of the lunar surface is required. Missions could be designed with a large robustness built in to the system to be able to operate within a range of possible feedstock compositions; however, the more knowledge and certainty that one has about the composition of the feedstock in use, the more efficiently the entire system will be able to be designed. This architecture also has applications for other planetary bodies as well.

Processing plant missions to asteroids could be even more beneficial due to the decreased gravity fields. Missions to Mars would greatly benefit from the use of this architecture although the mission design would be fairly different because of the different resources available in the Martian environment. Overall, currently this architecture is a beneficial means of lunar exploration for mare and glassy feedstocks but not for highland feedstocks; however, with expected increases in RTG efficiency this architecture can be expected to be very beneficial for all regions of the lunar surface with a 0% water ice content. The processing plant architecture could provide for the exploration of many more lunar sites in non-polar regions for a lower cost than both the multiple mission and fully fueled architectures. Future models will be created to better analyze the mission design, narrow constraints on the system parameters, and define the maximum degradation requirements of the system that still produce beneficial results.

REFERENCES

Allen, Carleton C. et al, Oxygen extraction from lunar soils and pyroclastic glasses, *Journal of Geophysical Research*, vol. 101, 26085-26095, 1996.

Chambers, J. G. et al, Quantitative mineralogical characterization of lunar high-Ti mare basalts and soils for oxygen production, *Journal of Geophysical Research*, vol. 100, 14391-14401, 1995.

Chinese National Space Agency website, <http://www.cnsa.gov.cn>

Crider, Hurley; Vondrak, Richard, The solar wind as a possible source of lunar polar hydrogen deposits, *Journal of Geophysical Research*, vol. 105, 26773-36782, 2000.

Criswell, D.; Waldron, R., International lunar base and lunar-based power system to supply Earth with electric-power, *Acta Astronautica* 29 (6), pp469-480, 1993.

Duke, Michael et al, Silicon PV cell production on the Moon as the basis for a new architecture for space exploration, *Space Technology and Applications International Forum*, American Institute of Physics, 2001.

Ekhart, Peter, The Lunar Base Handbook, McGraw-Hill, 1999.

Feldman, W. C. et al, Polar Hydrogen deposits on the Moon, *Journal of Geophysical Research*, vol. 105, 4175-4195, 2000.

Feldman, W. C. et al, Evidence for water ice near the lunar poles, *Journal of Geophysical Research*, vol. 106, 23231-23251, 2001.

Heiken, Grant H., Lunar Sourcebook, Cambridge University Press: New York, 1991.

Hodges, Richard R., Ice in the lunar polar regions revisited, *Journal of Geophysical Research*, vol. 107, no E2, 2002.

Hodges, Richard R., Reanalysis of Lunar Prospector neutron spectrometer observations over the lunar poles, *Journal of Geophysical Research*, vol. 107, no E12, 2002.

McKay, David S.; Allen, Carleton C., Hydrogen reduction of lunar materials for oxygen extraction on the Moon, AIAA meeting papers, paper 96-0488, 1996.

Mendell, W., Lunar bases and space activities of the 21st century, NASA CP 3166, 1988.

Nozette, Stewart et al, Integration of lunar polar remote-sensing data sets: Evidence for ice at the lunar south pole, *Journal of Geophysical Research*, vol. 106, 23253-23266, 2001.

Ogiwara, Sachio et al, Study on a hydrogen-reduced reactor design for lunar water production, Space 2000, American Society of Civil Engineers, 2000.

Rice, Eric E.; Hermes, Paul A.; Musbah, Omran A., Carbon based reduction of lunar oxides for oxygen production, AIAA meeting papers, paper 97-0890, 1997.

Robie, Richard; Hemingway, Bruce, Thermodynamic properties of minerals and related substances at 298.15K and 1 bar and at higher temperatures, USGS Bulletin 2131, 1995.

Rosenberg, S., Concepts in Lunar Resource Utilization, AIAA paper no. 91-2446, AIAA papers, 1991.

Rosenberg, S., Lunar resource utilization – the production of lunar oxygen, Space 98, American Society of Civil Engineers, 1998.

Sherwood, Brent; Woodcock, Gordon, Cost and Benefits of Lunar Oxygen: Economics, Engineering and Operations, Resources of Near Earth Space, pp199, University of Arizona Press, 1993.

Stefanescu, D. M. et al, In Situ resource utilization for processing of metal alloys on lunar and mars bases, AIAA, 1998.

Taylor, Lawrence A.; Carrier, W. David, Oxygen production on the Moon: an overview and evaluation, Resources of Near Earth Space, pp 69, University of Arizona Press, 1993.

Zhao, Y; Shadman, F., Production of oxygen from lunar ilmenite, Resources of Near Earth Space, pp 149, University of Arizona Press, 1993.